Validation of Gyratory Mix Design in Iowa

Final Report
July 2016

IOWA STATE UNIVERSITY
Institute for Transportation

Sponsored by
Iowa Highway Research Board
(IHRB Project TR-667)
Iowa Department of Transportation
(InTrans Project 14-492)
Federal Highway Administration

About InTrans

The mission of the Institute for Transportation (InTrans) at Iowa State University is to develop and implement innovative methods, materials, and technologies for improving transportation efficiency, safety, reliability, and sustainability while improving the learning environment of students, faculty, and staff in transportation-related fields.

About AMPP

The Asphalt Materials and Pavements Program (AMPP) at InTrans specializes in improving asphalt materials and pavements through research and technology transfer and in developing students' technical skills in asphalt.

Disclaimer Notice

The contents of this report reflect the views of the authors, who are responsible for the facts and the accuracy of the information presented herein. The opinions, findings and conclusions expressed in this publication are those of the authors and not necessarily those of the sponsors.

The sponsors assume no liability for the contents or use of the information contained in this document. This report does not constitute a standard, specification, or regulation.

The sponsors do not endorse products or manufacturers. Trademarks or manufacturers' names appear in this report only because they are considered essential to the objective of the document.

ISU Non-Discrimination Statement

Iowa State University does not discriminate on the basis of race, color, age, ethnicity, religion, national origin, pregnancy, sexual orientation, gender identity, genetic information, sex, marital status, disability, or status as a U.S. veteran. Inquiries regarding non-discrimination policies may be directed to Office of Equal Opportunity, Title IX/ADA Coordinator, and Affirmative Action Officer, 3350 Beardshear Hall, Ames, Iowa 50011, 515-294-7612, email eooffice@iastate.edu.

Iowa DOT Statements

Federal and state laws prohibit employment and/or public accommodation discrimination on the basis of age, color, creed, disability, gender identity, national origin, pregnancy, race, religion, sex, sexual orientation or veteran's status. If you believe you have been discriminated against, please contact the Iowa Civil Rights Commission at 800-457-4416 or the Iowa Department of Transportation affirmative action officer. If you need accommodations because of a disability to access the Iowa Department of Transportation's services, contact the agency's affirmative action officer at 800-262-0003.

The preparation of this report was financed in part through funds provided by the Iowa Department of Transportation through its "Second Revised Agreement for the Management of Research Conducted by Iowa State University for the Iowa Department of Transportation" and its amendments.

The opinions, findings, and conclusions expressed in this publication are those of the authors and not necessarily those of the Iowa Department of Transportation or the U.S. Department of Transportation.

Technical Report Documentation Page

1. Report No. IHRB Project TR-667	**2. Government Accession No.**	**3. Recipient's Catalog No.**	
4. Title and Subtitle Validation of Gyratory Mix Design in Iowa		**5. Report Date** July 2016	
		6. Performing Organization Code	
7. Author(s) R. Christopher Williams (orcid.org/0000-0002-8833-6232), Ashley Buss (orcid.org/0000-0002-8563-9553), Grace Mercado, Hosin "David" Lee (orcid.org/0000-0001-9766-1232), and Ashkan Bozorgzad		**8. Performing Organization Report No.** InTrans Project 14-492	
9. Performing Organization Name and Address Institute for Transportation Iowa State University 2711 South Loop Drive, Suite 4700 Ames, IA 50010-8664		**10. Work Unit No. (TRAIS)**	
		11. Contract or Grant No.	
12. Sponsoring Organization Name and Address Iowa Highway Research Board Iowa Department of Transportation 800 Lincoln Way Ames, IA 50010	Federal Highway Administration U.S. Department of Transportation 1200 New Jersey Avenue SE Washington, DC 20590	**13. Type of Report and Period Covered** Final Report	
		14. Sponsoring Agency Code IHRB and SPR Project TR-667	
15. Supplementary Notes Visit www.intrans.iastate.edu for color pdfs of this and other research reports.			

16. Abstract

The design number of gyrations (N_{design}) introduced by the Strategic Highway Research Program (SHRP) and used in the Superior Performing Asphalt Pavement (Superpave) mix design method has been commonly used in flexible pavement design throughout the US since 1996. N_{design}, also known as the compaction effort, is used to simulate field compaction during construction and has been reported to produce air voids that are unable to reach ultimate pavement density within the initial 2 to 3 years post-construction, potentially having an adverse impact on long-term performance.

Other state transportation agencies have conducted studies validating the N_{design} for their specific regions, which resulted in modifications of the gyration effort for the various traffic levels. Validating this relationship for Iowa asphalt mix designs will lead to better correlations between mix design target voids, field voids, and performance.

A comprehensive analysis of current N_{design} levels investigated the current levels with existing mixes and pavements and developed initial asphalt mix design recommendations that identify an optimum N_{design} through the use of performance data tests.

17. Key Words asphalt air voids—asphalt density—asphalt mixture compaction—asphalt mixture design—asphalt pavement performance—gyratory compaction—optimum binder content—Superpave mix design		**18. Distribution Statement** No restrictions.	
19. Security Classification (of this report) Unclassified.	**20. Security Classification (of this page)** Unclassified.	**21. No. of Pages** 103	**22. Price** NA

Form DOT F 1700.7 (8-72) **Reproduction of completed page authorized**

VALIDATION OF GYRATORY MIX DESIGN IN IOWA

Final Report
July 2016

Principal Investigator
R. Christopher Williams, Director
Asphalt Materials and Pavements Program
Institute for Transportation, Iowa State University

Research Assistants
Grace Mercado, Iowa State University
Ashkan Bozorgzad, University of Iowa

Authors
R. Christopher Williams, Ashley Buss, Hosin "David" Lee, and Ashkan Bozorgzad

Sponsored by
Federal Highway Administration,
Iowa Highway Research Board, and the
Iowa Department of Transportation
(IHRB Project TR-667)

Preparation of this report was financed in part
through funds provided by the Iowa Department of Transportation
through its Research Management Agreement with the
Institute for Transportation
(InTrans Project 14-492)

A report from
Institute for Transportation
Iowa State University
2711 South Loop Drive, Suite 4700
Ames, IA 50010-8664
Phone: 515-294-8103 / Fax: 515-294-0467
www.intrans.iastate.edu

TABLE OF CONTENTS

LIST OF FIGURES

LIST OF TABLES

ACKNOWLEDGMENTS

The authors would like to thank the Iowa Department of Transportation (DOT) and the Iowa Highway Research Board (IHRB) for sponsoring this project and the Federal Highway Administration (FHWA) for state planning and research funds that were used. We would also like to thank Scott Schram with the Iowa DOT for his assistance during the duration of the project. Special thanks go to the asphalt contractors for providing additional project information, the asphalt materials research team/staff with the Iowa DOT, and district personnel for assisting in field work, such as extracting cores required for this project.

EXECUTIVE SUMMARY

The design number of gyrations (N_{design}) introduced by the Strategic Highway Research Program (SHRP) and used in the Superior Performing Asphalt Pavement (Superpave) mix design method has been commonly used in flexible pavement design throughout the US since 1996. N_{design}, also known as the compaction effort, is used to simulate field compaction during construction and has been reported to produce air voids that are unable to reach ultimate pavement density within the initial 2 to 3 years post-construction, potentially having an adverse impact on long-term performance.

Other state transportation agencies have conducted similar validating the N_{design} for their specific regions, which resulted in modifications of the gyration effort for the various traffic levels. This study focused on the validation of N_{design} in Iowa.

Problem Statement and Objectives

The compaction effort is critical in asphalt mix design. Over-compaction during laboratory design may lead to under-compaction in the field, reduced asphalt content, and can affect overall durability. The objective of this study is to determine if the current mix design gyratory levels are creating mixes that will attain target densification under traffic. The quality control and quality assurance (QC/QA) information at construction were matched with field densities to determine if traffic loading is adequately compacting the surface mix. Detailed objectives for the project are outlined as follows:

1. Evaluate the ultimate in-place densities by performing volumetric testing for 300,000 to 30,000,000 equivalent single-axle loads (ESALs) for surface mixes in Iowa.

2. Determine the compatibility of mixes under the existing mix design procedures by recalculating the gyratory slope from the QC/QA data.

3. Estimate and compare the post-construction compaction effort (PCCE) for each selected project and determine the theoretical N_{design} at construction and post-construction.

4. Evaluate the optimum asphalt contents and aggregate structures due to different N_{design} values adopted for the mixtures under three different traffic levels.

Experimental Plan

A total of 20 projects were selected within the six different Iowa Department of Transportation (DOT) districts to evaluate the post-construction compaction effort and determine if 4% target air voids were being achieved. Pavement sections constructed in 2011 for 300,000, 1,000,000, 3,000,000 and 10,000,000 ESALs, in addition to sections with varying construction and post-construction years for 30,000,000 ESALs, were selected for the study.

All testing was done in accordance with the American Association of State Highway and Transportation Officials (AASHTO) and ASTM International standards. Three sections per ESAL level were selected, and pavement cores were removed by the Iowa DOT at three different mileposts per project (excluding the 30,000,000 ESAL sections).

Pavement conditions were also evaluated based on available data using the Iowa DOT's Pavement Management Information System (PMIS) survey information and the *Distress Identification Manual for the Long-Term Pavement Performance Program* (Miller and Bellinger 2003) to determine if the selected pavement sections displayed any anomalies during post-construction.

The field densities, bulk specific gravity (G_{mb}), and theoretical maximum density (G_{mm}) of the mixes were compared to the QC/QA data to determine the density during post-construction. The field densities, in addition to the mix data, were also used to recalculate the gyratory compaction slope.

With the determination of the compaction slope, the PCCE and the theoretical N_{design} at construction and post-construction were determined for each mix. The theoretical N_{design} at construction is the theoretical number of gyrations during construction, and, similarly, the theoretical N_{design} post-construction is the theoretical amount of compaction induced by traffic volume. Additionally, this study identifies the N_{design} values adopted for laboratory-produced/laboratory-compacted mixes for low-, medium-, and high-traffic levels.

Conclusions and Recommendations

Based on the findings of the study, the following conclusions were found:

- The current N_{design} compaction levels are higher than the targeted optimal value, creating mixes that do not reach 4% air voids after traffic densification at 4 years post-construction. These findings are consistent with other research studies conducted for other state transportation agencies.

- The majority of the mixes did not achieve 96% G_{mm} (or 4% air voids) at 1, 2, 4, and 12 years post-construction (Note: Only ESAL levels below 30,000,000 were analyzed at 4 years post-construction).

- The overall pavement conditions displayed no signs of premature distresses on the pavements studied. Pavement distresses showed that the overlay construction placed in 2011 provided significant improvements in pavement performance.

- The G_{mm} from the QC/QA data can be used to determine the density of the pavement since the values of G_{mm} tested in the laboratory using field cores were close to the hotbox G_{mm} values from the QC/QA data.

- Air void analysis showed that traffic volumes at the 300,000 and 3,000,000 ESAL levels compacted better post-construction; whereas the 1,000,000, 10,000,000, and 30,000,000 ESAL levels were unable to densify to the target 4% in-situ air voids. The majority of the sections at the two highest traffic volumes were unable to reach ultimate pavement density with the current design gyrations.

- Distribution of the $\%G_{mm}$ in years 2011, 2012, and 2013 indicate that at 4 years post-construction there is a high probability that approximately 25% of the hot-mix asphalt (HMA) mixtures will not attain ultimate pavement density.

- In laboratory-produced/laboratory-compacted mixes for low-, medium-, and high-traffic levels, the optimum asphalt content of the mixtures for a high-traffic level was lowest (at 4.8% for 4% air voids), followed by the medium-traffic level (at 5.68% for 4% air voids), and the low-traffic level (at 5.8% for 3% air voids).

- As N_{design} standards are reconsidered for the Iowa DOT, close attention to the design target air voids, voids in the mineral aggregate (VMAs), and aggregate sources/types will need to be addressed.

CHAPTER 1: INTRODUCTION

Background

The use of asphalt pavements, which cover about 94% of paved roads, has gradually increased since the late 19th century(Brown et al. 2009). The mix design of asphalt pavements has undergone continual evolution since initial development, relying heavily on empirical knowledge. Past challenges with pavement distresses in asphalt concrete have shaped design considerations in mix design and analysis. In the US, Superior Performing Asphalt Pavement (Superpave) mix design is used in a majority of states.

One of the most important factors in design is the compaction effort of the asphalt mixture. The compaction effort in the laboratory is known as the number of gyrations (N) and is denoted as the initial number of gyrations ($N_{initial}$), design number of gyrations (N_{design}), and maximum number of gyrations (N_{max}) in the Superpave mix design system. N_{design} is one of the most significant design considerations/parameters in the laboratory and is selected based on the corresponding equivalent single-axle load (ESAL) levels for the proposed pavement structure. The initial Superpave values were selected based on studies that matched in-place densities to a number of gyrations conducted by the Strategic Highway Research Program (SHRP) (Prowell and Brown 2007).

Over time, many agencies and researchers have performed additional studies to validate gyratory design levels (Harmelink and Aschenbrener 2002). Previous studies concluded that the N_{design} in the Superpave mix design method is considerably higher than necessary, and, as a result, the compaction effort conducted in the laboratory may not be reasonably attained in the field due to differences in the compaction equipment, compaction procedure, and the difficultly of compacting in the field.

During construction, the pavement is compacted in multiple lifts using rollers. Post-construction compaction is expected to occur over time from traffic loading to achieve an ultimate pavement density of 4% air voids within 2 to 3 years. However, studies have shown that if the N_{design} is too high, the ultimate pavement density cannot be achieved within that timeframe. The primary reason is the difficulty of compacting in the field, which consequently results in under-compaction that can cause durability issues in the pavement. In addition, the aging of the asphalt mixture is considerably affected by the initial air voids and temperature during production (Brown et al. 2009).

Examination and modification, if needed, of the existing N_{design} table in Superpave mix design would allow agencies to tailor the laboratory mix design process so 4% air voids can be achieved from ultimate density.

While freight transportation begins to transition into more efficient and lower costs of moving goods, the ability to store additional goods is more desired. As the evolution to modern highway technology continues to grow rapidly, the industry will need to continuously improve and modify

standards/regulations to accommodate the changes in traffic volumes, environment, and the automotive industry. Validation of the existing N_{design} table in the Superpave mix design will allow agencies/researchers to better evaluate the field and laboratory pavement responses more accurately. Ensuring adequate pavement density will reduce pavement distresses and improve overall durability in the pavement.

Problem Statement

N_{design} has been used in the laboratory to compact specimens to a design ESAL level. The existing N_{design} table in the Superpave mix design method has been reported to result in under-compaction and thus lower asphalt content in the field. This may lead to difficulties in further densifying the pavement, in addition to durability issues. Validating the asphalt mixes in Iowa will provide better correlation between the target air voids and field air voids.

Objectives

The objective of this research was to validate current N_{design} levels for 300,000 to 30,000,000 ESAL level surface mix designs. Sections in Iowa from 2011 for ESAL levels below 30,000,000 were randomly selected at each ESAL level to evaluate 4 years post-construction. The 30,000,000 ESAL level sections were selected with varying post-construction years. Collection of field cores and subsequent testing provided measurements of in-place densities 1, 2, 4, and 12 years post-construction.

The second objective was to determine the compactability of mixes under the current mix design procedures by using the gyratory slope from quality control and quality assurance (QC/QA) data. The post-construction compaction effort (PCCE) was evaluated as well as the optimum asphalt content and aggregate structures with different N_{design} levels for laboratory-produced/laboratory-compacted mixes for low, medium, and high traffic, and adjustments as needed were recommended.

The third objective was to provide N_{design} recommendations for the laboratory designs used in gyratory mix designs to the Iowa Department of Transportation (DOT), based on the findings of this study.

Methods and Approach

The overall study focused primarily on the laboratory compaction effort or $N_{design.}$ Testing was done in accordance with the American Association of State Highway and Transportation Officials (AASHTO) and ASTM International methods and procedures. The field cores used for the study were provided by the Iowa DOT. The selected sections for the study were randomly chosen throughout Iowa in the six Iowa DOT districts and varied in traffic volume. Pavement condition surveys were also evaluated based on available data using the Pavement Management Information System (PMIS) and the Long Term Pavement Performance Program (LTPP) manual surveys.

Determination of air voids, both pre- and post-construction, were compared to QC/QA data and analyzed accordingly. In addition, the gyratory slope and PCCE were evaluated for each project.

The research focused primarily on validating the effectiveness of the existing laboratory compaction effort in Iowa; the theory or assumption of over-compaction in the laboratory leading to under-compaction in the field has be examined in this study. Additionally, evaluation of the optimum asphalt content from laboratory-produced/laboratory-compacted mixes for low, medium, and high traffic were identified. The experimental plan is described in detail in Chapter 3.

Significance of Work

The study has provided a better understanding of the overall effect of the existing N_{design} used in Iowa. The outcome of the project will determine whether or not the N_{design} for Iowa should be changed. The data collected will be used to provide a new N_{design} recommendation that will influence asphalt mix designs and will be proposed for implementation upon laboratory performance testing validation.

Organization

The following report is divided into five chapters. Chapter 1 provides the background to the importance of the compaction effort in hot-mix asphalt (HMA), a problem statement, objectives, methods and approach, and significance of work. Chapter 2 is the literature review, which presents the previous studies conducted on the importance of lab and field compaction focused on validating N_{design}. Chapter 3 provides details on the experimental plan and testing methods used in this study. Chapter 4 presents the overall results and analyses. Chapter 5 summarizes the conclusions and recommendations and provides ideas for future research in regards to identifying an optimum N_{design} for Iowa and validating the performance of recommendations.

CHAPTER 2: LITERATURE REVIEW

History of Asphalt Mix Design

Early asphalt mixtures were primarily based on empirical design analysis (i.e., selecting optimum asphalt content). Industries and agencies relied heavily on precedent experience to evaluate and determine the appropriate mix type for selected sections at different locations with varying temperatures. A good or bad mix would be differentiated based on the pavement performance of the existing pavement structure, and the mechanics of the asphalt material was not taken into consideration.

The use of HMA concrete significantly increased throughout the years, and the need for standardized testing was essential to the design process (Christensen and Bonaquist 2005). Over time, the use of empirical design was insufficient due to factors/variables varying significantly with time. In the 1920s, the most popular early asphalt mix design method was the Hubbard-Field mix design (Brown et al. 2009). The Hubbard-Field method later influenced the Marshall and Hveem methods from the 1940s through the 1960s. In 1987, the Strategic Highway Research Program (SHRP) began developing the Superpave mix design system, and, by 2008, most states, including Iowa, adopted this mix design method (Prowell and Brown 2007).

The importance of simulating field compaction in the laboratory became one of the primary concerns for the industry during the early implementation of mix design methods. Hveem developed the Hveem mix design method in the mid-1920s for the California DOT (Caltrans, as it's known today), and the method was primarily used by western states (Brown et al. 2009). The method was developed to improve pavement performance with the use of "oil mix" (a combination of asphalt oil and aggregate) for low-traffic volume highways in California (Brown et al. 2009). Hveem concluded that fine mixes required higher optimum asphalt content due to their larger surface area as well as the appropriate amount of asphalt content from the particle size distribution or gradation (Prowell and Brown 2007). The gradation in HMA is one of the most effective means in determining the effectiveness of the performance of aggregate materials as a pavement structure. Gradation is determined by passing aggregate materials through a series of stacked sieves, which is known as sieve analysis (Brown et al. 2009). Figure 1 shows an example of gradation curves used in HMA design.

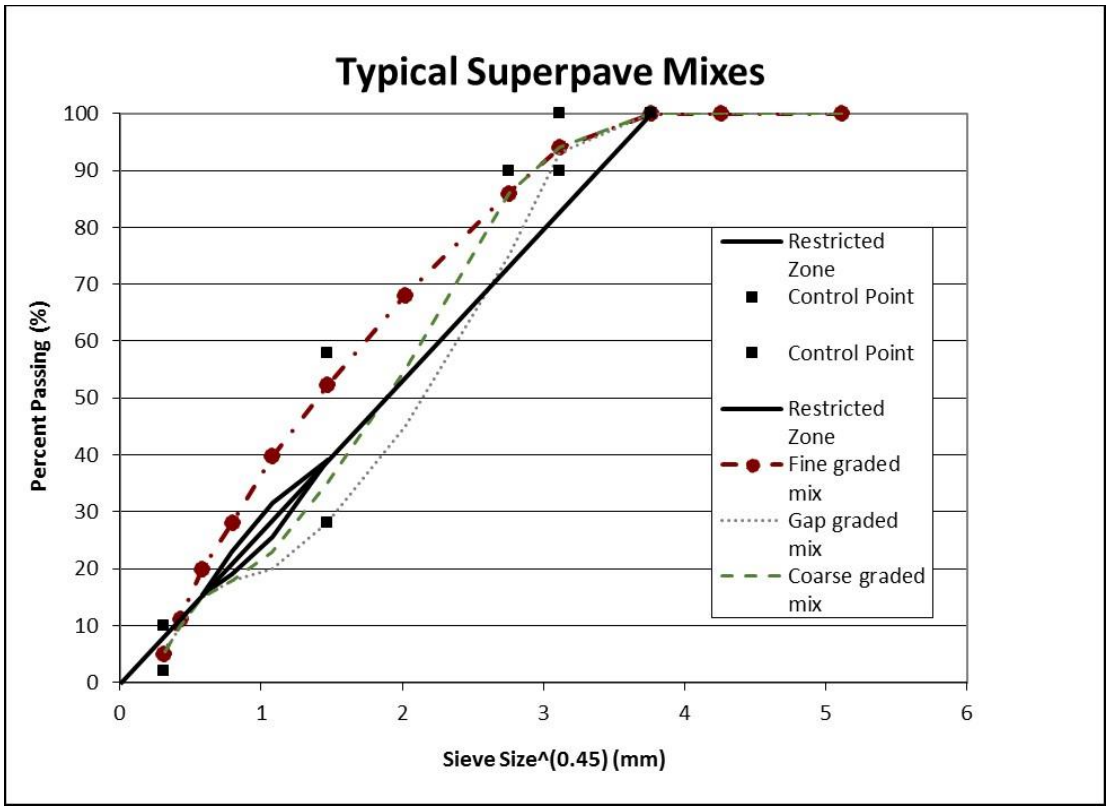

Figure 1. Gradation curves used in typical Superpave mixes

Previous studies show that using more asphalt content on the aggregate particle thickens the film and improves pavement durability (Hmoud 2011). The strength (or stability) of the mix was tested using the Hveem stabilometer, and the kneading compaction was used to simulate field compaction in the laboratory.

Because other states were unable to use the Hveem mix design method, in the late 1930s, the Marshall method, introduced by Bruce Marshall, was implemented. The Marshall method focused widely on the compaction effort of HMA and emphasized greatly on air voids.

In the early 1990s, with the limitations of the early mix design methods, SHRP developed the Superpave mix design method (Brown et al. 2009). The Superpave mix design method primarily focused on limiting/controlling detrimental pavement distresses. In order to do so, the mix design takes into account the changes in environmental conditions, traffic load, and axle configurations. Additionally, Superpave evaluates the asphalt binder, aggregate properties/characteristics, mixture analysis, and the material and volumetric properties (of compacted samples) in the HMA. These volumetrics were primarily used to determine the optimum asphalt content in the mixture. The compaction device used to compact laboratory specimens is known as the Superpave gyratory compactor (SGC), a compaction device similar to the original Texas gyratory. The gyrations were heavily dependent on the traffic levels and were generally expressed as 18,000 lbs ESAL. SHRP initially compacted samples at an angle of 1.0° but later changed the internal angle of gyration to 1.16° (external angle 1.25°), with a constant vertical

pressure of 600 kilopascal (kPa) (Prowell and Brown 2007). Based on the National Cooperative Highway Research Program (NCHRP) Project 9-9(1), Refinement of the Superpave Gyratory Compaction Procedure, different levels of compaction effort were recommended for Superpave and were denoted as $N_{initial}$, N_{design}, and N_{max}, as shown in Table 1 (Prowell and Brown 2007).

Table 1. NCHRP compaction parameters

Design ESALs (millions)	Compaction Parameter		
	$N_{initial}$	N_{design}	$N_{maximum}$
< 0.3	6	50	75
0.3 to < 3	7	75	115
3 to < 30	8	100	160
> 30	9	125	205

Source: FHWA 2001

Because Superpave was designed only to test for asphalt binder and volumetric properties of a mixture, agencies were hesitant to rely only on this, and as a result many researchers began using supplemental tests such as the Hamburg Wheel-Tracking Device and the Asphalt Pavement Analyzer (Brown et al. 2009). Inconsistent results were also observed between the density of samples compacted at N_{design} and the density backcalculated from the N_{max}. As a result, the original N_{design} table was consolidated by creating an experimental matrix with 4 aggregate sources, 2 gradations, and 6 N_{design} levels (40, 68, 93, 113, 139, and 172). As N_{design} was increased, the optimum asphalt content, voids in the mineral aggregate (VMA), and voids filled with asphalt (VFA) decreased with coarse-graded mixes being more sensitive than fine-graded mixes.

Comparison of the Mix Design Methods

While the Hveem method is excellent in simulating field densities, this method is only developed primarily for the western part of the US and is generally not recommended for use outside of that region. In addition, the kneading compaction device is expensive and not portable and thus not widely implemented. Alternatively, the Marshall mix design method uses an inexpensive and simple compaction device. Both methods focused on the voids, strength, and durability of the mix (NAPA 2015). Today, the Superpave mix design method is the most widely used method in hot-mix asphalt design and analysis. In terms of compaction methods, the primary difference between Superpave and the Marshall and Hveem methods is the ability of the SGC device to monitor the change in height during the compaction process. The use of the gyratory compactor lowered the VMA and optimum asphalt contents compared to the Marshall system. See Figure 2 and Figure 3for compaction devices.

FHWA (left and center) and ISU (right)

Figure 2. HMA compaction device with California kneading compactor (left), Marshall hammer (center), and Superpave Gyratory Compactor (right)

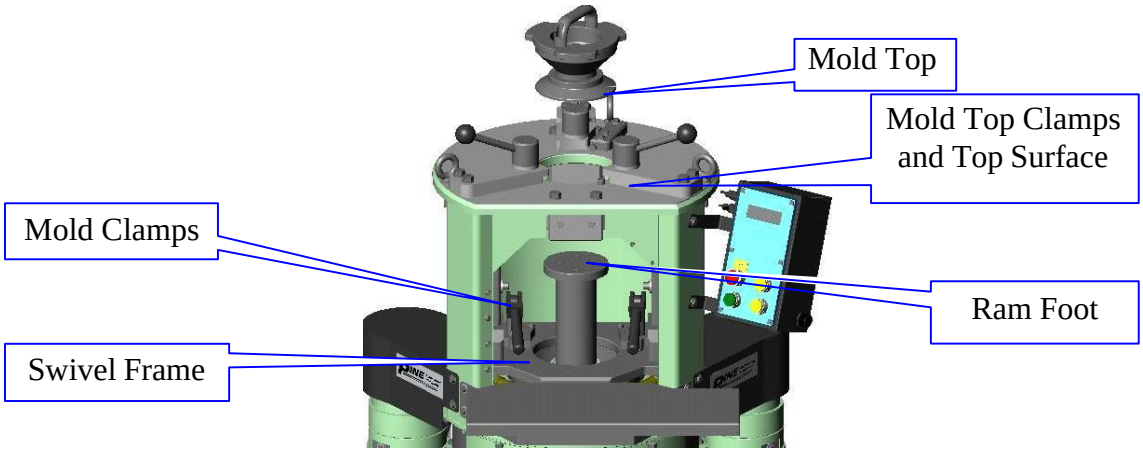

Figure 3. AFG2 Superpave Gyratory Compactor

While it is relatively simple to conclude that the evolution of mix design has led to improved design practices, the validation of the gyratory levels, mainly the N_{design} table, still requires further evaluation in terms of its' effectiveness of compaction effort in the field.

Superpave N_{design}

The Significance of Ndesign

N_{design} is the design number of gyrations or compaction effort used in Superpave HMA. The designated N_{design}, or the number of design gyrations for the gyratory compactor, is used to simulate the calculated ESAL for a project. To simulate field compaction in the laboratory, SHRP conducted numerous studies and extracted core samples from randomly selected sections. This allowed SHRP researchers to match in-place densities to a number of gyrations, and, as a result, generated the N_{design} table (Prowell and Brown 2007). The optimum N_{design} was developed with two factors: the improvement in pavement life associated with improved fatigue life and rutting resistance and the economic benefits from the reduced use of asphalt binder (Qarouach

2013). The ultimate purpose of conducting a laboratory test is to produce small-scale specimens and test for material characterization and volumetric properties and predict the pavement performance/distresses of HMA. This allows researchers to produce the most cost-effective solution for owner/agencies while conducting a large-scale pavement test to further evaluate/validate the pavement performance tested in the laboratory. Standardized tests state that test specimens are compacted to a target air void of 4% or 96% theoretical maximum density (G_{mm}) using the design number of gyrations corresponding to the appropriate traffic level. The G_{mm} of a mixture is the specific gravity of the HMA, excluding air voids (Brown et al. 2009). In the field, asphalt concrete is initially targeted to be compacted to 7% air voids, and traffic loading over time further densifies the pavement to its 4% target air voids (Peterson et al. 2003).

NCHRP Project 9-9(1) concluded that the ultimate pavement density was achieved 2 to 3 years post-construction. However, other studies monitored ultimate pavement densities to occur over a more extended period of time. The laboratory mix designs with a high level of SGC compaction effort have led to field mixtures that are difficult to place and compact to 7% air voids in the field. This lack in attaining the target field voids during construction results in the pavement not densifying further and never reaching the 4% target air voids. The relationship between the laboratory compaction effort and the field compaction does not provide a strong correlation. The levels of gyration is critical in design because over-compaction in the laboratory design can lead to higher air voids in the field due to under-compaction during the compaction process, which can consequently lead to durability issues in the pavement (Huang 2003). Similarly, under-compaction in the field will cause a higher ultimate pavement density, which can lead to bleeding or rutting (Huang 2003). A desirable, stiff asphalt mixture consists of a good aggregate skeleton and/or a low asphalt content that generally compacts to 4% air voids after the pavement has been densified by traffic; whereas a weak asphalt mixture with the same compaction effort over-compacts to 2% air voids (Anderson et al. 2002).

N_{design} is important in the determination of the optimum asphalt content as well as approximating the ultimate pavement density in the field. The optimum asphalt content is critical in design because mixes that have excessive asphalt will undergo permanent deformation, while too little asphalt causes difficulty in field compaction, which often leads to early fatigue cracking (VMA will subsequently be affected). Generally, achieving target pavement density and excellent construction quality are essential in producing a durable and long lasting pavement structure.

Disadvantages/Issues

The optimum binder content is one of the most important design parameters in HMA design. Several agencies claim that under the Superpave method, the asphalt binder content is reported to be too low and thus has been known to cause durability issues in the pavement (Maupin 2003). Additionally, other agencies believe the existing N_{design} values were higher than required and consequently pavements were unable to achieve ultimate pavement density within 2 to 3 years post-construction (Hornbeck 2008). As a result, many states have conducted local studies to verify/validate the N_{design} values in the Superpave method.

Validation of N_{design}

NCHRP Report 573

The National Center for Asphalt Technology at Auburn University was awarded NCHRP Project 9-9(1) ; the final report is entitled NCHRP Report 573: *Superpave Mix Design: Verifying Gyration Levels in the N_{design} Table* (Prowell and Brown 2007). The primary goal of the project was to validate the current design gyration levels in the AASHTO Standard Practice R 35 (AASHTO 2015a) for 4 consecutive 20 year design traffic levels at the following traffic volumes: less than 300,000, 1,000,000 to 3,000,000, 3,000,000 to 30,000,000, and greater than 30,000,000 ESALs) while monitoring field performance (Prowell and Brown 2007).

The research team studied 40 field projects in 16 states with different traffic volume levels, aggregate and gradation types, and asphalt binder performance grades (see Figure 4 for locations).

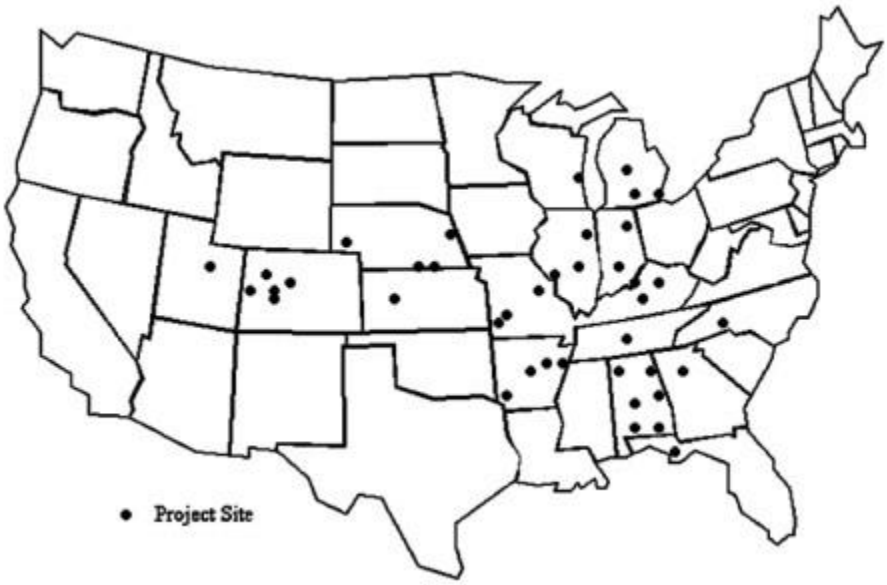

Prowell and Brown 2007 © 2007 Transportation Research Board

Figure 4. Locations of NCHRP Project 9-9(1) field studies

One out of 40 projects used a compaction effort of 50 gyrations, 12 projects used 75 (68-86), 18 projects used 100 (90-109), and 9 projects used 125 gyrations. In addition, 11 projects, 26 projects, and 3 projects used a nominal maximum aggregate size (NMAS) of 9.5 mm, 12.5 mm, and 19.0 mm, respectively. For each project location, prior to construction, loose mix was sampled at the asphalt plant and 3 specimens were replicated and compacted to 100 and 160 gyrations; a total of about 26 to 36 specimens per project were compacted.

Researchers extracted 3 cores along the right of the wheel path shortly after construction, 3 months, 6 months, 1 year, 2 years, and 4 years post-construction. Each project was monitored

until the ultimate in-place density was achieved. The ultimate in-place density would then be matched with the N_{design} used in the initial mix design. The recorded average in-place density for the 40 projects was 91.6% G_{mm}, where 55% of the projects showed densities below 92% G_{mm} and 78% displayed densities less than 93% G_{mm} (Prowell and Brown 2007). Based on the results, about 63% of the pavement densification occurred in the first 3 months after construction. The densification showed little to no difference between 3 months and 6 months after construction. This occurred because projects completed in the summer would experience cooler temperature in the following months after construction, thus the change in densification from 3 months to after 6 months were insignificant. At 50% frequency, the percent G_{mm} between 6 months and 1 year increased by 0.8% (93.6 to 94.4% G_{mm}) and showed a slight increase of 0.2% between 1 year and 2 years. The project extended to monitor after 4 years post-construction to ensure pavement reached ultimate in-place density. The recorded average in-place density for the 40 projects after 2 and 4 years was 94.6% G_{mm}.

To verify, a test comparing the 2 year and 4 year in-place densities was conducted, where the null hypothesis tested that the average 2 year density was identical to the average 4 year density. The test concluded that there was no statistically significant difference in the 2 year and 4 year in-place densities. Thus, it is evident to conclude that pavement densification occurs after 2 years. However, numerous factors may contribute to pavement densification, such as the performance binder grade, weather conditions, high oxidation, etc. Researchers conducted 4 different analyses to match the ultimate in-place density to the N_{design}. The following analyses were conducted: (1) regression of the predicted N_{design} and traffic volume after 2 years, (2) regression between ESAL levels at different time intervals and the predicted gyration matching in-place density at the corresponding time intervals, (3) models, and (4) ultimate in-place density related to N_{design}. Additionally, researchers attempted to use the concept of the locking point developed by the Illinois DOT (IDOT) (Prowell and Brown 2007).

Gyratory Locking Point (LP)

The LP concept is considered an alternative to N_{design} and is created to prevent over-compaction and aggregate deterioration. It is assumed that during the compaction process, the aggregates in the mixture are damaged as the rollers continue to compact to its construction design air voids. The concept was developed to prevent damage in the aggregates and instead provide good aggregate interlock. Out of the 4 different LPs tested, only 3-2-2 showed the best relationship to the 2 year in-place densities, but the results were weaker compared to the design traffic (see Figure 5) (Prowell and Brown 2007). As a result, this approach was no longer evaluated based on these findings.

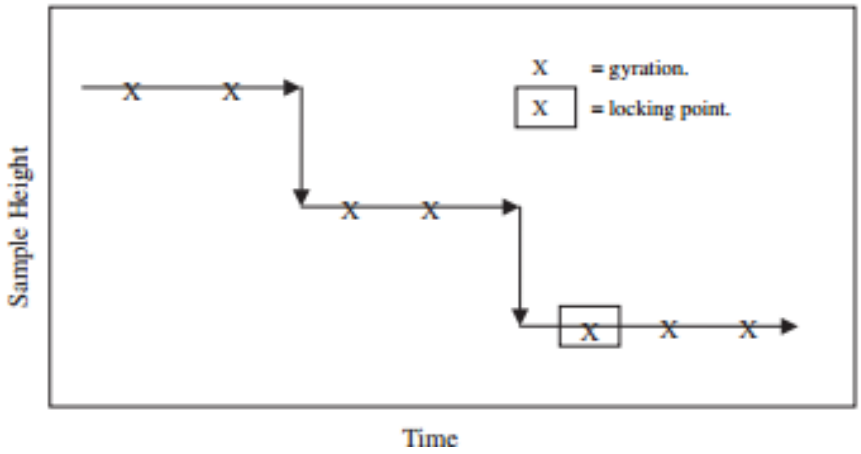

Prowell and Brown 2007 © 2007 Transportation Research Board

Figure 5. Illinois 3-2-2 locking point

$N_{initial}$ and N_{max}

Initially, Superpave produced three levels of gyrations for each traffic level: $N_{initial}$, $N_{design,}$ and N_{max}. The air voids were measured based on these three levels to determine the quality of the mixture (Brown et al. 2009). The specification states that air voids should meet a minimum value at $N_{initial}$, 11% air voids at $N_{design,}$ and 2% air voids at N_{max}. The use of $N_{initial}$ in design is to guarantee that the HMA mixture is not too soft or tender during the compaction process and to ensure rutting resistance (Anderson et al. 2003). Similarly, N_{max} is used in design to validate rutting resistance. The $N_{initial}$ and N_{max} for the 40 projects were also evaluated. It was recorded that 11 out of 40 projects had at least one sample that failed $N_{initial}$ and 25 of 40 projects had at least one sample that failed N_{max}. The research team concluded, based on the results obtained from this study, that the current N_{design} levels used in AASHTO R 35 (AASHTO 2015a) were significantly higher than the ultimate pavement density, primarily at ESAL levels greater than 300,000. Figure 6 displays the general concept of N_{design}.

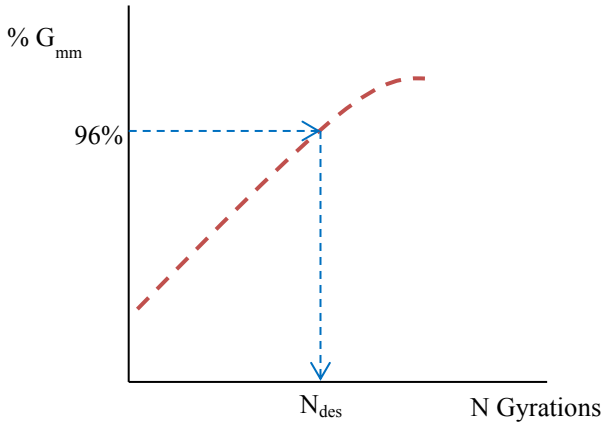

Figure 6. Concept of N_{design}

NCHRP Recommendations

The research team presented the following recommendations: (1) reduction of the existing N_{design} table primarily for mixes designed with modified asphalt binder with a performance grade of PG76-XX or greater, (2) removal of $N_{initial}$ and N_{max} in the existing N_{design} table, (3) specification for the angle of gyration revised to a dynamic internal angle (DIA) of 1.16°± 2°, and (4) an option to consider the N_{design} at the 2 year design traffic volume. Table 2 summarizes the final recommendation as a result of validating the N_{design} for NCHRP Project 9-9(1) (Prowell and Brown 2007).

Table 2. NCHRP recommended N_{design} levels for a SGC DIA of 1.16° ± 2

20 year Design Traffic, ESALs	**2 year Design Traffic, ESALs**	**N_{design} for Binders < PG 76-XX**	**N_{design} for binder ≥ PG 76-XX or mixes placed > 100 mm from surface**
< 300,000	< 30,000	50	NA
300,000 to 3,000,000	30,000 to 230,000	65	50
3,000,000 to 10,000,000	230,000 to 925,000	80	65
10,000,000 to 30,000,000	925,000 to 2,500,000	80	65
> 30,000,000	> 2,500,00	100	80

Source: Prowell and Brown 2007

Reduction of N_{design} in other States

It was evident, based on pavement surveys collected, that Superpave mixes performed significantly well against rutting due to lower binder contents used. However, researchers observed that many pavements experienced early fatigue cracking (Aguiar-Moya et al. 2001). Fatigue or alligator cracking is a form of pavement distress generally caused by fatigue failure on the HMA surface under repeated loading (Brown et al. 2009). Fatigue cracking can be due to an increase in loading; inadequate compaction and structural design; stripping; and possible loss of supporting base, subbase, and/or subgrade layers (Brown et al. 2009). Additionally, NCHRP Report 573 concluded that mixes with higher gyration levels provided better rut resistance but may lack sufficient durability (Prowell and Brown 2007). As a result, many states conducted various tests to verify the existing design number of gyrations and evaluated the effect on pavement performance. Such states include Colorado, Georgia, Virginia, Ohio, and others. The primary focus of each study was to validate the in-place design number of gyrations of HMA in each state over a span of 5 to 6 years, depending on the project specification.

The Colorado DOT (CDOT) found that none of the pavements randomly selected reached the design air voids after 6 years. The average in-place field voids for years 3, 4, 5, and 6 years displayed a difference of 1.2% air voids at Superpave N_{design} between the line of equality at 4% air voids, see Figure 7 for a visual interpretation (Harmelink and Aschenbrener 2002).

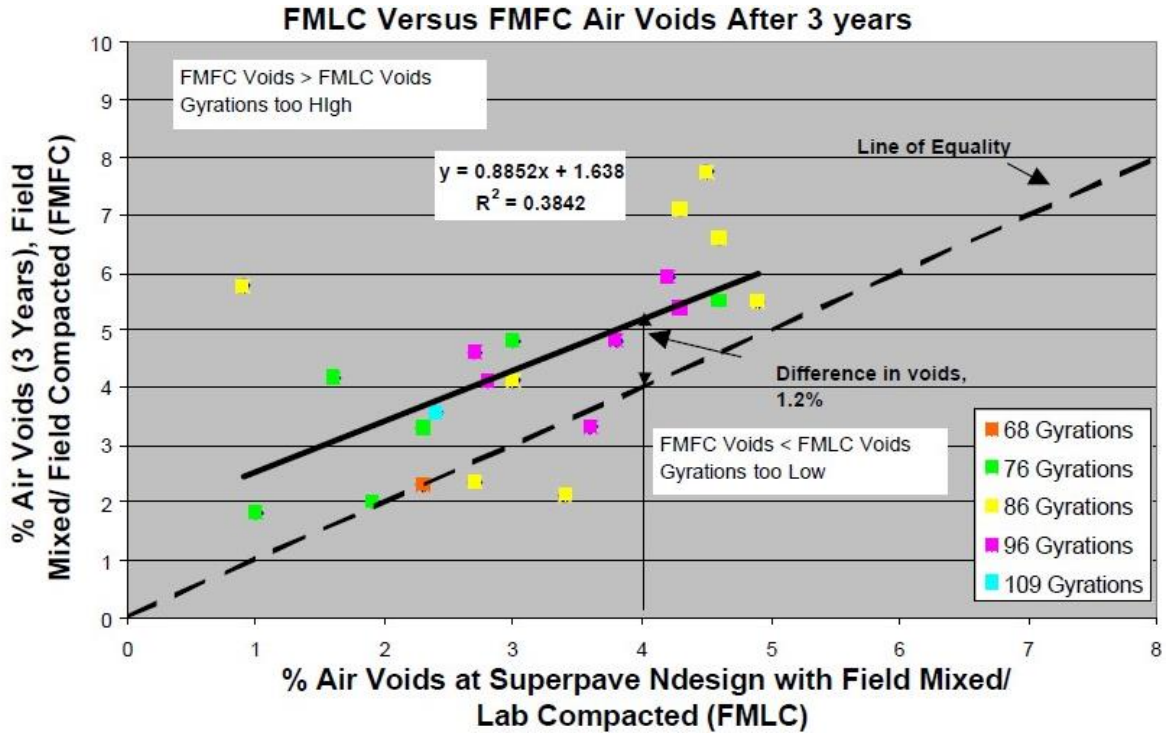

Harmelink and Aschenbrener 2002

Figure 7. Field-mix/laboratory-compacted (FMLC) versus field-mixed/field-compacted (FMFC) air voids after 3 years

In this case, the line of equality is used for comparing the percent air voids at Superpave N_{design} with the percent air voids at a specific year. In Figure 7, the average in-place field voids at 3 years show that there is a difference of 1.2% air voids between the 2 parameters. The results indicate that the field air voids are under-compacted, and thus the current design number of gyrations being used is too high. CDOT determined that a reduction of 30 gyrations is required in order to match the in-place ultimate pavement densities. However, such a reduction was not desired for CDOT. The pavement performance was also evaluated throughout the study; low to moderate rutting was detected but no major distresses were observed. The final recommendations by CDOT concluded 75 gyrations were to be used for lower traffic levels and 100 gyrations for higher traffic levels. The Georgia DOT (GDOT) found the average in-place air voids after 5 years was 5.7%. GDOT concluded that 66 gyrations matched the in-place densities in Georgia and thus selected a design number of gyration of 65 for Superpave mixes (performance grade should be adjusted according to the traffic level) (Watson et al. 2008). The Ohio DOT (ODOT) specified the design number of gyrations to about 65, based on the annual average daily traffic (AADT) (ODOT 2013). In Virginia, the Virginia DOT's (VDOT's) primary concern was slightly different than simply verifying N_{design} levels (Maupin 2003). VDOT's concern was that the existing Superpave mixes do not have sufficient asphalt content, thus reducing the pavement life and serviceability (Huang 2003). The primary goal was to provide better pavement serviceability while controlling rutting or bleeding in the pavements in Virginia. Virginia has lowered the number of gyrations since using the Superpave mix design method in order to accommodate for the low asphalt content. The lower gyration levels required an increase

in asphalt content and, as a result, increased the overall durability of the pavement (Maupin 2003).

Effects on Pavement Performance

To design an adequate flexible pavement structure, the three principle pavement distresses considered in design are fatigue cracking, rutting, and low temperature cracking. Each are examined further below in regard to the effects on gyration level.

Rutting

Rutting occurs due to an accumulation of permanent deformation along the wheel paths caused by excessive traffic loading (rut depth) and/or high temperature and, as a result, causes compressive strain at the top of each layer (see Figure 8).

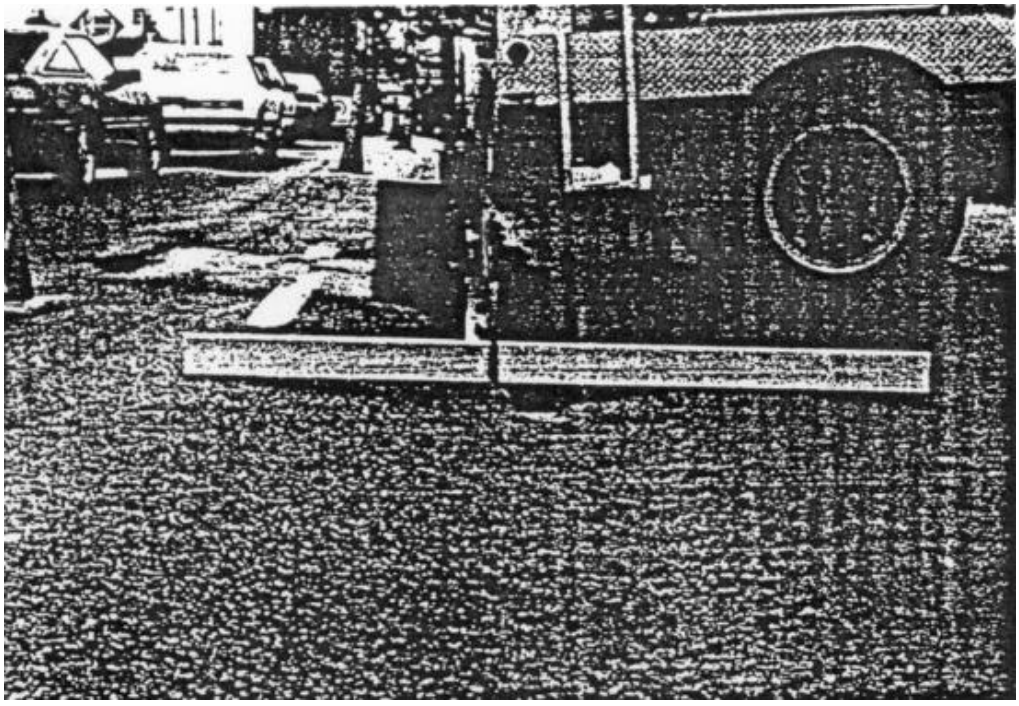

Brown and Cross 1989 Association of Asphalt Paving Technologists (AAPT)

Figure 8. Severe rutting in flexible pavement

Rutting can also occur due to inadequate compaction during construction (Brown et al. 2009). The severity level can be detected by following the *Distress Identification Manual for the Long-Term Pavement Performance Program* (Miller and Bellinger 2003). High-severity rutting, if left untreated, can lead to hydroplaning caused by the build-up of water in ruts and to more concentrated loading, which results in less wheel water and an increase in structural failures (Huang 2003). Additionally, excessive rutting can cause serviceability issues, because the ride quality becomes inadequate for travelers (Brown et al. 2009). About 32% of rutting occurs in the

surface layer and 14% and 45% in the base and subbase, respectively (Huang 2003). Generally, with the existing N_{design} used in Superpave, rutting resistance has not been reported to cause major inadequacies to the pavement structure. Thus, reducing the N_{design} value can negatively affect the rutting resistance and consequently increase permanent deformation in the structure due to higher asphalt content (Anderson et al. 2003).

The most common problem with conducting pavement performance testing is the cost of the test devices. NCHRP Report 478 conducted a study to determine the relationship of SGC properties to HMA rutting behavior (Anderson et al. 2002). It has been believed that there is a relationship between the compaction slope of the SGC and the rutting behavior of HMA. Based on a previous study involving Watsonville Granite, the results showed that for higher compaction slope mixtures the shear stiffness was higher but the permanent shear strain was lower (Anderson et al. 2002). According to NCHRP Report 478, "the main problem in relating compaction slope to mixture performance properties is that the compaction slope, unlike mixture performance, is not sensitive to asphalt binder content" (Anderson et al. 2002). Researchers involved in the study developed a compaction parameter to correlate the SGC to the rutting performance of an asphalt mixture. However, further research is needed to validate the compaction parameter determined in this study. Meanwhile, tests such as the Hamburg Wheel-Tracking Device and the Asphalt Pavement Analyzer may be used to test for rutting resistance (Prowell and Brown 2007).

Fatigue Cracking

Fatigue cracking in flexible pavements causes horizontal tensile strain at the bottom of the asphalt or base layer under repeated traffic loading (see Figure 9 (left)).

Pavement Interactive 2009a Copyright ©2012 Pavia Systems, Inc. (left) and ©2003 Steve Muench (right)

Figure 9. Fatigue cracking (left) and pothole caused by fatigue cracking (right)

The small cracks typically start at the bottom of the asphalt or base layer and propagate to the surface layer resulting in a series of interconnecting cracks caused by fatigue failure (Huang 2003). There are many factors that contribute to fatigue cracking, such as improper design and/or construction, pavement material characteristics, weak subgrade soil, traffic loading, and moisture due to poor drainage and temperature. While too much binder causes bleeding in pavements, too

little can cause fatigue cracking, because the pavement is unable to flex or bend to accommodate traffic load and/or temperature changes (Huang 2003).

If left untreated, excessive fatigue cracking will result in loose surface materials that will ultimately lead to potholes, as shown in Figure 9 (right).

Pavement rehabilitation is required in order to restore pavement conditions and increase serviceability. However, the underlying pavement layers, in addition to the traffic loads, must be evaluated and considered in design prior to the rehabilitation process, because weak layers do not provide sufficient support to accommodate or withstand traffic loads (Brown et al. 2009). Previous studies have shown that mix design using Superpave showed early signs of fatigue cracking. In order to reduce the fatigue cracking, different agencies suggested adding enough binder to reduce/delay cracking.

Thermal Cracking

Thermal cracking occurs due to the ultimate tensile strength being exceeded at low temperatures, either in a single low-temperature drop or through low-temperature thermal cycling (see Figure 10).

Pavement Interactive 2009b Copyright ©2012 Pavia Systems, Inc.

Figure 10. Block cracking, type of thermal cracking

Thus, there are two types of distresses under this category: low-temperature cracking and thermal fatigue cracking. Low-temperature cracking occurs primarily in the northern part of the US, where temperatures drop below -10°F, whereas thermal fatigue cracking occurs in locations with moderate temperatures where the asphalt becomes too oxidized (Huang 2003).

To reduce/delay thermal cracking, the proper asphalt binder type used for locations with low temperatures should be used. Additionally, the asphalt binder should not be overheated during construction, because the binder oxidizes and stiffens. Hornbeck suggested that increasing the film thickness may also assist in preventing thermal cracking (Hornbeck 2008).

Relative Performance

If a lower gyration level is used, the fatigue resistance increases whereas the rutting resistance decreases. Relative performance for fatigue and rutting can be determined using Equations 1 and 2 (Cominsky et al. 1994).

$$RP_{fatigue} = \frac{P_{N_{design=i}}}{P_{N_{design=50}}} \quad (1)$$

$$RP_{rutting} = \frac{P_{N_{design=i}}}{P_{N_{design=125}}} \quad (2)$$

The relative performance for fatigue is a proportion between the fatigue resistance of the compacted sample at N_{design} and the sample compacted at 50 gyrations. The 50 gyration level was selected because tested mixes with 50 gyrations showed to have the highest fatigue resistance. The relative performance equation for rutting is similar to the equation for fatigue resistance, but with the rutting being compared to 125 gyrations since it has been shown to produce the most rutting resistant samples.

CHAPTER 3: EXPERIMENTAL PLAN AND TESTING METHOD

Introduction and Overview

This study evaluated the concerns with the use of the nationally recommended N_{design} levels in Iowa and identified the problematic ESAL levels. The outcome of the study determined how the current N_{design} levels affect the overall pavement density.

This research focused primarily on field sections. The evaluation of existing pavement conditions was closely examined using the PMIS surveys and the *Distress Identification Manual for the Long-Term Pavement Performance Program* (Miller and Bellinger 2003). Identified field pavements throughout Iowa were randomly selected with the assistance of the Iowa DOT.

Based on the availability of pavement condition data, eight projects were selected to evaluate existing pavement conditions. Field density measurements were collected and compared to QC/QA data to ensure quality in design and construction. Additionally, the gyratory slope and the PCCE were calculated and evaluated in this study. The hypothesis of over-compaction in the laboratory leading to under-compaction in the field was validated. An additional study will be conducted to determine optimum asphalt content in the laboratory for varying traffic levels. Figure 11 summarizes the experimental plan for the project.

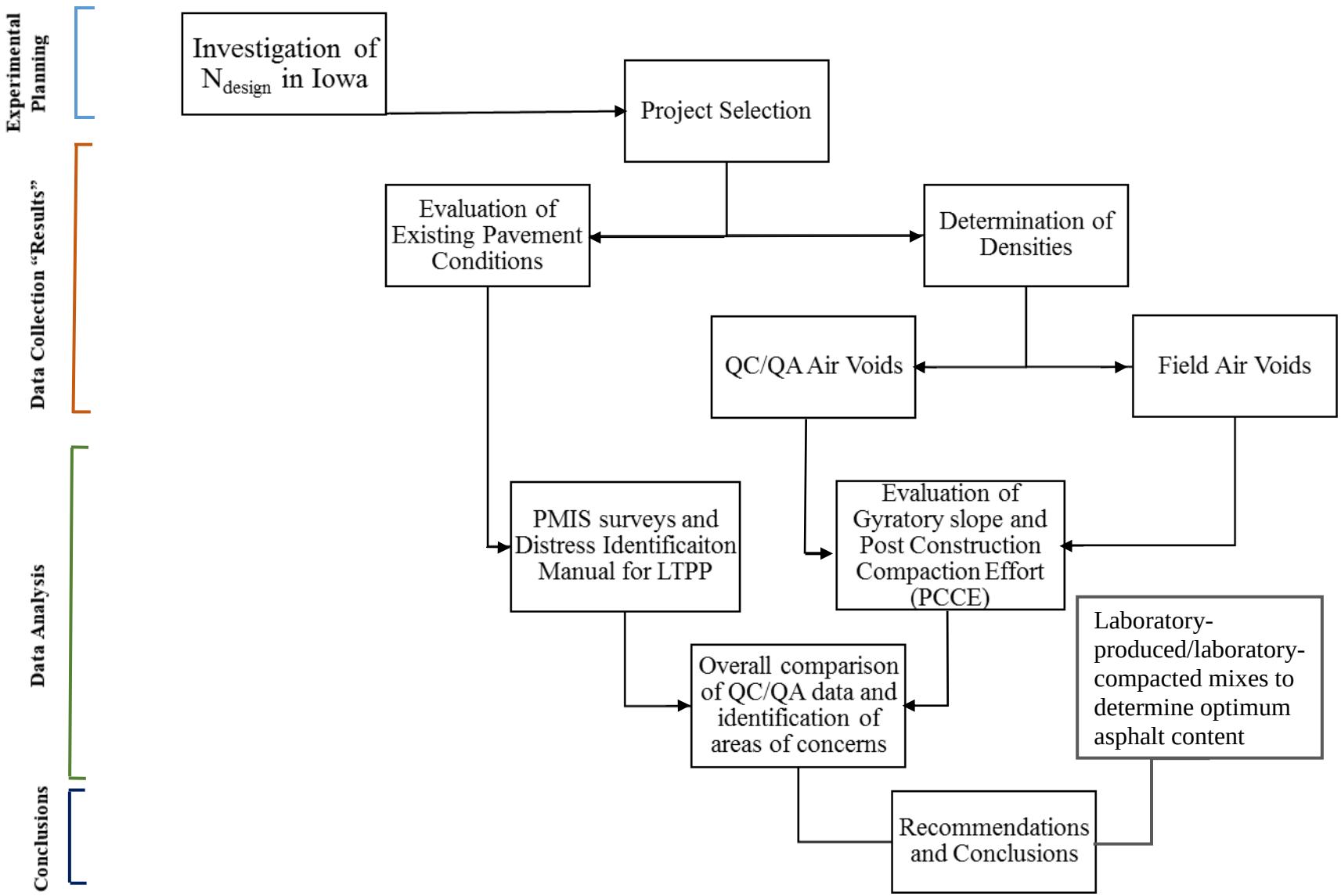

Figure 11. Flowchart of experimental plan for the study

Project Selection

Three asphalt pavement projects for each ESAL category below 30,000,000 ESALs from the 2011 construction season and eight projects for 30,000,000 ESALs were randomly selected throughout Iowa to evaluate the design number of gyrations and to validate whether or not ultimate pavement density was achieved. Projects selected varied in traffic levels ranging from 300,000 to 30,000,000 ESALs, as well as the N_{design}. The project details, such as the AADT, are shown in Table 3, and locations for each project are displayed in Figure 12. Additional project information is located in Appendix A.

Table 3. Project details

Project No.	Project Location (County and Highway)	Milepost	AADT	ESAL Level	N_{des}
1	Boone E-26	0.59	690	300,000	68
		0.77	690		
		1.26	690		
2	Emmet A-34	0.46	320		
		1.16	320		
		1.64	730		
3	Story E-29	0.18	560		
		0.4	560		
		1.91	560		
4	Clinton IA 136	4.5	1230	1,000,000	76
		5.9	1230		
		13.6	2110		
5	Guthrie IA 25 MI	78.1	1100		
		80.31	1100		
		83.05	1100		
6	Tama E-43	1.43	740		
		5.42	740		
		7	740		
7	Polk IA 17	7.99	980	3,000,000	86
		9.83	980		
		11.84	980		
8	Polk IA 160	0.16	21600		
		0.28	21600		
		0.51	21600		
9	Lyon IA 9	1.73	3290		
		1.74	3290		
		3.66	3290		
10	Linn US 151	31.42	7300	10,000,000	96
		32.93	7300		
		33.03	7300		

Project No.	Project Location (County and Highway)	Milepost	AADT	ESAL Level	N_{des}
11	Jefferson US 34	204.38	5200		
		216.97	5200		
		217.78	5200		
12	Hamilton US 20	136.22	8200		
		136.38	8200		
		137.07	8200		
13	Pottawattamie I-29 NB	I-29 NB 70.0 mp	19500		
		I-29 NB 69.10 mp	19500		
		I-29 NB 68.0 mp	19500		
14	Warren I-35	Warren I-35 NB 59.50	21100		
		I-35 NB 57.75 Warren	21100		
		I-35 NB 58.3 Warren	21100		
15	Fremont I-29 NB	I-29 NB 5.0 mp	12000		
		I-29 NB 3.0	12000		
		I-29 NB 4.0	12000		
16	Story I-35	Story I-35 NB 123.90	25800		
		Story I-35 NB 123.85	25800		
		I-35 NB 122.50 Story	25800		
17	Iowa I-80	I-80 EB between 210.20 and 210.25	26300		
		I-80 EB 211.30	26300		
18	Pottawattamie I-680	I-680 WB 2.10	6000		
		I-680 EB 2.0 mp	6000		
		I-680 WB 1.75	6000		
19	Johnson I-80 EB/WB	I-80 WB 234.10	31300		
		I-80 Wb 235.80	31300		
20	Johnson I-380	I-380 North 3.50	51700		
		I-380 North 2.40	51700		

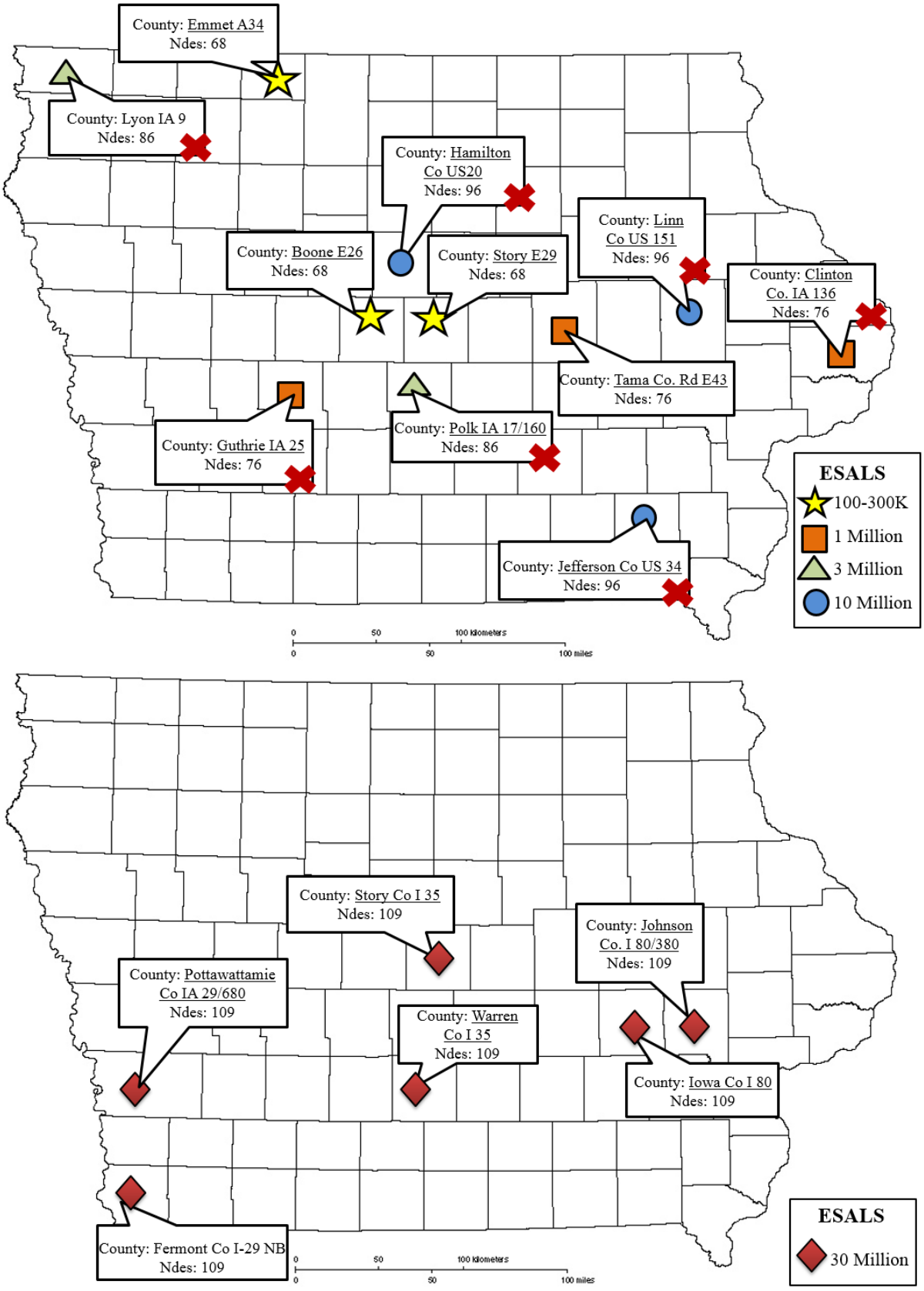

Figure 12. Identification of field sections in Iowa, specific project locations in Iowa

Three projects per ESAL level below 30,000,000 and eight projects for 30,000,000 ESALs were selected, and three specified milepost locations were randomly chosen for field coring/testing within the projects. The Iowa DOT assisted in the removal of three 4 in. field cores along the wheel path at each milepost, 4 years post-construction for 300,000 to 10,000,000 ESALs. For 30,000,000 ESALs, the cores extracted were 8 in. in diameter. Only the surface mixes were used to evaluate densification due to traffic loads.

The ESAL levels selected for the experimental plan are representative of more than 90% of the mixes that were constructed in Iowa for the 2011 construction season. The cumulative distribution of surface mixtures constructed in 2011 is presented in Figure 13.

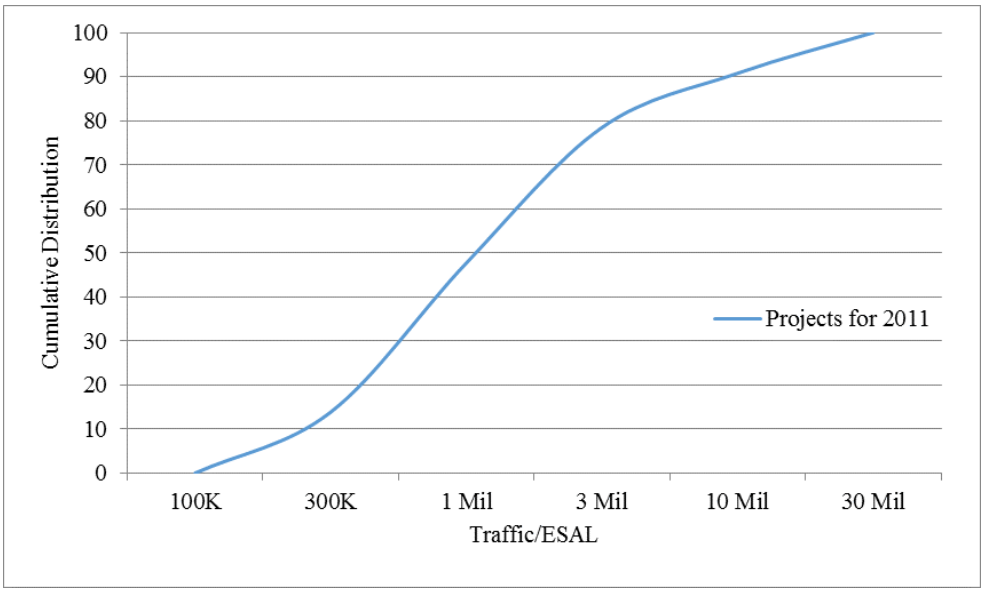

Figure 13. Cumulative distribution of surface mixes

In Figure 13, a small distribution of the projects selected were approximately 14% at 300,000 ESALs. Traffic levels ranging from 1,000,000 to 3,000,000 ESALs constitute about 65% of the asphalt pavements constructed in 2011.

Evaluation of Existing Pavement Conditions

Flexible Pavement Distresses

Distresses in a flexible pavement structure are an important consideration in design, because it is an initial indication of pavement failure. According to the *Distress Identification Manual for the Long-Term Pavement Performance Program*, the main structural pavement distresses in flexible pavements are fatigue cracking, block cracking, edge cracking, longitudinal cracking (wheel path/non-wheel path), reflective cracking at joints, and transverse cracking (Miller and Bellinger 2003). In addition to the structural distresses, functional distresses, such as the International Roughness Index (IRI), were also examined. There are three levels of severity for each type of

distress: low, moderate, and high. Estimated measurements of the amount (length) of distresses were recorded and categorized in its appropriate severity level, based on Table 4.

Table 4. Level of severity corresponding to type of distress

Type	Severity Levels
Fatigue	**Low:** A small percentage of cracks present; not spalled or sealed.
	Moderate: An initial formation of interconnecting cracks developing into a pattern; somewhat spalled; possible cracks sealed
	High: Moderate to high interconnected cracks formed complete pattern; severely spalled; possible cracks sealed; possible pumping present.
Transverse	**Low:** Unsealed crack with a mean width of 6 mm or less; a decent condition sealed crack with sealant material, mean width unable to determine.
	Moderate: Any cracks with a mean width greater than 6 mm but less than or equal to 19 mm; or any cracks adjacent to low severity with a mean width of 19 mm or less.
	High: Any cracks with a mean width greater than 19 mm; or any cracks adjacent to moderate to high severity with a mean width of 19 mm or less.
Longitudinal	**Low:** Unsealed crack with a mean width of 6 mm or less; a decent condition sealed crack with sealant material, mean width unable to determine.
	Moderate: Any cracks with a mean width greater than 6 mm but less than or equal to 19 mm; or any cracks adjacent to low severity with a mean width of 19 mm or less.
	High: Any cracks with a mean width greater than 19 mm; or any cracks adjacent to moderate to high severity with a mean width of 19 mm or less.
Patch/Patch deterioration	**Low:** Patch has low severity distress (rutting < 6 mm); pumping is not present.
	Moderate: Patch has moderate severity distress (rutting < 6 mm to 12 mm); pumping not present.
	High: Patch has high severity distress (rutting > 12 mm); or additional patch material within original patch; pumping present.

Source: Miller and Bellinger 2003

In accordance to the *Distress Identification Manual for the Long-Term Pavement Performance Program* (Miller and Bellinger 2003), Table 4 provides a brief description of each severity level corresponding to the type of distress. In short, a suitable functional pavement performance yields low IRI; high present serviceability rating (PSR); high skid number (SN), and minimum transverse, longitudinal, and fatigue cracking; note that all distresses are due to tensile strain or stress in the asphalt concrete (AC) layer.

Selection and Determination of Pavement Condition using PMIS

In pavement design and analysis, the primary purpose is to construct a pavement structure that is able to support traffic/environmental loads while providing users with a safe, comfortable, and efficient mode of transportation. The performance and serviceability of pavements are ways to evaluate the condition of the structure. Pavement performance reflects condition changes or any

structural inadequacies in the pavement structure to accommodate traffic volume over time, whereas serviceability is the ability of the pavement system to serve traffic throughout the pavement life cycle (Huang 2003).

Distresses in pavements negatively impact performance, and, if left untreated, contribute to the deterioration and subsequent loss in structural integrity. The PMIS surveys are useful in primarily evaluating the overall condition of the pavement and can additionally be used to recommend an appropriate rehabilitation/maintenance strategy for a given pavement section based on collected distress data. Graphical visualization of the severity of distresses before and after rehabilitation was generated to show if pavement conditions improved after rehabilitation and if there were anything unusual in the sections.

Selected projects were categorized into corresponding ESAL levels and severity levels (low, moderate, high) when applicable, as shown in Table 5. Within the selected projects, eight projects were selected based on the availability of pavement condition data and were evaluated using the PMIS surveys. The PMIS data should demonstrate the severity in distresses induced on the pavement structure prior to rehabilitation. The selected projects chosen are shown in Figure 12, denoted with an X. Pre- and post-construction field performance was analyzed based on manual classifications in the *Distress Identification Manual for the Long-Term Pavement Performance Program* (Miller and Bellinger 2003). Post-construction performance was compared with material characteristics of field cores and QC/QA collected at construction. The QC/QA provided by the Iowa DOT presented design parameters, such as the bulk specific gravity (G_{mb}) and G_{mm} of the mixture at construction, which was tested by both the contractor and the Iowa DOT, in addition to the intended thickness and actual thickness of the HMA. The pavement performance data contained both the following structural and functional distresses: rutting, fatigue or alligator cracking, transverse cracking, longitudinal cracking, and IRI.

Table 5 displays the county and ESAL levels for projects with accessible state network PMIS data.

Table 5. Projects selected to evaluate pavement condition

Project No.	County	ESALs
4	Clinton	1,000,000
5	Guthrie	1,000,000
7	Polk	3,000,000
8	Polk	3,000,000
9	Lyon	3,000,000
10	Linn	10,000,000
11	Jefferson	10,000,000
12	Hamilton	10,000,000

Pavement condition surveys were used to compare the pavement performance in low-, moderate-, and high-traffic volumes, or specifically 1,000,000, 3,000,000, and 10,000,000 ESALs. The N_{design} for each ESAL category varied; the higher the traffic volume, the greater the value for N_{design}. The results identified which ESAL level(s) required further monitoring/evaluation.

Determination of Field Densities

Field cores were collected 4 years post-construction in June and July 2015 for ESAL levels below 30,000,000. Field cores with 30,000,000 ESALs were drilled in 2009 and varied in construction years. The surface mixture from the field cores was isolated for testing by sawing off the appropriate thickness, as shown in Figure 14; refer to Appendices A through E for detailed QC/QA data. The field core densities were then compared to densities at construction obtained from the mix data.

Figure 14. Actual field core samples

The G_{mb} of the field specimen was determined in accordance to ASTM D6752/D6752M (2011) and AASHTO T166-13 (2013). There are two methods to measure the bulk specific gravity of a mixture: the Corelok method (Figure 15) and the conventional method (Figure 16).

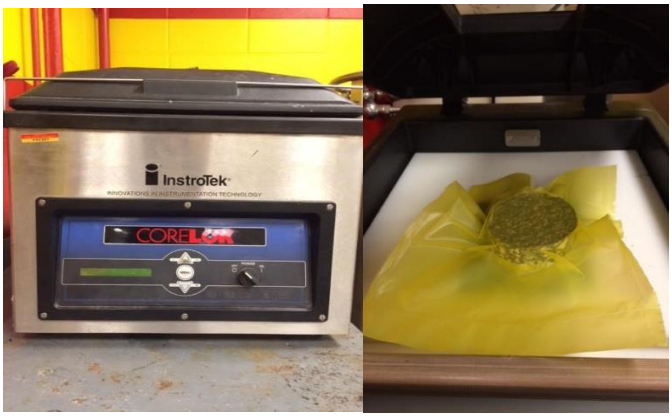

Figure 15. Corelok method

Figure 16. Water bath used in conventional method

The Corelok method uses a Corelok device, which consists of a vacuum chamber and a water tank while the conventional method primarily uses only the water tank. The Corelok method requires vacuum sealing bags, with different sizes that correlate to the appropriate bag volume correction factor to determine the air voids. Dry weights are obtained prior to and after sealing as well as the submerged and dry weights after submersion. The volume of the sample is determined, and the bulk specific gravity can then be calculated.

The Corelok method is known to produce more accurate results for the specific gravity of the field and laboratory specimens. The concern of excess water absorption as well as water draining rapidly when samples are removed from the water tank causes problems with measurements and thus does not produce accurate results. Both methods were used in the determination of the bulk specific gravity of the field cores.

The first half of the samples were tested using the Corelok method. The results of the Corelok method did not have a significant difference in the bulk specific gravity in comparison to the conventional saturated surface dried method. Thus, the remaining samples were tested using the conventional method. Using the conventional method, the dry, submerged, and saturated surface dry (SSD) weights were obtained to calculate the bulk specific gravity. The SSD is defined as the condition when the external surface is "dry," but the internal part of the sample is saturated. The SSD weight obtained by patting the entire sample with a rag or towel.

The G_{mm} was initially estimated per project milepost based on the closest stationing from the G_{mm} measured from the QC/QA hotbox of loose mix recorded by the Iowa DOT at construction. The actual G_{mm} for each core sample was then verified in accordance to AASHTO T 209 (AASHTO 2015b). Two methods in AASHTO T 09 were used to determine the G_{mm} in the laboratory: the flask and metal bucket methods, as shown in Figure 17.

Figure 17. Metal bucket method (left) and flask method (right)

The surface mix samples were heated in the oven at 105 ± 5°C for 30 minutes or until the core was tender enough to break apart. For the flask method, a total of 2000 grams of sample was tested. Similar to the bulk specific gravity in the Corelok method, the flask method is known to produce accurate values for G_{mm}. Both methods yielded the same results.

Evaluation of the Gyratory Slope and PCCE

As previously stated, as reported in NCHRP Report 478, the NCHRP 9-16 project was conducted to determine if there was a relationship between the gyratory compaction parameters, particularly the gyratory slope and the rutting behavior of a mixture. The findings showed that the number of gyrations at maximum shear stress could be related to the stiffness and rutting of a mixture. However, additional research was recommended. While no definitive conclusion can be drawn relating compaction slope to rutting from the report, evaluation of the slope may still provide valuable information in relation to the study (Anderson et al. 2002).

In this research, mix design information was provided and the compaction slope was recalculated from $N_{initial}$ to N_{design}. From this, the PCCE, which showed the difference in theoretical N_{design} four years post-construction and at construction due to traffic, was determined, as shown in Figure 18.

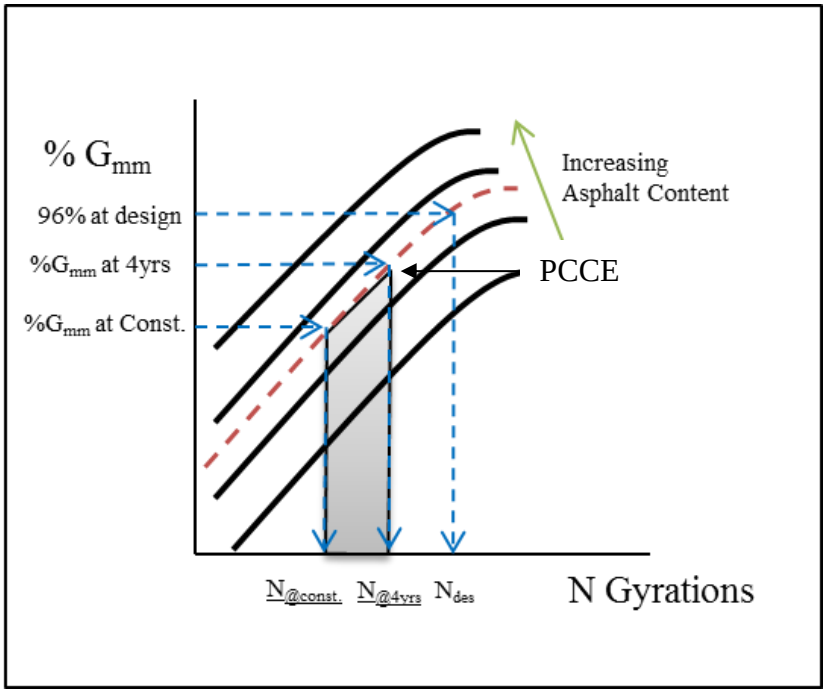

Figure 18. Conceptual representation of theoretical PCCE

The theoretical N_{design} four years post-construction and N_{design} at construction is calculated by using the compaction slope equation presented in Equation (3) from *The Superpave Mix Design Manaul for New Construction and Overlays* (Cominsky et al. 1994).

$$\text{Compaction slope} = 100\times [(C_{des} - C_{ini})/(\log(N_{des}) - \log(N_{ini}))] \quad (3)$$

Where, C_{des} = levels of compaction obtained at N_{design}
C_{ini} = levels of compaction obtained at N_{inital}

The average for each ESAL category was computed and is taken as the PCCE for that specific ESAL level.

Determination of Optimum Asphalt Content using Laboratory Compacted Mixes

Mix Design

The Superpave mix design consists of four steps: material selection, aggregate structure design, optimum binder content, and moisture susceptibility testing. To identify the influence of the gyration level on the mix design, this project's efforts were focused on performing mix design evaluations for three traffic levels (high, medium, and low). For each traffic level, the mix designs used typical aggregate structure and three different asphalt contents (5.0, 5.5, and 6.0%) of the same binder grade (PG64-22). The aggregate gradations for low-, medium-, and high-

traffic levels are summarized in Table 6, Table 7, and Table 8, respectively, and are plotted in Figure 19.

Table 6. Aggregate gradation of low level of traffic

Sieve Size		Virgin Aggregate Material Gradation (% passing)			
ID	**mm**	**Sand**	**TAT4 Man. Sand**	**3/8 in.**	**Batch Mix**
1/2 in.	12.5	100.0	100.0	99.6	99.9
3/8 in.	9.5	100.0	100.0	60.2	90.5
#4	4.8	100.0	96.5	3.8	76.0
#8	2.4	71.7	89.5	0.9	59.9
#16	1.2	40.4	79.1	0.8	42.0
#30	0.6	19.1	52.5	0.6	24.2
#50	0.3	6.5	11.5	0.5	6.5
#100	0.15	2.7	0.5	0.4	1.5
#200	0.075	1.6	0.2	0.2	0.8
% dry weight of aggregate		47.5%	28.6%	23.9%	

Table 7. Aggregate gradation of medium level of traffic

Sieve Size		Virgin Aggregate Material Gradation (% passing)			
ID	**mm**	**Sand**	**TAT4 Man. Sand**	**1/2 in. to Dust**	**Batch Mix**
1/2 in.	12.5	100.0	100.0	83.0	90.7
3/8 in.	9.5	100.0	100.0	64.0	80.2
#4	4.8	95.0	100.0	32.0	61.1
#8	2.4	90.0	73.0	20.0	49.0
#16	1.2	79.0	39.0	15.0	37.8
#30	0.6	53.0	19.0	12.0	25.4
#50	0.3	16.0	7.5	10.0	11.4
#100	0.15	2.0	4.3	8.0	5.6
#200	0.075	1.0	3.5	5.8	4.0
% dry weight of aggregate		30.0%	15.0%	55.0%	

Table 8. Aggregate gradation of high level of traffic

Sieve Size		Virgin Aggregate Material Gradation (% passing)			
ID	**mm**	**Sand**	**TAT4 Man. Sand**	**3/8 in.**	**Batch Mix**
1/2 in.	12.5	100.0	100.0	99.6	99.9
3/8 in.	9.5	100.0	100.0	60.3	85.3
#4	4.8	99.6	96.5	3.8	63.6
#8	2.4	71.7	89.5	0.9	48.5
#16	1.2	40.4	78.1	0.8	32.1
#30	0.6	19.1	52.4	0.6	17.9
#50	0.3	6.5	11.5	0.5	5.1
#100	0.15	2.7	0.5	0.4	1.5
#200	0.075	1.6	0.2	0.4	0.9
% dry weight of aggregate		46.0%	17.0%	37.0%	

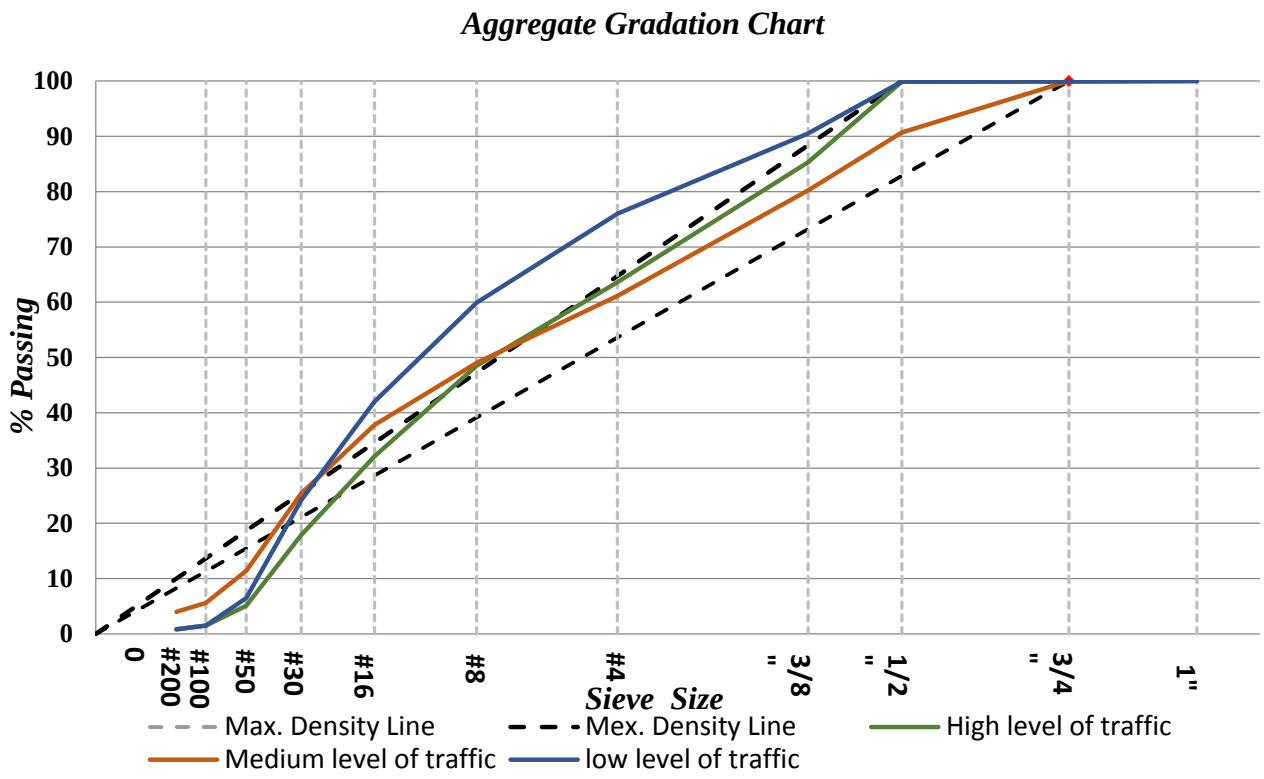

Figure 19. Aggregate gradation of different levels of traffic

These gradations are typical ones used by L.L. Pelling Co. in Iowa. The optimum binder content was identified to achieve 4% air voids. In order to analyze the change in air voids in mixtures designed for all 3 traffic levels, all mixtures were compacted up to N_{max}.

As can be seen in Figure 19, aggregates for a low level of traffic include higher amounts of fine aggregates compared to those for a high level of traffic. The gradation for a medium level of traffic is more gap-graded (finer small aggregates but coarser large aggregates) with a larger maximum size than that of the high level of traffic.

Mix design results for low-, medium-, and high-traffic levels are summarized in Table 9, Table 10, and Table 11, respectively.

Table 9. Mix design properties of low-traffic level mix

Mix Design Properties	**HMA**	**Mix Design Criteria**
Target Air Voids	3.00%	----
Optimum Binder Content (%)	5.80	----
Comb. Agg. Dust Content ($P_{0.075}$ %)	0.83	Maximum 10%
$\%G_{mm}$ at N_{ini} (8 gryrations)	86.39	≤ 89.0%
$\%G_{mm}$ at N_{des} (96 gyrations)	95.61	96% ± 0.5%
Voids in Mineral Aggregate (VMA, %)	15.7	Minimum 14%
Voids Filled with Asphalt (VFA, %)	80.9	75% - 85%
Dust to Binder Ratio ($P_{0.075}/P_{be}$)	0.15	0.6 - 1.4
Film Thickness (μm)	16.10	8.0 - 15 μm

Table 10. Mix design properties of medium-traffic level mix

Mix Design Properties	**HMA**	**Mix Design Criteria**
Target Air Voids	4.00%	----
Optimum Binder Content (%)	5.68	----
Comb. Agg. Dust Content ($P_{0.075}$ %)	4.02	Maximum 10%
$\%G_{mm}$ at N_{ini} (8 gryrations)	87.32	≤ 89.0%
$\%G_{mm}$ at N_{des} (96 gyrations)	95.61	96% ± 0.5%
Voids in Mineral Aggregate (VMA, %)	18.56	Minimum 14%
Voids Filled with Asphalt (VFA, %)	78.6	65% - 78%
Dust to Binder Ratio ($P_{0.075}/P_{be}$)	0.8	0.6 - 1.4
Film Thickness (μm)	12.8	8.0 - 15 μm

Table 11. Mix design properties of high-traffic level mix

Mix Design Properties	HMA	Mix Design Criteria
Target Air Voids	4.0%	----
Optimum Binder Content (%)	4.80	----
Comb. Agg. Dust Content ($P_{0.075}$ %)	0.89	Maximum 10%
%G_{mm} at N_{ini} (8 gryrations)	83.15	≤ 89.0%
%G_{mm} at N_{des} (96 gyrations)	95.61	96% ± 0.5%
Voids in Mineral Aggregate (VMA, %)	14	Minimum 14%
Voids Filled with Asphalt (VFA, %)	71.4	65% - 78%
Dust to Binder Ratio ($P_{0.075}/P_{be}$)	0.22	0.6 - 1.4
Film Thickness (μm)	14.44	8.0 - 15 μm

Dust content was very low for mixtures designed for low- and medium-traffic levels and did not meet the minimum dust-binder requirement of 0.6. The optimum binder content of the mixture designed for a high-traffic level was lower than that for the mixtures designed for low- and medium-traffic levels. The mixture designed for a medium-traffic level met all mix design requirements.

CHAPTER 4: RESULTS AND ANALYSES

Pavement Performance Evaluation using PMIS and LTPP

The PMIS surveys were useful in evaluating the condition of the pavement structure prior to being overlaid. The state-owned roadways were selected because the PMIS data was readily available. The primary purpose of evaluating the PMIS data was to identify external factors that may impact the analysis. The projects were categorized into corresponding ESAL levels and the pavement distresses were categorized by type and severity levels when applicable. Figure 20, Figure 21, and Figure 22 display a distress for each project with time in years on the x-axis and the corresponding pavement distress on the y-axis.

The negative years represent time prior to rehabilitation while positive years indicate observations post-rehabilitation. The year "zero" represents 2011, the year of construction. The 2011 pavement distress surveys appear to have taken place both before and after reconstruction, depending on the project. The lines represent the mean distresses for the corresponding severity level (if applicable); higher values represent more severe distress levels in the pavement structure.

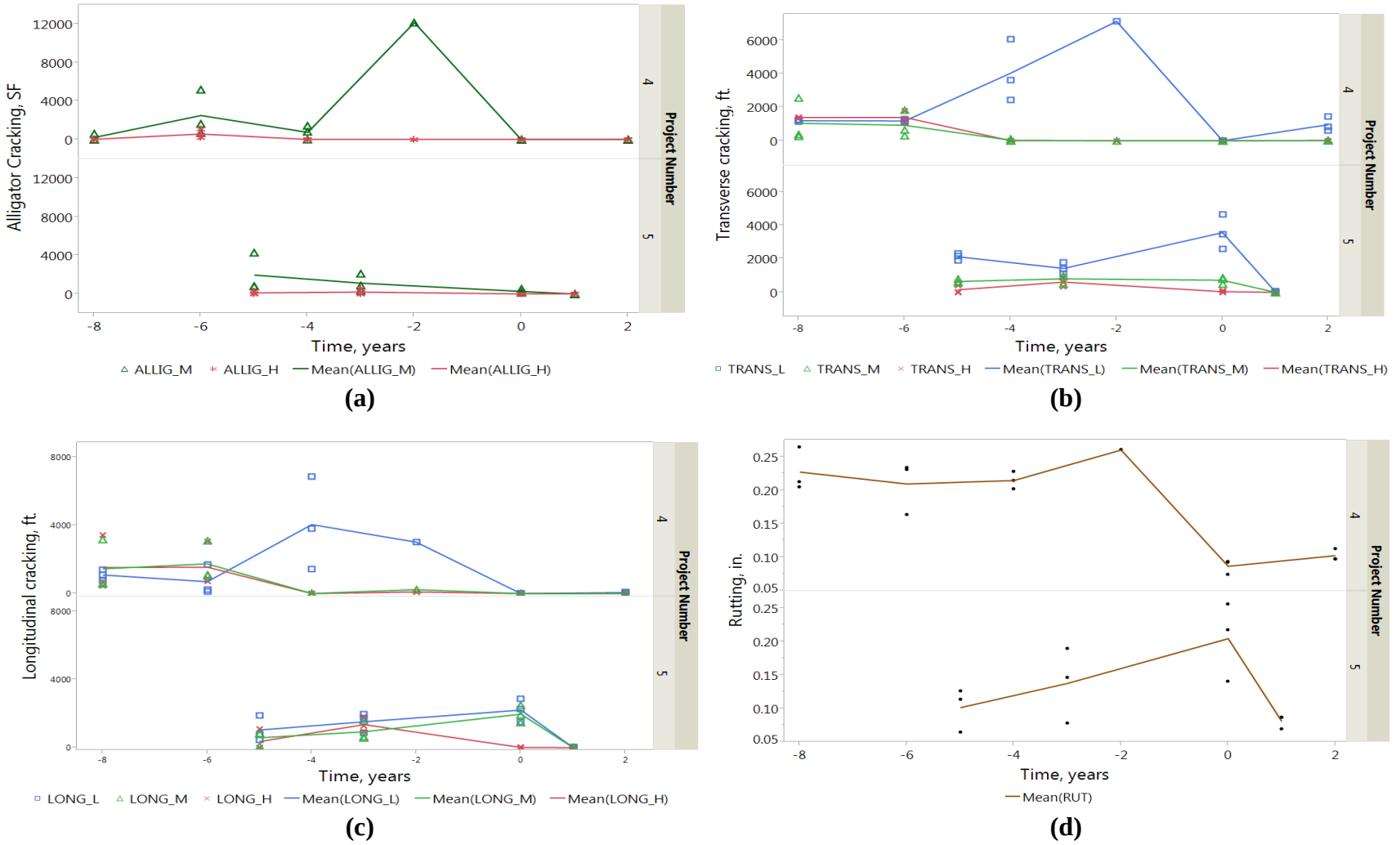

Figure 20. At 1 million ESALs: (a) alligator or fatigue cracking, (b) transverse cracking, (c) longitudinal cracking, and (d) rutting

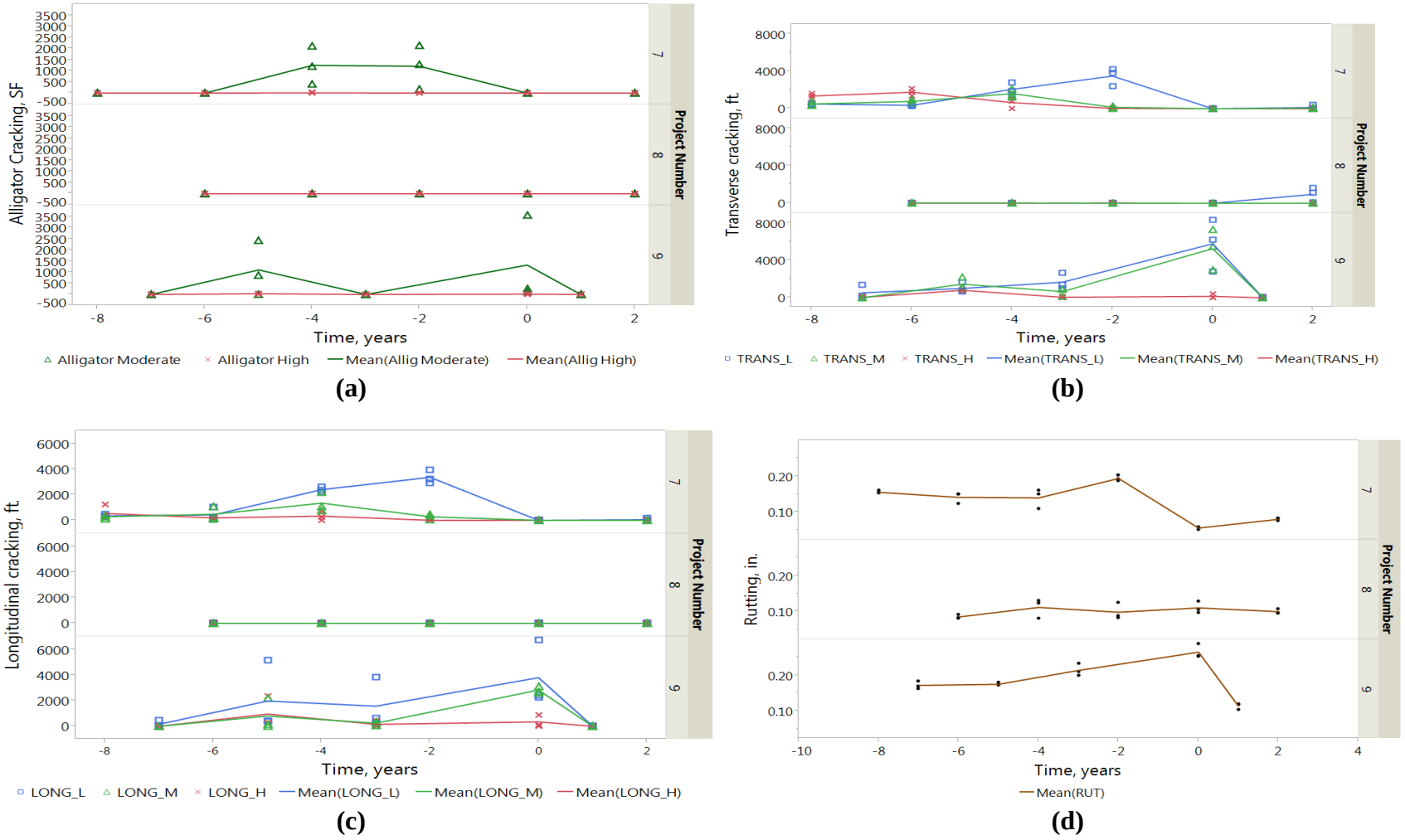

Figure 21. At 3 million ESALs: (a) alligator or fatigue cracking, (b) transverse cracking, (c) longitudinal cracking, and (d) rutting

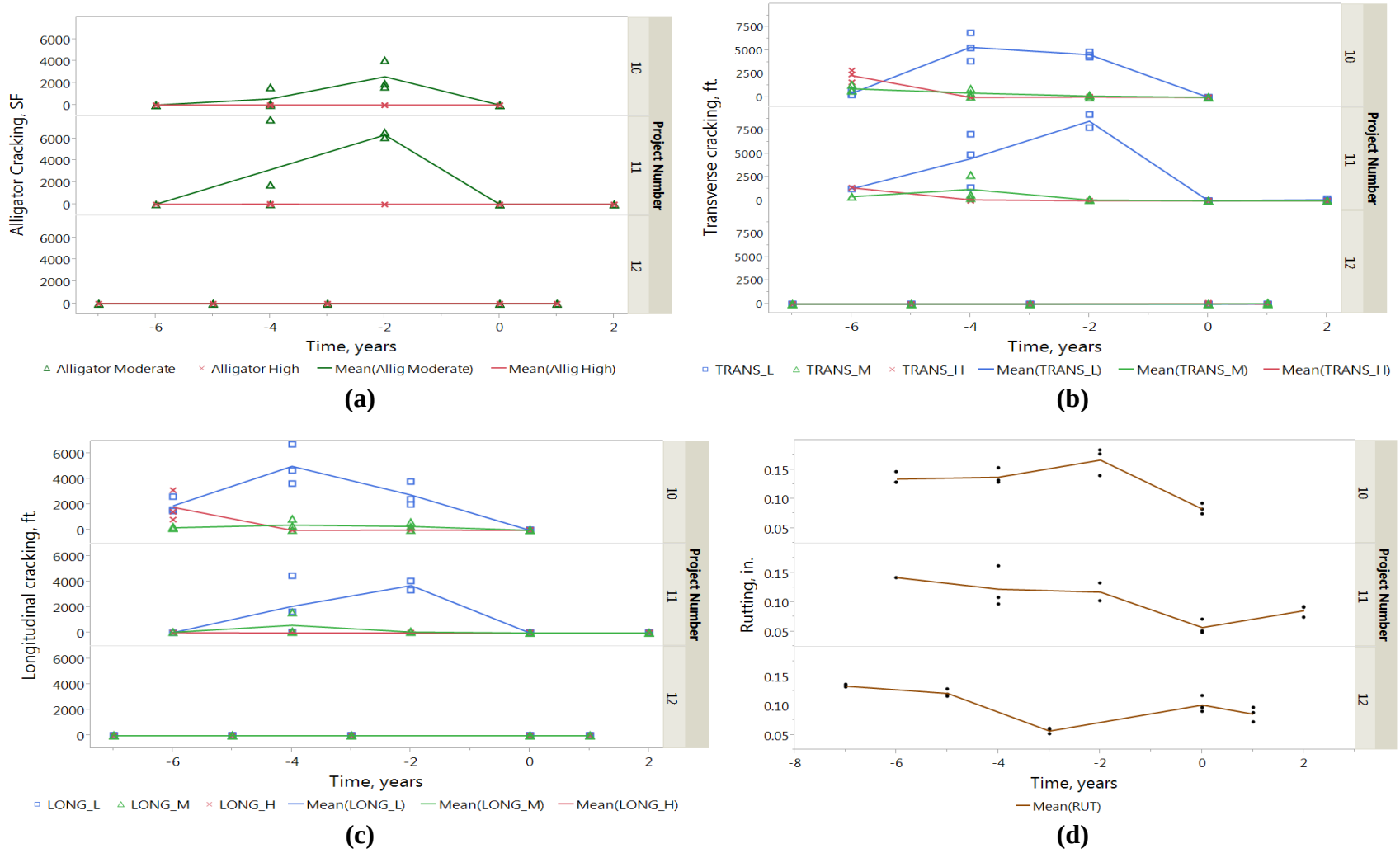

Figure 22. At 10 million ESALs: (a) alligator or fatigue cracking, (b) transverse cracking, (c) longitudinal cracking, and (d) rutting

The IRI was selected as an overall indicator of ride quality and is shown in Figure 23.

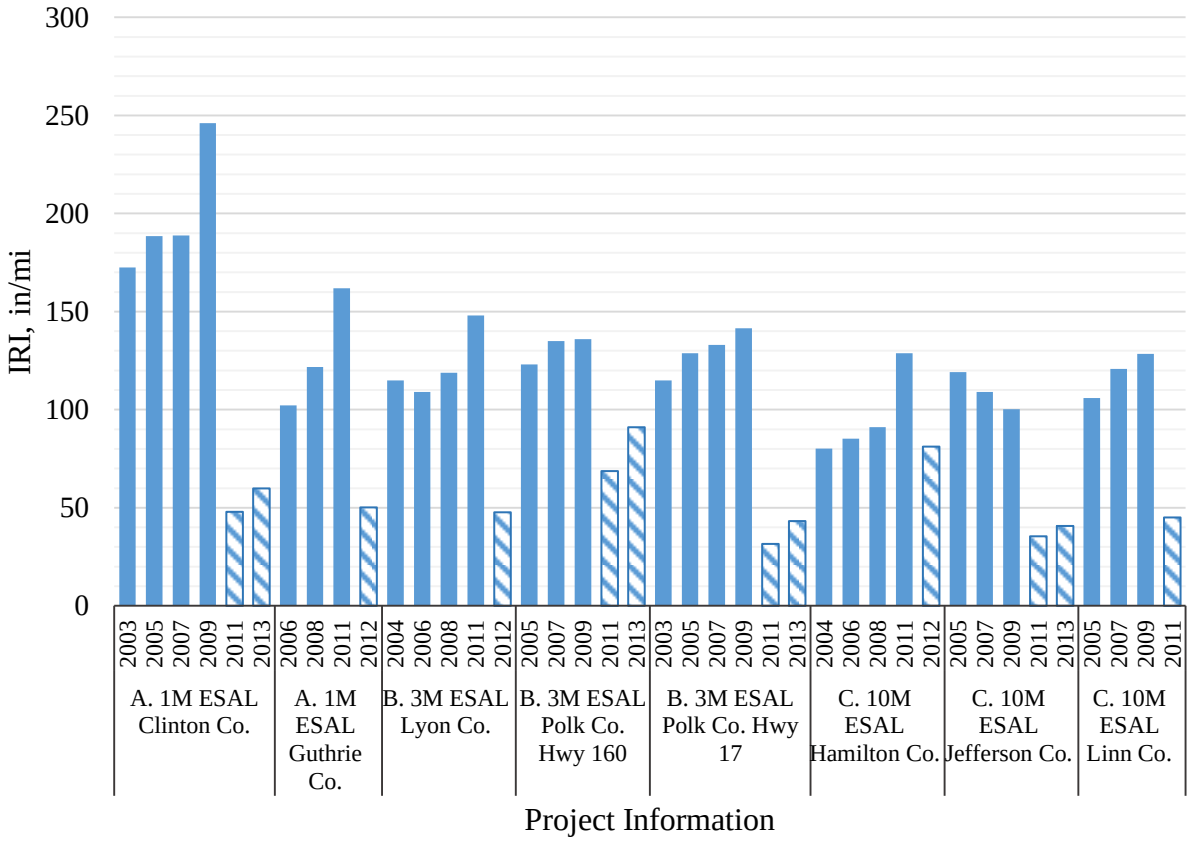

Figure 23. IRI indication at each ESAL level

The IRI values for this research are summarized in the figure. Pavement conditions post-rehabilitation for all projects showed significant improvement for all sections. PMIS data is collected on pavements in Iowa every two years and thus projects will continue to be evaluated under the State's PMIS program. The highest IRI was from the 1,000,000 ESAL mix in Clinton County. The post-construction IRI was highest for the 10,000,000 ESAL Hamilton County project followed by the Polk County Hwy 160 3,000,000 ESAL project. The hatched bars indicate the years the pavement sections were rehabilitated.

According to the Iowa DOT's Interstate Corridor Plan, the following IRI criteria was developed: IRI < 95 indicates good pavement condition, IRI between 95 and 170 suggests fair condition, and if the IRI is greater than 170 the condition is poor (Iowa DOT 2013). For the selected projects, the pavement with the historically highest IRI was a 1,000,000 ESALs project located in Clinton County, but all pavements showed significant improvement after rehabilitation. In addition to the IRI, other distresses such as transverse cracking, longitudinal cracking, and rutting were investigated.

1 Million ESALS

Pavement conditions for Projects 4 and 5 are displayed in Figure 21, where Project 4 is shown in the upper portion of the graphs. Fatigue cracking for Project 4, in Figure 21(a), indicates minor high severity cracking; whereas, moderate cracking displayed a sharp drop in distress after pavement rehabilitation. Project 4 showed no sign of high severity fatigue cracking but displayed a significant increase in moderate cracking 2 years prior to rehabilitation and subsequently improved thereafter. In Figure 23, Project 5 showed fair IRI roughness levels and Project 4 indicated a poor IRI condition prior to rehabilitation, according to the Iowa DOT criteria. Although the average IRI value for Project 4 showed a slight increase 2 years after rehabilitation, the results still indicate good pavement condition. The longitudinal cracking for Projects 4 and 5 is shown in Figure 20(c). High and moderate longitudinal cracking was not as much of a concern as the low longitudinal cracking for Project 5. The maximum average low and moderate cracking in Project 5 displayed an increase in distress until the year prior to rehabilitation; longitudinal cracking improved significantly after the treatment. In Project 4, low severity cracking reached a peak in distress four years prior to rehabilitation while the moderate and high cracking stabilized the same year and remained constant. Transverse cracking, shown in Figure 20(b), displayed similar trends to longitudinal cracking: low distress values in high severity cracking and high distress values for low severity cracking for both projects. The maximum low severity transverse cracking in Project 4 was nearly double the maximum low severity longitudinal cracking. There were small amounts of rutting recorded for both projects.

3 Million ESALs

Pavement conditions can be viewed in Figure 21 (for Projects 7 (top), 8 (middle), and 9 (bottom). Project 8 has the least (or no) distress in pavements. Large amounts of patching were evident in Project 8, specifically 4 years prior to rehabilitation. However, no conclusion can be drawn to relate the low pavement distress and the large patching conducted on the pavement section. Due to the findings in Project 8, the following discussion will focus on Projects 7 and 9. In all three projects, the average high severity fatigue cracking in Figure 21(a) remained constant at zero, while the average moderate fatigue cracking for Projects 7 and 9 fluctuated throughout the recorded years. Project 7 displayed an average of 1000 sq ft in moderate fatigue cracking prior to rehabilitation with post construction observations indicating no fatigue cracking. Project 8's IRI, shown in Figure 23, remained consistent and stable throughout the years examined. Based on the IRI, the graphs indicate fair pavement conditions. The pavements showed post-rehabilitation improvement in the majority of the pavement distresses except for low severity transverse cracking in Project 8 and rutting in Project 9. In Figure 21(b), the low severity transverse cracking for Project 8 had a slight increase in distress, but the effect may be negligible. The average rutting depth for all three projects shown in Figure 21(d) did not exceed 0.26 in. The average IRI values after rehabilitation indicated good pavement conditions in all three projects and were similar to 1,000,000 ESALs; low severity longitudinal and transverse cracking produced the greatest amount of distress in the pavements, as seen in Figure 21(b-c).

10 Million ESALs

The pavement conditions for Projects 10, 11, and 12 are shown in Figure 22 at the top, middle and bottom, respectively. Project 12 showed no sign of fatigue, longitudinal, and transverse cracking, as seen in Figure 22(a-c) in the top portion of the graph. Projects 10 and 11 show significant improvement in pavement performance after rehabilitation. In Figure 22(a), the fatigue cracking for both projects displayed similar trends; the average high severity cracking remained constant at zero while the average moderate cracking reached a peak 2 years prior to rehabilitation and subsequently decreased thereafter. In Figure 23, the average IRI for all three projects were below 200 and remained relatively constant over time. Figure 22(c) displayed large amounts of low severity longitudinal and transverse cracking in the pavement structure. The maximum low severity transverse cracking in Project 11 was approximately double the maximum low severity longitudinal 2 years prior to rehabilitation; a similar trend in Project 4, as shown in Figure 22. Additionally, the transverse and longitudinal cracking for Project 10 displayed similar trends in the level of severities. Figure 22(d), showed a slight increase in the average rutting in Project 11 after rehabilitation, but none of the projects exceeded an average rut depth of 0.17 in.

Theoretical Maximum Specific Gravity QC/QA versus AASHTO T 209

The $G_{mm\ (QC/QA)}$ is the G_{mm} measured during QC/QA at construction and was used initially to estimate the field air voids at construction with the actual calculated G_{mb} from the field cores. It is expected that the values for $G_{mm\ (QC/QA)}$ would yield equivalent values of G_{mm} directly measured from the core. To verify, G_{mm} testing was carried out to validate if \ $G_{mm\ (QC/QA)}$ values matched actual field core G_{mm} values. As shown in Figure 24 and Figure 25, based on the results, the percent air voids for $G_{mm\ (QC/QA)}$ yielded similar results to G_{mm} tested using AASHTO T 209 (AASHTO 2015b).

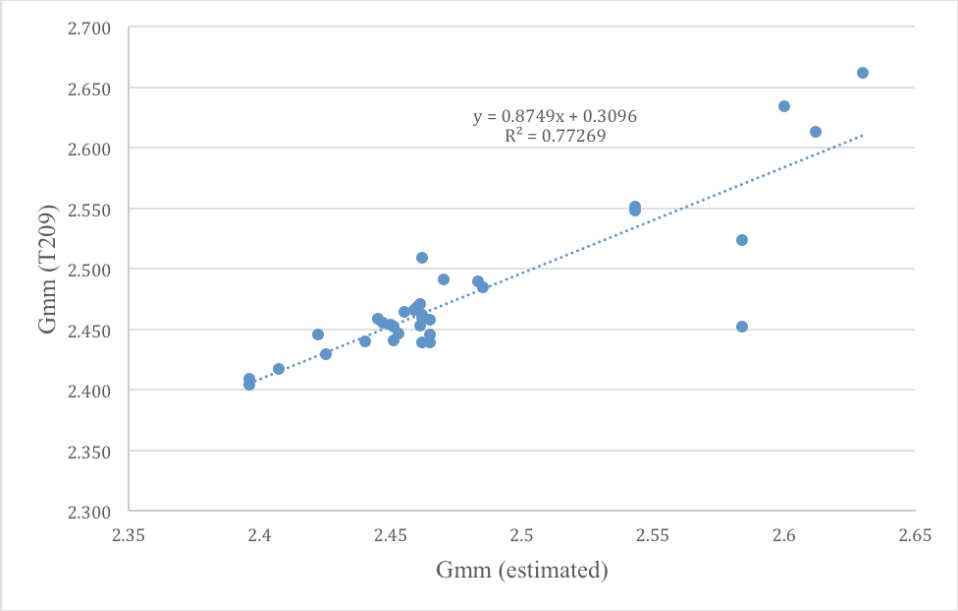

Figure 24. G_{mm} estimated or QC/QA versus actual G_{mm} or G_{mm} tested in accordance with AASHTO T 209

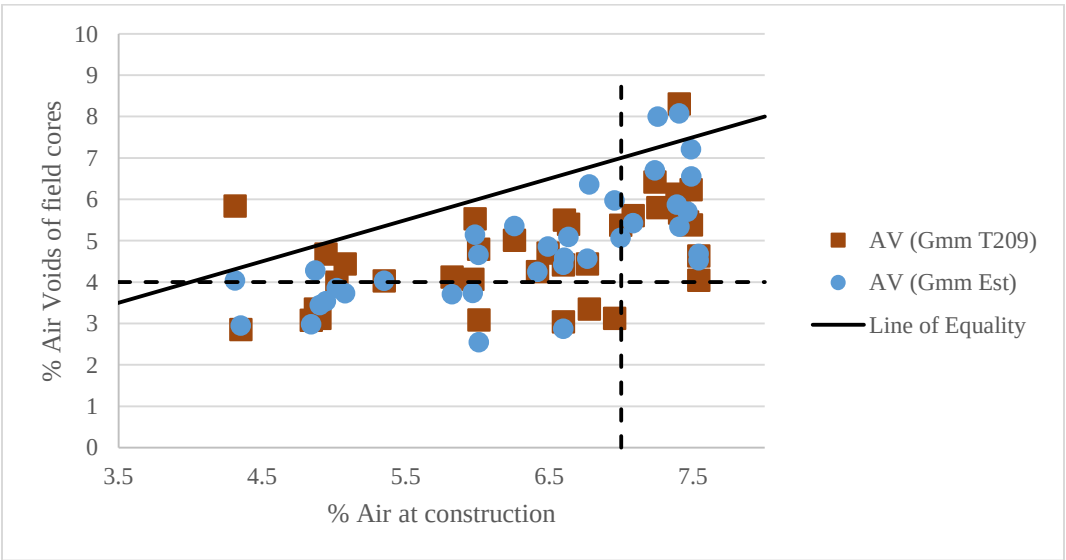

Figure 25. Calculated air voids with estimated G_{mm} from QC/QA data and air voids with G_{mm} measured from the field core tested in accordance with AASHTO T 209

The $G_{mm\ (QC/QA)}$ was also plotted against actual field G_{mm} with a linear fitted regression line. Figure 24 shows that G_{mm} values 2.50 and below displayed better correlation between the observed values and predicted $G_{mm\ (QC/QA)}$. Thus, for evaluating future air void information, the G_{mm} can accurately be used from QC/QA, as opposed to conducting additional laboratory testing to validate the G_{mm} directly from field cores.

Change in Air Voids Post-Construction

The air voids at construction and field air voids were collected and analyzed for this research project. The results show that air voids for 300,000, 1,000,000, 3,000,000, and 10,000,000 ESALs 4 years post-construction displayed an average of less than 2.0% change in air voids. Figure 26(a-d) categorizes the change in air voids for each project by ESAL level.

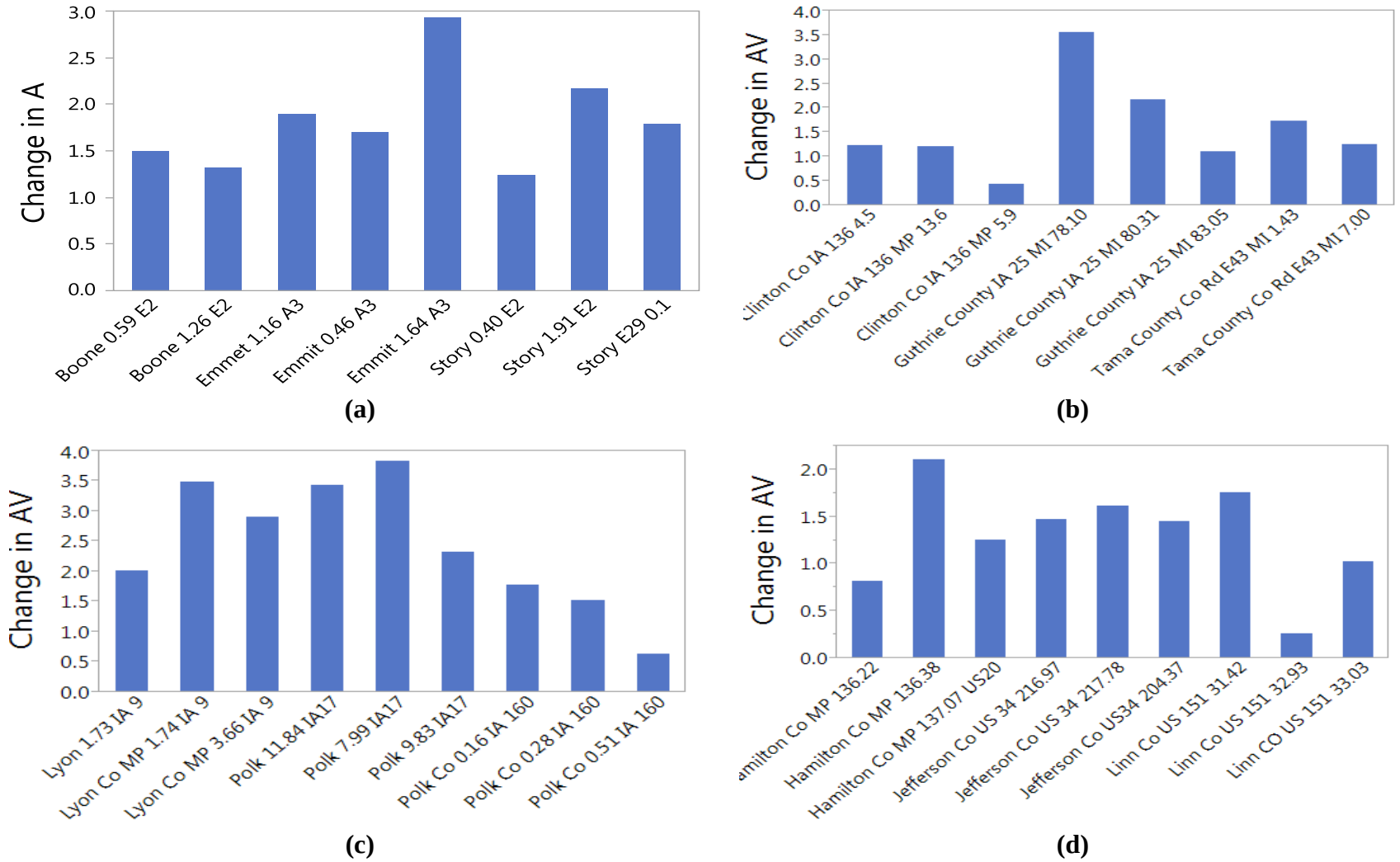

Figure 26. Change in percent air voids per ESAL level at (a) 300,000, (b) 1,000,000, (c) 3,000,000, and (d) 10,000,000

The overall averages are shown in Figure 27 (left), with the error bars representing the standard error (SE) bars in the change in air voids Figure 27 (right) shows the overall distribution of the change in air voids.

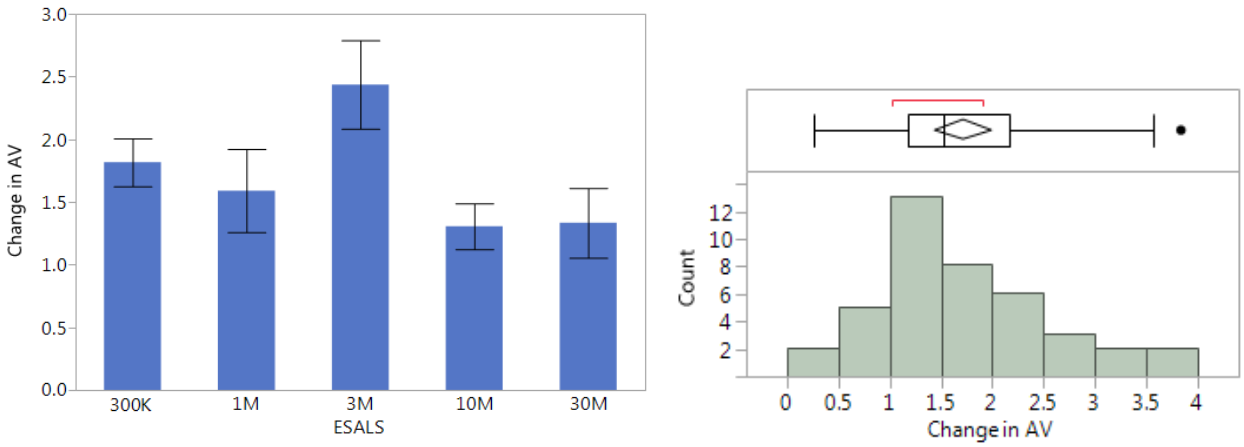

Figure 27. Change in percent air voids against ESALs (left) and distribution of the percent change in air voids with varying ESAL levels (right)

In Figure 27 (left), the change in air voids is similar for all mixes with the exception of 3,000,000 ESALs, which shows the highest average change. There was high variability in the change of air voids for ESAL levels of 1,000,000, 3,000,000, and 30,000,000, compared to traffic levels at 300,000 and 10,000,000 ESALs. Traffic volumes at 3,000,000 ESALs tended to have a higher change in air voids. One explanation may be the distribution of traffic on rural highways in the 3,000,000 ESAL category for IA 9 in Lyon County and Hwy 17 in Polk County.

The average air voids 4 years post-construction for the 300,000 ESAL level was about 4% air voids, which indicates that the pavements under this specific ESAL level reached ultimate pavement density. At construction, the air voids were compacted to an average of 6% at this ESAL level range. At 1,000,000 ESALs, the construction air voids were compacted to 7% and after 4 years post-construction, the average field air voids were 5%. The results for 3,000,000 ESALs varied, specifically for projects paved on IA 160 in Polk County, Iowa (Project 8). The overall average air voids 4 years post-construction and at construction was approximately 5 and 6.5%, respectively. In Project 8, the air voids at construction were approximately 5%, significantly lower than the desired initial target air voids compared to the other two projects. Pavement density for Project 8, 4 years post-construction, reached to about 4% air voids, a 2% change in air voids. At the 10,000,000 ESAL level, the average air voids at construction for projects located on Hwy US 20 in Hamilton County, Iowa, and Hwy US 34 in Jefferson County, Iowa, (Projects 12 and 11, respectively) were about 7.3% air voids, which is above the initial target air voids; and the project located on Hwy US 151 in Linn County, Iowa (Project 10) was over-compacted to about 5.0% air voids at construction. The air voids 4 years post-construction for Projects 12 and 11 did not densify to 4% and field density was determined to be in the range of 6.2 to 6.8%, whereas in Project 10, the air voids were approximately 3%.

See Figure 28 for the average air voids per ESAL level 4 years post-construction and at construction.

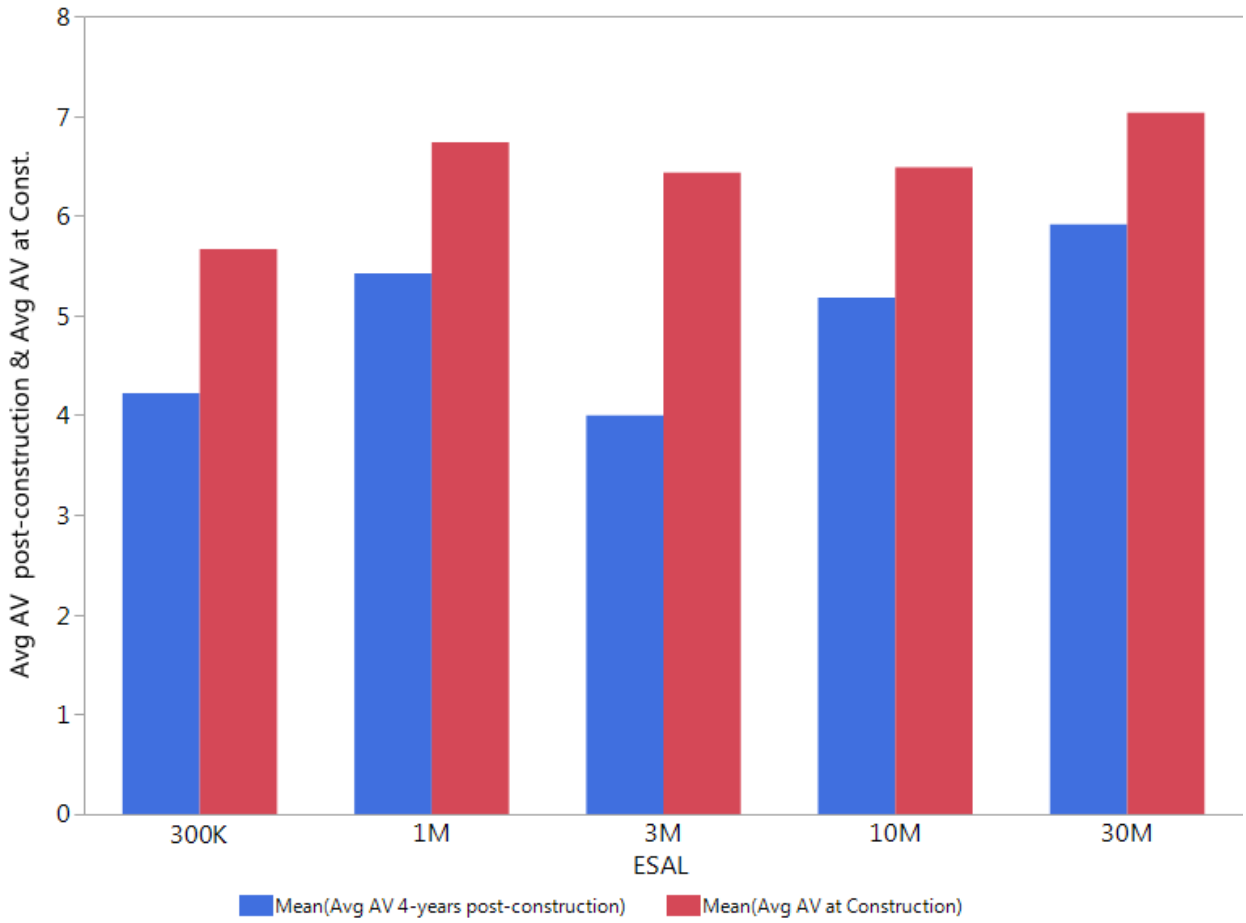

Figure 28. Average air voids at construction and 4 years post-construction

Figure 28 shows the differences in average air voids at construction and 4 years post-construction with varying ESAL levels. The figure shows that ESAL levels for 300,000 and 3,000,000 had lower air voids at construction and both were able reach ultimate pavement density 4 years post-construction. For 30,000,000 ESALs, the average air voids 1 year or less post-construction is about 6.0% and about 7.0% at construction. At 2 years post-construction for Fermont I-29 NB and at 12 years post-construction for Pottawattamie I-680, the air voids were 5.6 and 5.7%, respectively, with average air voids at construction of 6.8 and 6.9%, respectively. The densities for 30,000,000 thus had an average change in air voids of about 1% or less.

Air Voids at Construction and 4 Years Post-Construction

The comparison between air voids at construction and air voids 4 years post-construction was done. Figure 29 displays the overall percent air voids at construction plotted against percent air voids of the field cores 4 years post-construction.

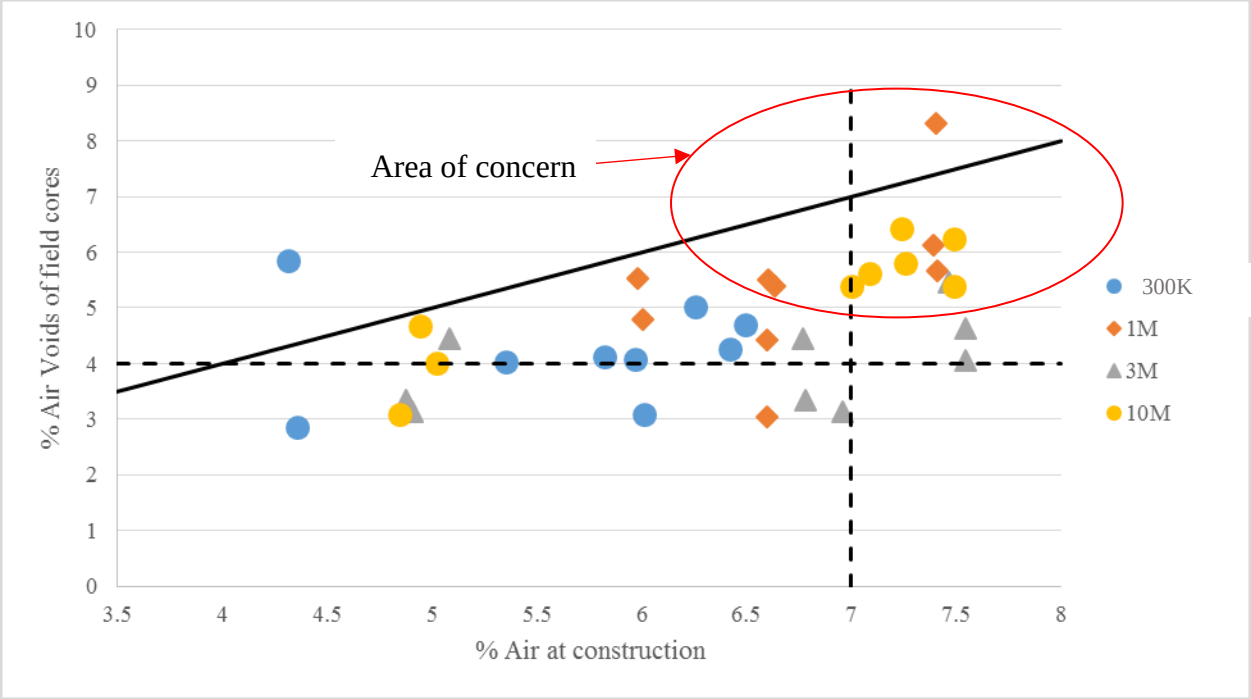

Figure 29. Percent air voids at construction versus air voids 4 years post-construction

Based on the results, the ultimate pavement density has not been achieved for the majority of the projects. The percent air voids at construction plotted beyond 7% and were unable to densify with traffic with the exception of 1 mixture. About 33% of the pavement sections for 1,000,000 and 3,000,000 ESALs as well as 56% for 10,000,000 ESALs of samples collected have not and will likely never reach the ultimate pavement density of 4%. Samples with a traffic volume of 300,000 ESALs did not fall beyond the 7% air voids at construction. Only 11% of the samples collected reached the 4% target air voids, mainly projects at 300,000 ESALs. This can possibly be due to different aggregate specifications and requirements that generally allows for better compaction, such as higher criteria for fractures faces in a coarse aggregate angularity test, shape, texture, etc. As shown in Figure 29 , the most problematic traffic levels were projects with 10,000,000 ESALs.

Although projects with 300,000 ESALs were not compacted to 7% air voids at construction, 75% of the samples were within or were significantly close to the target air void of 4% at 4 years post-construction. The solid red circle line plotted beyond the 7% air voids at construction in Figure 29 represents the area of most concern.

Air Voids at Construction and Post-Construction for 30,000,000 ESALs

The air voids at construction and post-construction for 30,000,000 ESALs were also evaluated in this study. The cores selected had different construction years but were all drilled in the same year. As shown in Figure 30, none of the projects with 30,000,000 ESALs densified to the target air voids.

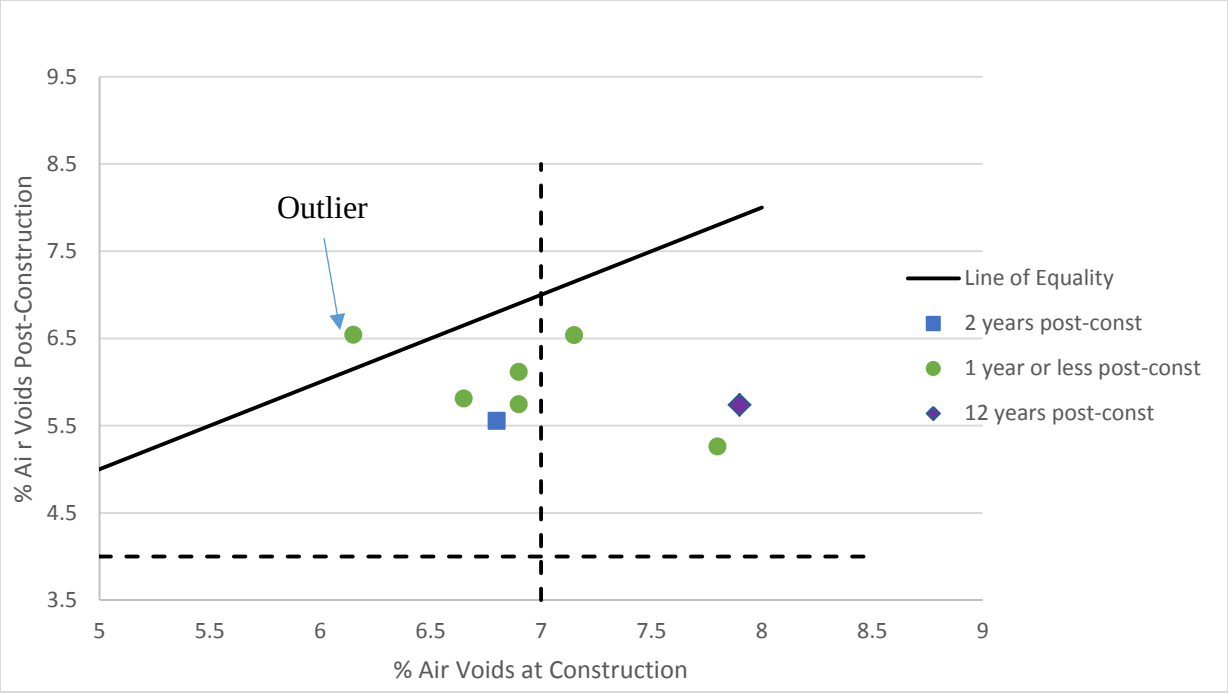

Figure 30. Air void analysis for 30,000,000 ESALs

Most of the densification is said to occur within the first 2 years. However, the air voids for cores extracted 1 year or less and 2 years post-construction did not densify in the pavements significantly. The change in air voids for these years ranged between 0.6 to 2.5%. For the project 12 years post-construction, the results displayed a similar change in air voids with 1 year and 2 years post-construction. Throughout the 12 years of traffic loading induced on the pavement, about 2% change in air voids occurred post-construction. The results indicate that, with traffic induced at 30,000,000 ESALs, the pavements were unable to reach the ultimate pavement density of 4%. There are no air voids that plotted at 4% air voids or below, and those that plotted beyond 7% air voids at construction will not likely attain the desired target air voids. All of the air voids were plotted below the line of equality.

Table 12 shows the tabulation of average air voids for 30,000,000 ESALs.

Table 12. Tabulation of average air voids for 30,000,000 ESALs

Project No.	Project Name	Avg. AV Post-Construction	Avg. AV at Construction
13	Pottawattamie I-29 NB	6.54	7.15
14	Warren I-35	5.74	6.9
15	Fremont I-29 NB	5.55	6.8
16	Story I-35	6.12	6.9
17	I-80 EB/WB 80(242)	6.54	6.15
18	Pottawattamie I-680	5.74	7.9
19	Johnson I-80 EB/WB	5.81	6.65
20	Johnson I-380	5.26	7.8

Gyratory Compaction Slope and PCCE

The compaction slope for projects with available mix data is shown in Table 13.

Table 13. Compaction slope, theoretical $N_{@field}$, and $N_{@const}$

Project No.	Project Location	N_{design}	ESALs	$\%G_{mm}$	Gyratory Slope Semi log method N_{ini} to N_{design}	Avg Theory $N_{@field}$	Avg Theory $N_{@const}$
1	Boone E-26	68	300K	96	6.651	84.14	51.39
2	Emmet A-34	68	300K	96	6.363	75.32	33.79
3	Story E-29	68	300K	96	6.382	53.99	28.74
4	Clinton IA 136	76	1M	96	5.859	46.98	32.13
5	Guthrie	76	1M	96	6.747	72.28	31.29
6	Tama E-43	76	1M	96	6.393	38.46	22.34
7	Polk IA 17	86	3M	96	7.148	52.48	34.53
8	Polk IA 160	86	3M	96	6.414	92.50	61.15
9	Lyon IA 9	86	3M	96	5.680	59.30	20.68
10	Linn US 151	96	10M	96	6.465	101.46	68.81
11	Jefferson US 34	96	10M	96	6.405	54.14	31.38
12	Hamilton US 20	96	10M	96	7.899	42.35	35.61
13	Pottawattamie I-29 NB	109	30M	96	8.823	66.18	13.21
14	Warren I-35	109	30M	96	9.673	92.73	56.54
15	Fremont I-29 NB	109	30M	96	9.720	115.82	49.34
16	Story I-35	109	30M	96	7.896	72.41	46.79
17	I-80 EB/WB 80(242)	109	30M	96	9.122	69.96	55.86
18	Pottawattamie I-680	109	30M	96	6.370	46.92	15.28
19	Johnson I-80 EB/WB	109	30M	96	9.197	57.90	43.29
20	Johnson I-380	109	30M	96	8.000	65.77	23.73

During the mix design, the N_{design} for 300,000, 3,000,000, and 10,000,000 ESALs were 68, 86, and 96 gyrations, respectively. Mix designs are optimized for 4% target air voids or 96% G_{mm}. With the use of the slope for each mix and the $\%G_{mm}$, a theoretical compaction effort can be attained 4 years post-construction. A theoretical compaction effort is calculated using the $\%G_{mm}$ at construction and the gyratory slope; the parameter is designated $N_{@const}$, $N_{@const}$ represents the theoretical compactive effort in units of gyrations and the compactive effort achieved at the time of construction. Similarly, $N_{@4yrs}$ indicates the theoretical compactive effort in units of gyrations achieved 4 years post-construction. The difference in theoretical $N_{@4yrs}$ and $N_{@const.}$ represents the applied PCCE. This concept is graphically displayed in Figure 18.

It is anticipated that as the mixes become more difficult to compact, the PCCE will decrease because the mixes become less likely to compact under traffic loading conditions. However, it did not follow the expected trend, as shown in Figure 31: the traffic volumes at 300,000 and 3,000,000 ESALs displayed the highest PCCE.

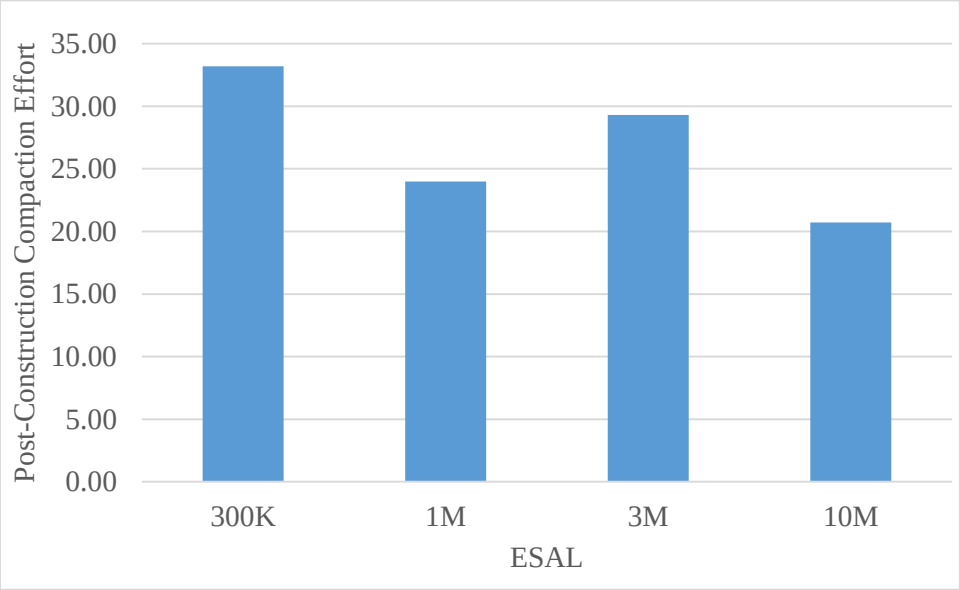

Figure 31. PCCE per ESAL level at 96 percent G_{mm}

For the mixes at 300,000 ESALs, the average theoretical $N_{@4yrs}$ was 71 gyrations, which indicates that the mixes were slightly over-compacted in the field by 3 gyrations; thus reaching the ultimate density. The outcome yielded similar results to the air void analysis. Pavement sections under this specific ESAL level reached ultimate density 4 years post-construction.

The mixes for 1,000,000 and 10,000,000 ESAL levels had an average theoretical $N_{@4yrs}$ of 53 and 66 gyrations, respectively, thus, the gyrations needed to reach the desired N_{design} for both ESAL levels were calculated to be 23 and 30 gyrations, respectively. The most problematic ESAL levels were at 1,000,000 and 10,000,000. These two ESAL levels displayed lower PCCE in comparison to the 300,000 and 3,000,000 ESAL levels. Most projects at 10,000,000 and a few at 1,000,000 ESALs were unable to densify with traffic. The PCCE for 30,000,000 could not be compared directly to the results obtained for the other ESAL levels due to the differences in the

post-construction years. Nevertheless, the average PCCE for 30,000,000 ESALs was 36 gyrations, and previously stated variability in the results could possibly be due to the different years after construction. Overall, the results support the validation of under-compaction during construction for those ESAL levels of concern. To better understand the $\%G_{mm}$ as N changes, each gyration curve for different ESAL levels were plotted and can be seen in Figures 44 through 48 in Appendix E. The line in the graphs is the gyratory slope based on 96% $G_{mm,}$ excluding ESAL levels at 300,000, which was at 96.5% G_{mm}.

Due to the high variability within each ESAL level category, the projects were separately plotted for each ESAL level to better understand the effects of PCCE. Figure 32 and Figure 33 show the average $N_{@4yrs}$, $N_{@const}$, and PCCE for 4 years post-construction and the results for 30,000,000 ESALs for each project selected. Based on Figure 32 and Figure 33, there appears to be high variability within each project for a given ESAL level.

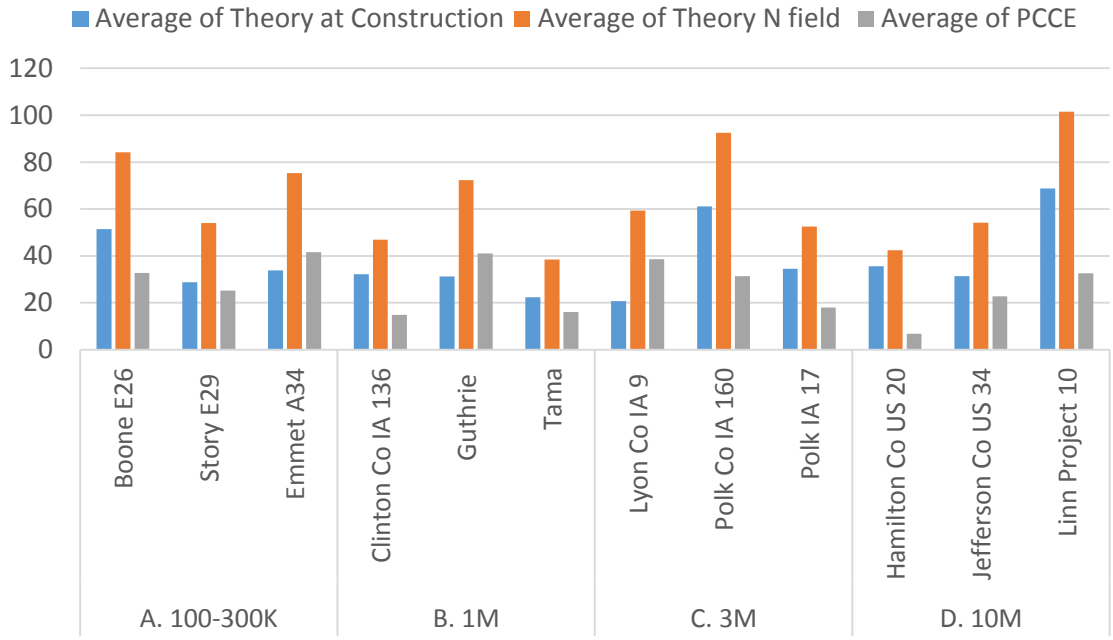

Figure 32. Average of theory for $N_{@4yrs}$ and $N_{@const}$ and PCCE for each ESAL level at 96 percent G_{mm}

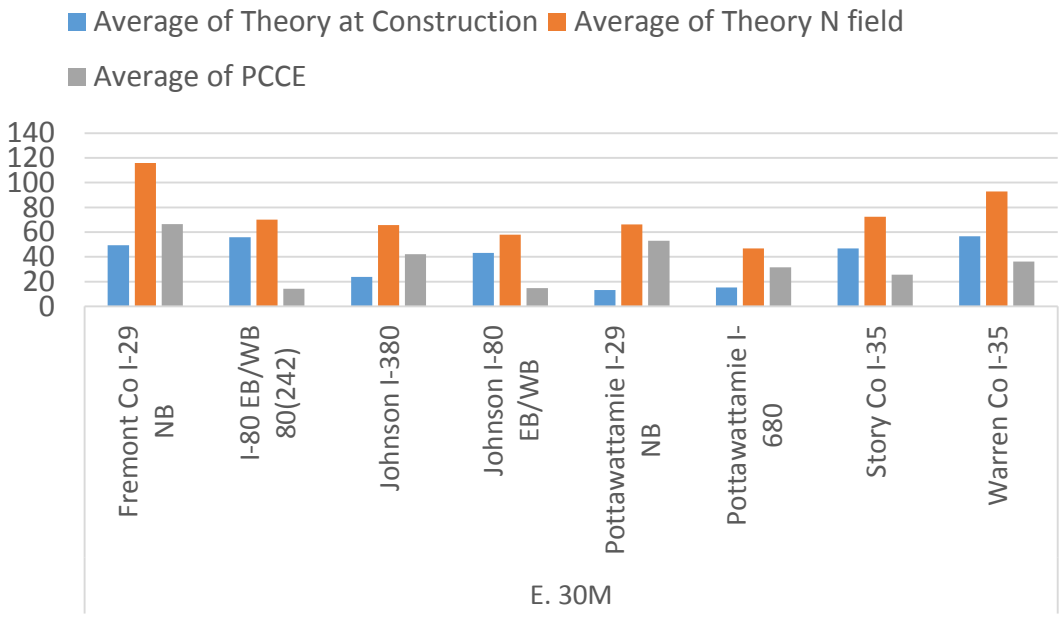

Figure 33. Average of theory for $N_{@4yrs}$ and $N_{@const}$ and PCCE for 30,000,000 ESALs

These graphs show that the highest level of PCCE induced is the 300,000 ESAL level for Emmet County, Iowa, for 4 years post-construction. The results match the air voids analyses, where ultimate pavement density was achieved at 300,000 and 1,000,000 ESALs. This indicates that higher PCCE was applied at these ESAL levels. While the other ESAL levels varied in terms of PCCE, the results still indicate that target air voids 4 years post-construction were not reached with the use of the gyratory slope. Thus, at 4 years post-construction, the higher N_{design} levels will generally see a decrease in the post-construction compaction due to traffic.

The previous analysis provides an estimate of how much densification from a pavement can be expected by traffic over a period of several years. The densification is expected and necessary for reducing the infiltration of water, reducing asphalt oxidation, and improving pavement performance. On average, the change in air voids was approximately 1.75% from construction to 4 years post-construction. The highest average change observed was 2.5% for the 3,000,000 ESAL pavements. The analysis of air voids also showed that the higher air voids at construction had a decreased likelihood of ever reaching the 4% final air voids from the traffic compaction. The following histograms in Figure 34 show all $\%G_{mm}$ values at construction from 2011 to 2013 in Iowa.

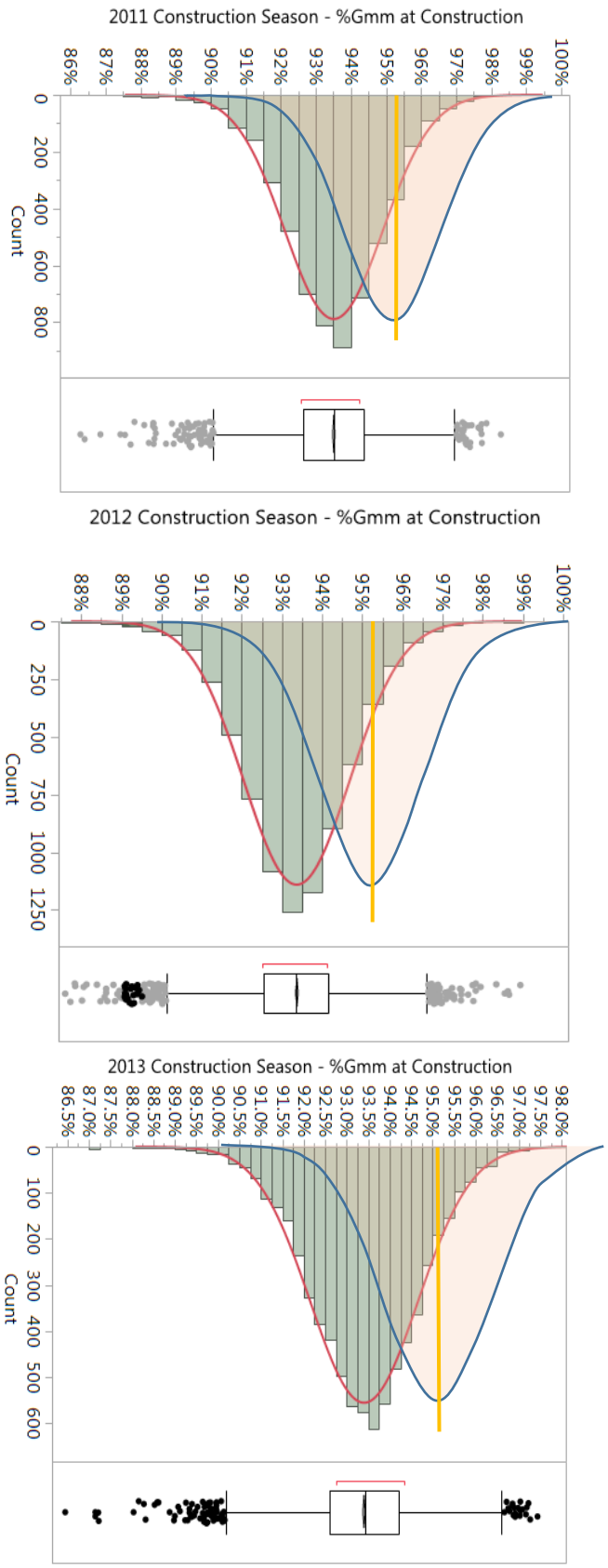

Figure 34. Distribution of percent of theoretical maximum density at construction with an expected shifted distribution for air voids at 4 years post-construction

The histograms indicate that there is a high probability that 25% of these pavements will never reach 4% air voids (or 96% G_{mm}). The histograms also show that the average percent G_{mm} in the field is 93.5%. The lower quartile is approximately 92.5 to 93.5%. If the average densification is applied and the distributions shifted, the average pavement will reach 95.25% densification. The shifted histogram in Figure 34 (i.e., the solid line) indicates the predicted distribution of $\%G_{mm}$ 4 years post-construction for 2011, 2012, and 2013, based on the analyses conducted from the randomized field samples collected in 2011. This information provides an understanding of typical pavement densities in the field, along with an explanation of how best to approach the N_{design} specification and continue to track the pavement densification process over time.

Optimum Binder Content Selection

The optimum binder content corresponds to 4% air voids for high and medium levels of traffic and 3 or 3.5% air voids for low levels of traffic, depending on the aggregate gradation. A temperature range for mixing where viscosity lies between 150 and 190 centistokes (cSt) is suggested. As summarized in Table 14, a mixing temperature was selected as 155˚C and compaction temperature as 145˚C.

Table 14. Mixing and compaction temperatures

	Mixing	**Compaction**
Viscosity Range	150 to 190 cSt	250 to 310 cSt
Temperature Range	150 to 160˚C	140 to 150˚C
Temperature used in this Report	155˚C	145˚C

Asphalt mixtures were compacted using a gyratory device. Table 15 summarizes the initial number of gyrations (N_{ini}), N_{design}, and N_{max} that were adopted for low-, medium-, and high-traffic levels. For all specimens in this study, however, 152 gyrations was selected as N_{max}.

Table 15. Number of gyration for different levels of traffic

Level of Traffic	**Design ESAL**	**N_{ini}**	**N_{des}**	**N_{max}**
Low	0-0.3 M	7	68	104
Medium	0.3-1 M	7	76	117
High	3-10 M	8	96	152

Volumetric Characteristics of Mixtures

Air voids, VMA, and VFA of mixtures for low-, medium-, and high-traffic levels are plotted against asphalt contents in Figure 35, 36, and 37, respectively.

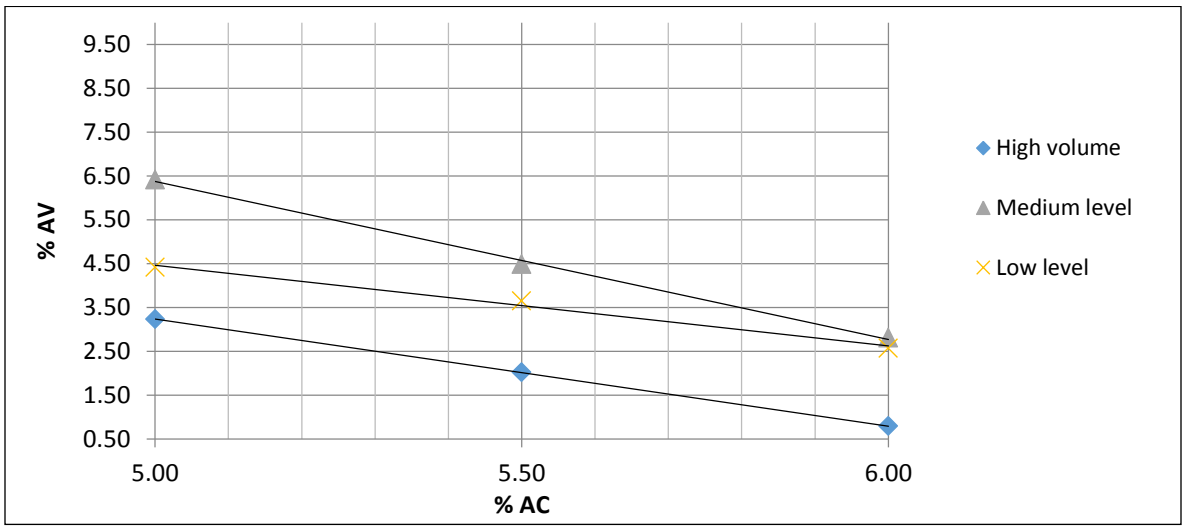

Figure 35. Percent air void versus percent asphalt for all traffic levels

As Figure 35 shows, when the asphalt content is increased, the air voids decrease. Due to the higher number of gyrations, the mixture for a high-traffic level exhibited the lowest air voids. However, the mixture for a medium-traffic level exhibited the highest air voids due to its coarser gradation and a larger maximum aggregate size. As a result, the optimum asphalt content of the mixture for a high-traffic level was lowest (at 4.8% for 4% air voids), followed by the medium-traffic level (at 5.7% for 4% air voids), and the low-traffic level (at 5.8% for 3% air voids).

As shown in Figure 36, the same trend for air voids can be observed from VMA where the mixture for a high-traffic level exhibited the lowest VMA, followed by the low-traffic level, and then the medium-traffic level. For low and medium levels of traffic, VMA met the requirement of 14%, but for a high level of traffic, VMA did not meet the requirement.

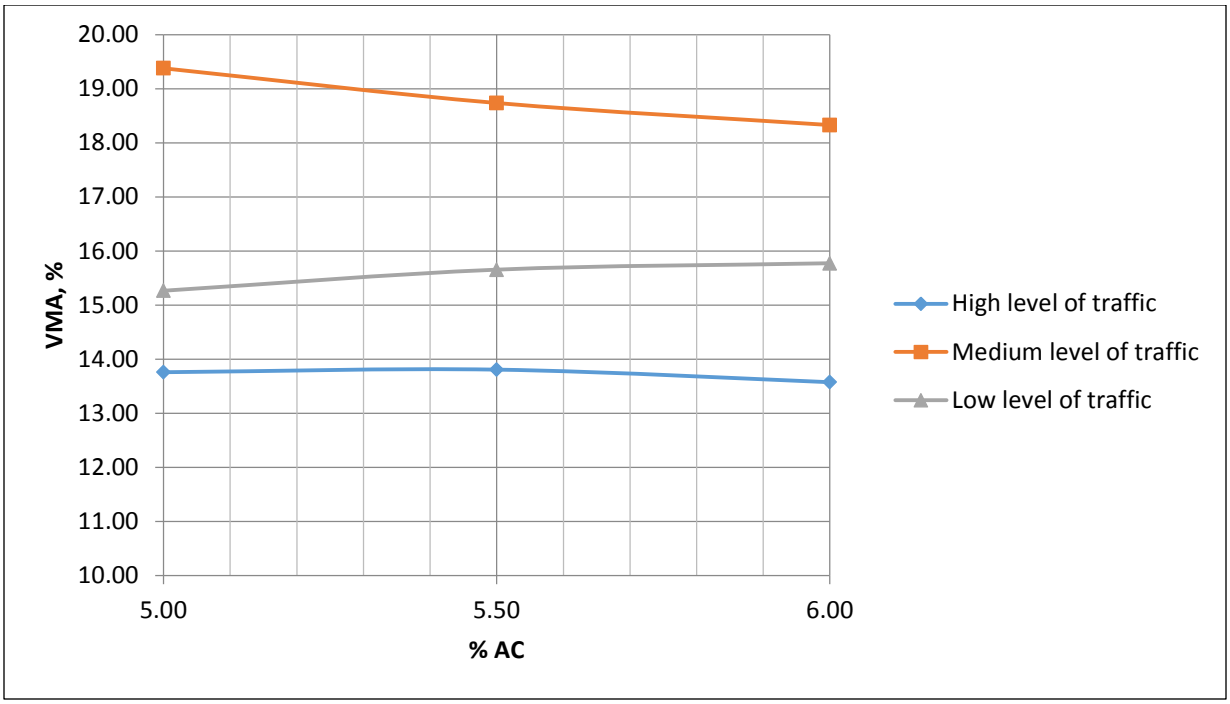

Figure 36. Percent voids in asphalt mixture versus percent asphalt for all traffic levels

Overall, as Figure 37 shows, the VFA was highest in the mixture for the high-traffic level rather than for the low and medium levels of traffic. The mixtures with the optimum asphalt content for all traffic levels met the VFA requirements. It should be noted that the VFA for the low-traffic level was highest at 5% AC content but the lowest at 6%.

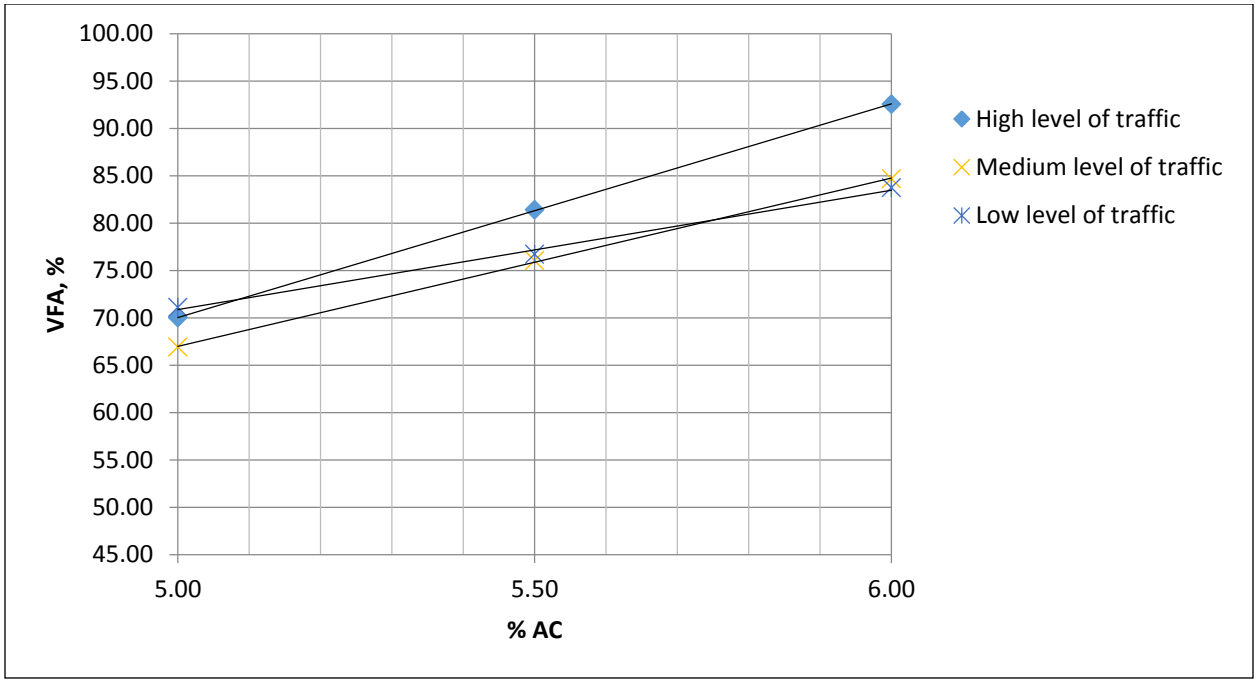

Figure 37. Percent voids filled with asphalt versus percent asphalt for all traffic levels

Table 16 summarizes the optimum asphalt content for low-, medium-, and high-levels of traffic. As the traffic level was increased from low to high, the optimum asphalt content decreased.

Table 16. Summary of optimum asphalt content for all levels of traffic

Mixtures for Traffic Levels	Optimum Asphalt Content
Low (3% AV)	5.8%
Medium (4% AV)	5.7%
High (4% AV)	4.8%

The $\%G_{mm}$ values of the mixtures with 5.0, 5.5, and 6.0% binder contents are plotted against the number of gyrations up to 152 for low-, medium-, and high-traffic levels in Figure 38, 39, and 40, respectively.

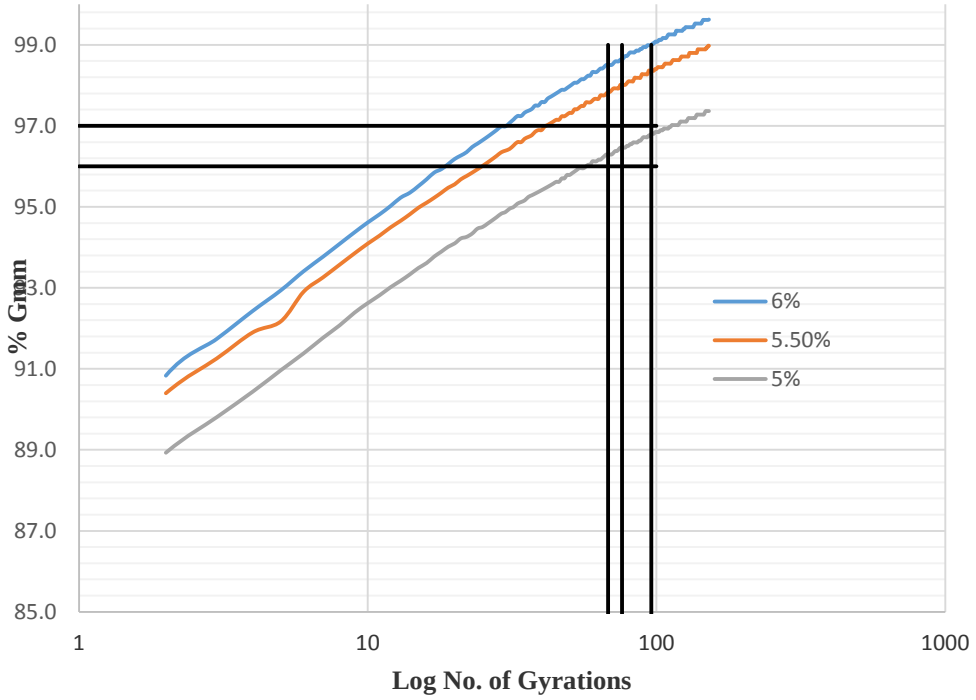

Figure 38. Percent of theoretical maximum density versus number of gyrations for high level of traffic

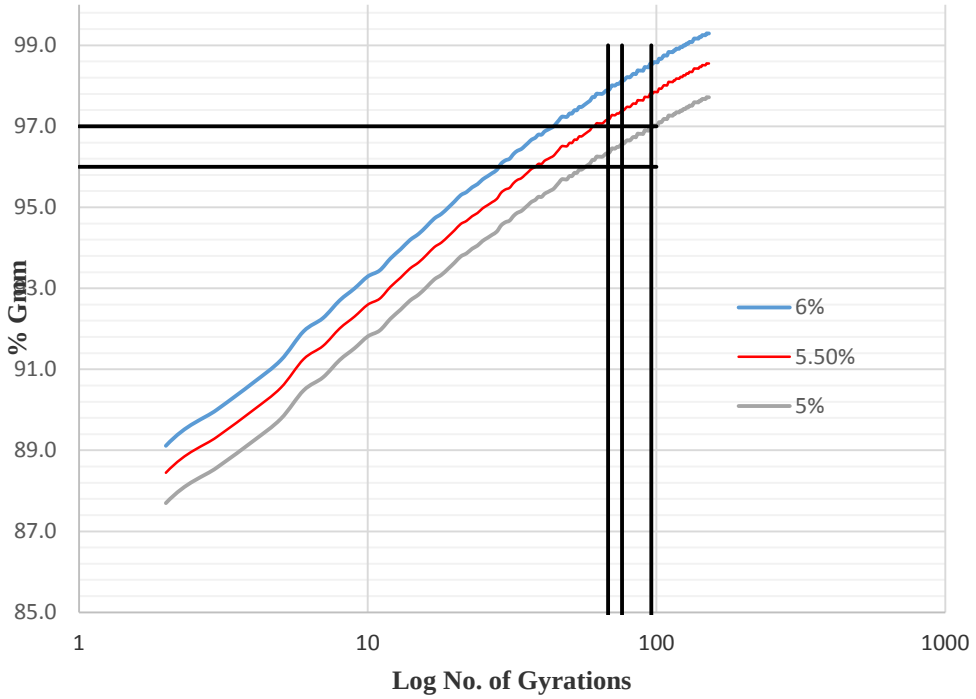

Figure 39. Percent of theoretical maximum densityversus number of gyrations for medium level of traffic

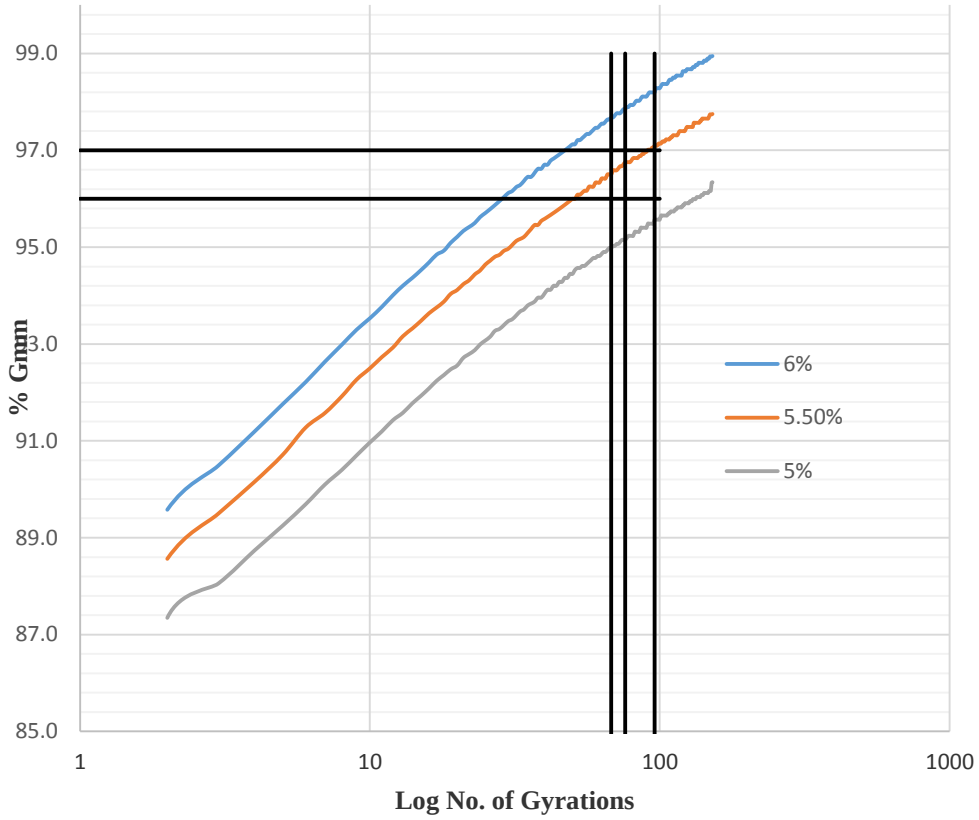

Figure 40. Percent of theoretical maximum densityversus number of gyrations for low level of traffic

As shown in these figures, three vertical lines indicate 68, 76, and 96 gyrations and 2 horizontal lines corresponds to 3 and 4% of air voids. As expected, the $\%G_{mm}$ values increased as the binder content increased.

Based on these plots, the optimum binder contents for three different design number of gyrations of 68, 76, and 96 were determined for the mixtures for low, medium, and high levels of traffic and summarized in Table 17.

Table 17. Optimum asphalt contents for three types of mixtures under three different design gyration numbers

Mixtures for Traffic Levels	**Number of Gyrations**		
	68	**76**	**96**
Low (3%AV)	5.7%	5.6%	5.45%
Medium (4% AV)	5.3%	4.7%	4.4%
High (4% AV)	5.7%	4.9%	4.8%

As expected, the optimum binder content decreased as the design number of gyrations increased from 68 to 96. For example, if the design gyration number of 68 is adopted for all mixtures, the optimum binder content would be 5.7, 5.3, and 5.7 for low-, medium-, and high-traffic levels, respectively. The optimum asphalt contents for the medium-traffic level are lower than the ones for the high-traffic level at all gyration levels because it is easier to compact to achieve 4% air voids with less asphalt. The optimum asphalt contents for the low-traffic level were highest for all gyration numbers because it needs more binder to achieve 3% air voids.

Table 18 shows the optimum asphalt contents, assuming that the target air voids of 4% is adopted for the low-traffic level.

Table 18. Optimum asphalt contents for three types of mixtures under three different design gyration numbers (4 percent air void for low level of traffic)

Mixtures for Traffic Levels	**Number of Gyrations**		
	68	76	96
Low	5.3%	5.25%	5.1%
Medium	5.3%	4.7%	4.4%
High	5.7%	4.9%	4.8%

As can be seen in Table 18, when the target air voids increased from 3 to 4% for the low-traffic level, the optimum asphalt content decreased for all gyration levels. However, the optimum asphalt content for the low-traffic level did not change much as the number of gyration was increased.

The $\%G_{mm}$ values of the mixtures for low-, medium-, and high-traffic levels are plotted against the number of gyrations up to 152 for 5.0, 5.5, and 6.0% binder contents in Figure 41, 42, and 43, respectively.

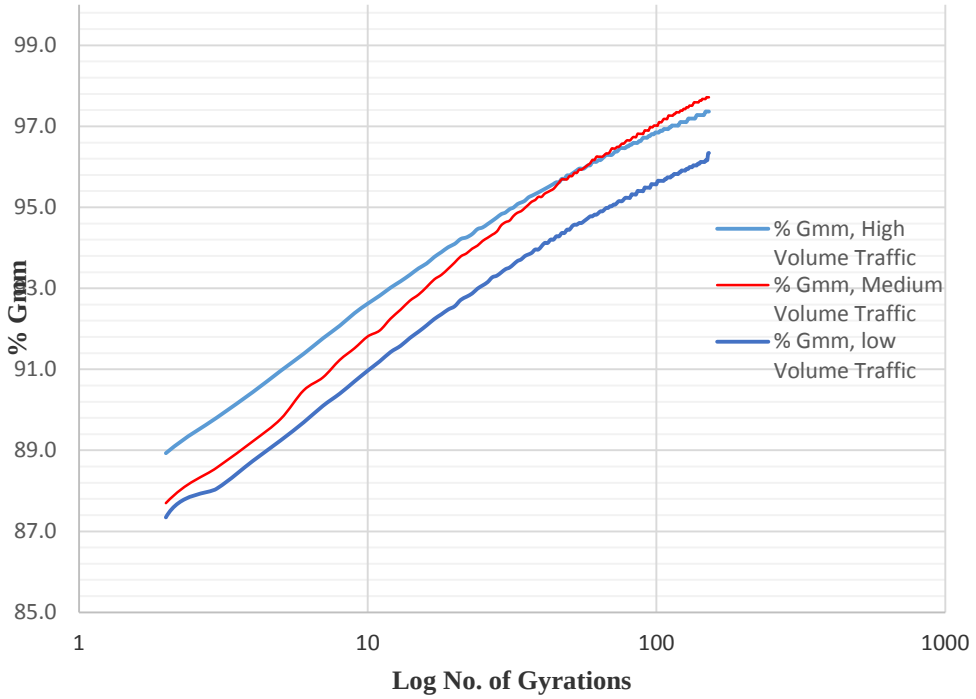

Figure 41. Percent of theoretical maximum density versus number of gyrations for 5 percent asphalt

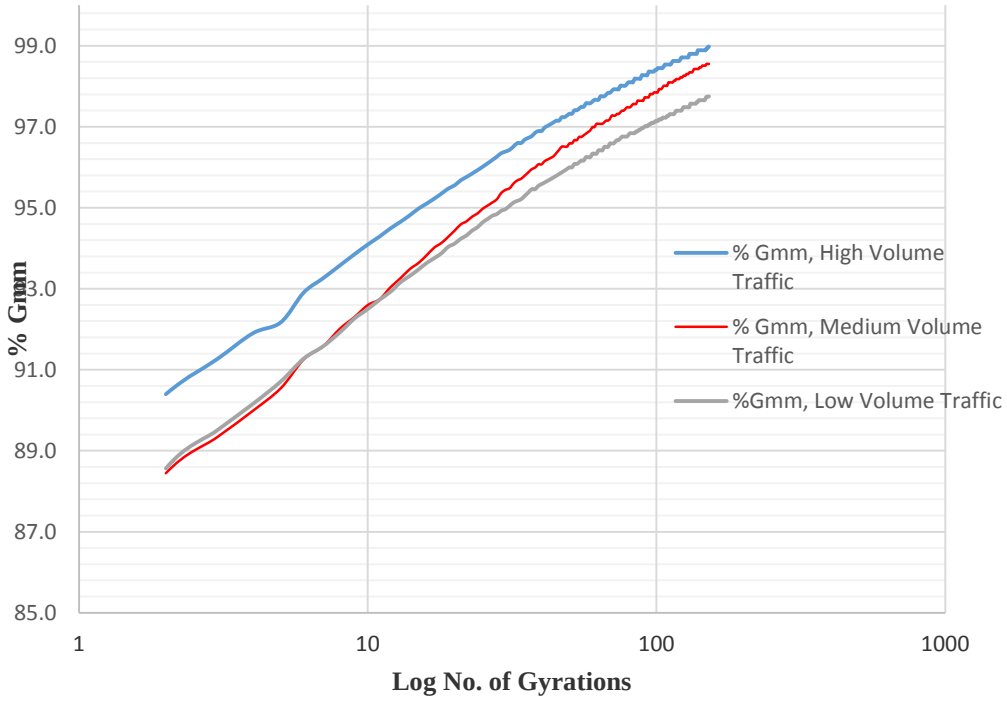

Figure 42. Percent of theoretical maximum density versus number of gyrations for 5.5 percent asphalt

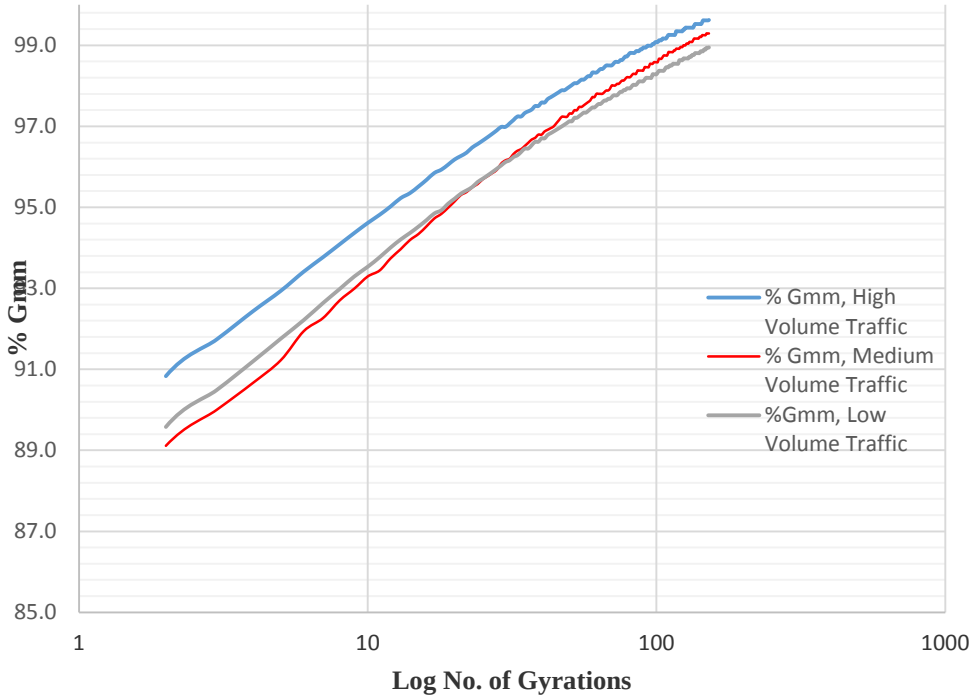

Figure 43. Percent of theoretical maximum density versus number of gyrations for 6 percent asphalt

These figures show that the initial $\%G_{mm}$ value of the mixture for the high-traffic level was higher than those for low- and medium-traffic levels, possibly due to a dense graded aggregate structure. However, the final $\%G_{mm}$ value of the mixture for the medium-traffic level reached $\%G_{mm}$ for the high-traffic level, because the rate of increase of the $\%G_{mm}$ values (the slope of the gyration curve) was higher than those for low and high levels of traffic. It can be postulated that the mixture for the medium-traffic level was easier to compact than mixtures for low- and high-traffic levels.

Based on the percentages in Table 19, air voids were derived for mixtures at three gyration levels (68, 76, and 96) and three asphalt contents (5.0, 5.5, and 6.0%).

Table 19. Percent air void for different levels of traffic, asphalt content, and number of gyrations

Asphalt Content		Mixes for Low Traffic			Mixes for Medium Traffic			Mixes for High Traffic		
		68	76	96	68	76	96	68	76	96
5.0%	1	5.10%	4.90%	4.50%	3.60%	3.30%	2.90%	3.80%	3.60%	3.20%
	2	5.0%	4.80%	4.40%	3.80%	3.50%	3.10%	3.60%	3.40%	3.30%
5.5%	1	3.60%	3.20%	2.90%	2.80%	2.60%	2.20%	2.20%	2.00%	1.70%
	2	3.50%	3.30%	2.90%	2.80%	2.60%	2.20%	2.10%	1.90%	1.60%
6.0%	1	2.20%	2.00%	1.70%	2.00%	1.80%	1.50%	1.40%	1.20%	1.0%
	2	2.40%	2.30%	1.90%	2.20%	2.00%	1.40%	1.60%	1.50%	1.0%

For a given gyration level and asphalt content, throughout the gyration process, air voids for the low-traffic level were higher than those of medium- and high-traffic levels, especially in the early stage of the gyration (up to 68 gyrations). As the specimens were gyrated more, the difference in air voids among specimens decreased. It can be concluded that it is easier to compact the mixtures for both medium- and high-traffic levels than those for the low-traffic level.

CHAPTER 5: CONCLUSIONS AND RECOMMENDATIONS

The literature showed that the current N_{design} table in the Superpave mix design method may be too high in some instances. The challenge this creates is over-compaction during laboratory design leading to under-compaction in the field. Difficulty in compaction may result in decreased durability and increased water penetration.

By evaluating the pavement conditions for some projects, the research team was able to determine if the sections selected showed any anomalies within the pavement sections prior to conducting compaction analyses after construction. Based on the PMIS data, the pavement sections selected for the study were adequate for post-construction analyses. Within the selected projects, the overall pavement conditions showed significant improvements in pavement performance after rehabilitation in year 2011 for ESAL levels below 30,000,000. No major pavement distresses were observed; the plan is for the projects to be continuously monitored every 2 years. Additionally, the average decrease in air voids ranged between 1 and 2%, and the majority of randomly selected locations did not reach 96% G_{mm} post-construction, specifically at the higher ESAL levels. A correlation between the density 4 years post-rehabilitation and the overall performance of pavements in Iowa will be investigated in future research.

Based on the field and construction air voids analyses, for future study, the G_{mm} from the QC/QA data can be utilized to determine the density of the pavement since the results showed that the field G_{mm} was close to the estimated G_{mm}. In addition, the study also showed that at ESAL levels of 300,000 and 3,000,000, ultimate pavement density was achieved. The outcome of the study showed that projects at ESAL levels of 1,000,000, 10,000,000 and 30,000,000 displayed the most concern. The majority of the projects at 10,000,000 and 30,000,000 ESALs were unable to densify with traffic due to under-compaction during construction. Due to this under-compaction, a target air void of 4% was not always achieved within at least four years for the majority of the pavement locations studied.

The binder content was also tested in the laboratory to determine if the target binder content from the QC/QA data was in the mixes. It is important to evaluate the binder content because it could possibly affect the N_{design} at construction. For instance, at 300,000 ESALs, if the binder content is higher, the N_{design} at construction may not be 68 but may be lower. However, the binder content tested showed that the binder contents for mixes were fairly close to the target binder content from the QC/QA data, thus this does not contribute to the concerns of achieving the ultimate pavement density.

Additionally, the PCCE, or estimated compaction due to traffic analyses, validated the results obtained from the air voids analyses. The results showed that PCCE does not necessarily decrease with increasing traffic volumes as expected. The results showed that there is more compaction effort induced at the 300,000 and 3,000,000 ESAL levels. As the ESAL levels increase, the difficulty to compact under traffic becomes more difficult, with the exception of the 1,000,000 ESAL level. Preliminary results suggest a decrease in the number of design gyrations compared to the ones currently being used in Iowa. Anomalies were present in the data analysis primarily in evaluating the gyratory slope and PCCE. There likely may be errors or

miscalculations in the QC/QA data. Although there was high variability in determining the theoretical N_{design} post-construction, at construction, and the PCCE within each project, this information is still valuable for the study. Additional projects and mix design information will be valuable in further evaluating the findings of the study. Ongoing data collection from the PMIS data will also be useful in tracking how these pavements perform over time. Although more research is needed, the outcome of the research concluded that the pavements constructed with high gyration mix designs were less likely to achieve ultimate density in the field, particularly at 10,000,000 and 30,000,000 ESALs. In addition, based on the distribution of $\%G_{mm}$ at construction and the expected shifted distribution at 4 years post-construction, the results estimate that there is a high probability that 25% of flexible pavements in Iowa will never reach ultimate pavement density; N_{design} being one of the major factors that contributes to this effect.

Lastly, the optimum asphalt content of the mixture for a high-traffic level was lowest (at 4.8% for 4% air voids), followed by the medium-traffic level (at 5.68% for 4% air voids), and the low-traffic level (at 5.8% for 3% air voids). The low asphalt content for the high-traffic level was mainly due to the high number of gyrations. Due to very low dust content, the mixtures for both low- and high-traffic levels did not meet the mix design requirements.

The mixtures with varying asphalt contents of 5.0, 5.5, and 6.0% were compacted up to a maximum number of 152 gyrations. The initial $\%G_{mm}$ value of the mixture for the high-traffic level was higher than those for the low- and medium-traffic levels, possibly due to a dense-graded aggregate structure. However, the final $\%G_{mm}$ value of the mixture for the medium-traffic level reached 152 gyrations for the high-traffic level because the rate of increase of the $\%G_{mm}$ values (the slope of the gyration curve) was higher than those for the low- and high-traffic levels. It can be postulated that the mixture for the medium-traffic level was easier to compact than the mixtures for low- and high-traffic levels. For any given gyration level and asphalt content, air voids for the low-traffic level were higher than those of the medium- and high-traffic levels.

As N_{design} standards are reconsidered for Iowa, close attention to the design target air voids, VMA, and aggregate source/type will be addressed. Future research will be conducted to validate and recommend the optimum design number of gyrations in Iowa. Again, the long standing premise of utilizing the greatest amount of asphalt binder in an aggregate structure without compromising rutting resistance in asphalt mix design is being met, but is conservative, and pavement life could be extended with an increased amount of binder. This increased life would be a result of improved durability and fatigue cracking performance as well as improved resistance to moisture sensitivity. The next important aspect of this research is to verify that proposed changes in gyration levels at the various traffic levels is not leading to rutting susceptibility.

REFERENCES

Aguiar-Moya, J. P., Prozzi, J. A., and Tahmoressi, M. 2007. Optimum Number of Superpave Gyrations Based on Project Requirements. *Transportation Research Record: Journal of the Transportation Research Board*, No. 2001, pp. 84-92.

AASHTO. 2013. *AASHTO T 166-13: Standard Method of Test for Bulk Specific Gravity (Gmb) of Compacted Hot-Mix Asphalt (HMA) Using Saturated Surface-Dry Specimens*, American Association of State Highway and Transportation Officals, Washington, DC.

AASHTO. 2015a. *AASHTO R 35: Standard Practice for Superpave Volumetric Design for Asphalt Mixtures*, American Association of State Highway and Transportation Officals, Washington, DC.

AASHTO. 2015b. *AASHTO T 209: Theoretical Maximum Specific Gravity and Density of Hot Mix Asphalt*. American Association of State Highway and Transportation Officals, Washington, DC.

Anderson, R. M., Turner, P. A., Peterson, R. L., and Mallick, R. B. 2002. *NCHRP Report 478: Relationship of Superpave Gyratory Compaction Properties to HMA Rutting Behavior*, National Cooperative Highway Research Program, Washington, DC.

Anderson, R., Christensen, D., and Bonaquist, R. 2003. Estimating the Rutting Potential of Asphalt Mixtures using SGC properties and IDT. *Journal of the Assocation of Asphalt Paving Technologists*, Vol. 72.

ASTM International. 2011. *ASTM D6752/D6752M: Standard Test Method for Bulk Specific Gravity and Density of Compacted Bituminous Mixtures Using Automatic Vacuum Sealing Method*, ASTM International, West Conshohocken, PA.

Brown, E. R. and S. A. Cross. 1989. A Study of In-Place Rutting of Asphalt Pavements. *Journal of the Association of Asphalt Paving Technologists*, Vol. 58, pp. 1–39.

Brown, E. R., Kandhal, S. P., Roberts, L. F., Kim, Y. R., Lee, D.-Y., and Kennedy, T. W. 2009. *Hot Mix Asphalt Materials: Mixture Design, and Construction*. National Asphalt Pavement Association (NAPA) Education Foundation, Lanham, MD.

Christensen, D. W. and R. Bonaquist. Rut Resistance and Volumetric Composition of Asphalt Concrete Mixtures. Proc., Technical Sessions, Assocation of Asphalt Paving Technologists, Vol. 74, pp. 410-439, 2005.

Cominsky, R. J., Huber, G. A., Kennedy, T. W., and Anderson, M. 1994. *SHRP-A-407: The Superpave Mix Design Manaul for New Construction and Overlays*, Strategic Highway Research Program, Washinton, DC.

FHWA. 2001. *Superpave Mixure Design Guide: WesTrack Forensic Team Consensus Report*, Federal Highway Administration Office of Infrastructure Research and Development, Washington, DC.

Harmelink, D. and T. Aschenbrener. 2002. *In-Place Voids Monitoring of Hot Mix Asphalt Pavements*, Colorado Department of Transportation (CDOT) Research Branch, Denver, CO.

Hmoud, H. R. 2011. Evaluation of VMA and Film Thickness Requirements in Hot-Mix Asphalt. *Modern Applied Sciences*, Canadian Center of Science and Education, 5(4): 166.

Hornbeck, N. C. 2008. *Effect of Compaction Effort on Superpave Surface Course Materials*, Master's Thesis (Civil Engineering), West Virginia University, Morgantown, WV.

Huang, Y. H. 2003. *Pavement Analysis and Design*, 2nd (Ed.), Pearson Prentice Hall, Upper Saddle Rive, NJ.

Iowa DOT. 2013. *Iowa in Motion – Iowa Interstate Corridor Plan*, Iowa Department of Transportation, Ames, IA.

Maupin, G. W. 2003. *Additional Asphalt to Increase the Durability of Virginia's Superpave Surface Mixes*, Virginia Transportation Research Council, Charlottesville, VA.

Miller, J. S. and W. Y. Bellinger. 2003. *Distress Identification Manual for the Long-Term Pavement Performance Program*, Federal Highway Administration Office of Infrastructure Research and Development, McLean, VA.

NAPA. 2015. *History of Asphalt*. National Asphalt Pavement Association, Lanham, MD. Available at www.asphaltpavement.org/index.php?option=com_content&view=article&id=21&Itemid=41.

ODOT. 2013. *Construction and Material Specifications*, Ohio Department of Transportation, Columbus, OH.

Pavement Interactive. 2009a. Pavement Management, Fatigue Cracking. April 7, 2009. www.pavementinteractive.org/article/fatigue-cracking/.

Pavement Interactive. 2009b. Pavement Management, Block Cracking. June 5, 2009. www.pavementinteractive.org/article/block-cracking/.

Peterson, R. L., Mahboub, K. C., Anderson, R. M., Masad, E., and Tashman, L. 2003. Superpave Laboratory Compaction Versus Field Compaction. *Transportation Research Record: Journal of the Transporation Research Board*, No. 1832(1): 201-208.

Pine Instrument Company. 2011. *AFG2 SUPERPAVE Gyratory Compactor Operation Manual*, Version 015. Available at www.abmbv.nl/files/pine_afg2_manual.pdf.

Prowell, B. D. and E. R. Brown. 2007. *NCHRP Report 573: Superpave Mix Design: Verifying Gyration Levels in the Ndesign Table*, National Cooperative Highway Research Program, Washinton, DC.

Qarouach, S. 2013. *An Investigation of the Effect of Ndesign Values on Performance of Superpave Mixtures*, Master's Thesis (Civil Engineering), North Carolina State University, Raleigh, NC.

Watson, D. E., Moore, J., Heartsill, J., Jared, D., and Wu, P. 2008. Verification of Superpave Number of Design Gyration Compaction Levels for Georgia. *Transportation Research Record: Journal of the Transportation Research Board*, No. 2057(1): 75-82.

APPENDIX A: QC/QA FIELD VOIDS DATA (300,000–10,000,000 ESALS)

Table 20. QC/QA field voids data for selected projects

County	Project No.	Iowa DOT Project No.	Core#/ Station	Intended Thickness, in.	Actual Thickness, in.	G_{mm} (est.)	AV at const. (%)	ESAL	N_{design}
Boone	1	FM-C008(55)--55-08	2/288+10	1.5	1.8	2.462	4.509	300,000	68
			3/297+18	1.5	2	2.462	4.468		
			4/323+23	1.5	1.7	2.466	5.312		
Emmet	2	STP-S-CO32--5E-32	4/61+31	N/A	2	2.396	5.968		
			7/86+61	N/A	1.825	2.396	6.010		
			3/24+56	N/A	1.75	2.407	5.941		
Story	3	STP-S-C085(107)--5E-85	8/21+69	1.5	1.6	2.461	6.258		
			5/101+19	1.5	1.6	2.462	6.418		
			8/9+80	1.5	1.6	2.465	6.491		
Clinton	4	STP-136-1(63)--2C-23	3/254+98	2	2	2.461	6.136	1,000,000	76
			8/664+05	2	2	2.45	6.122		
			8/182+93	2	1.875	2.46	6.179		
Guthrie	5	STP-025-4(40)--2C-39	7/223+98	1.5	1.7	2.425	6.598		
			5/340+97	1.5	1.875	2.44	6.598		
			4/485+60	1.5	1.84	2.422	6.606		
Tama	6	STP-S-CO86(077)--5E-86	7/286+12	1.5	1.52	2.458	7.404		
			5/369+35	1.5	1.75	2.449	7.391		
			3/75+54	1.5	1.48	2.457	7.407		

County	Project No.	Iowa DOT Project No.	Core#/ Station	Intended Thickness, in.	Actual Thickness, in.	G_{mm} (est.)	AV at const. (%)	ESAL	N_{design}
Polk	7	STP-017-1(16)--2C-77	3/237+83	2	1.5	2.468	6.767	3,000,000	86
			6/8+38	2	2.1	2.487	6.956		
			2/131+62	2	1.9	2.478	6.780		
Polk	8	STP-160-1(10)--2C-77	1/344.68	2	1.7	2.468	4.903		
			2/301.66	2	2.1	2.463	4.872		
			2/356.83	2	2.2	2.441	5.080		
Lyon	9	STP-009-1(39)--2C-60	7/92+27	1.5	1.63	2.452	7.463		
			4/193+93	1.5	1.38	2.453	7.542		
			8/92+65	1.5	1.63	2.453	7.542		
Linn	10	NHSX-151-3(119)--3H-57	3/171+75	2	1.75	2.63	4.981	10,000,000	96
			4/176+67	2	1.75	2.63	5.057		
			5/92+23	2	2	2.605	4.952		
Jefferson	11	NHSX-034-8(143)--3H-51	4/920+52	1.5	1.625	2.541	7.084		
			8/977+65	1.5	1.5	2.558	6.998		
			1/105+65	1.5	1.875	2.577	7.256		
Hamilton	12	MP-020-1(705)136--76-40	2/12+38	2	1.7	2.47	7.490		
			6/48+60	2	1.9	2.471	7.487		
			1/3+80	2	1.9	2.46	7.236		

APPENDIX B: QC/QA LABORATORY VOIDS DATA (300,000–10,000,000 ESALS)

Table 21. QC/QA laboratory voids data for selected projects

County	Project No.	Iowa DOT Project No.	Constructed		Iowa DOT			ESAL	N_{design}
			G_{mm}	AV	G_{mb}	G_{mm}	AV		
Boone	1	FM-C008(55)--55-08	2.458	3.295	2.383	2.463	3.248	300,000	68
			2.461	2.966					
			2.466	3.487					
			2.466	3.933	2.365	2.463	3.979		
			2.467	3.486					
			2.466	3.690					
Emmet	2	STP-S-CO32--5E-32	2.404	3.494	2.327	2.406	3.283		
			2.41	3.402					
			2.396	3.005	2.33	2.405	3.119		
			2.396	2.379					
			2.396	2.462					
			2.396	3.005	2.33	2.405	3.119		
			2.396	2.379					
			2.396	2.462					
Story	3	STP-S-C085(107)--5E-85	2.46	3.577	2.379	2.467	3.567		
			2.461	3.210					
			2.461	3.291					
			2.465	3.773					
			2.462	3.940	2.366	2.45	3.429		
			2.462	3.940					
			2.461	3.413					

County	Project No.	Iowa DOT Project No.	Constructed		Iowa DOT			ESAL	N_{design}
			G_{mm}	AV	G_{mb}	G_{mm}	AV		
Clinton	4	STP-136-1(63)--2C-23	2.472	4.814				1,000,000	76
			2.457	4.070					
			2.45	3.429	2.375	2.452	3.140		
			2.457	3.541	2.383	2.453	2.854		
			2.465	4.016					
			2.464	3.977					
			2.456	3.705					
			2.447	3.515					
			2.454	3.708	2.375	2.452	3.140		
			2.45	3.592					
Guthrie	5	STP-025-4(40)--2C-39	2.43	3.416					
			2.424	3.218					
			2.422	3.303					
			2.435	3.737	2.347	2.433	3.535		
			2.441	3.523					
			2.442	3.890					
			2.442	3.931					
			2.416	2.649	2.353	2.425	2.969		
			2.423	2.889					
			2.428	3.542					

County	Project No.	Iowa DOT Project No.	Constructed		Iowa DOT			ESAL	N_{design}
			G_{mm}	AV	G_{mb}	G_{mm}	AV		
			2.459	4.189					
			2.457	4.151					
			2.465	4.706					
			2.454	3.953	2.345	2.451	4.325		
			2.452	4.119					
Tama	6	STP-S-CO86(077)--5E-86	2.451	3.835					
			2.462	4.184	2.34	2.454	4.645		
			2.449	4.328					
			2.448	4.616	2.323	2.45	5.184		
			2.446	4.579					
			2.445	4.540					

County	Project No.	Iowa DOT Project No.	Constructed		Iowa DOT			ESAL	N_{design}
			G_{mm}	AV	G_{mb}	G_{mm}	AV		
Polk	7	STP-017-1(16)--2C-77	2.468	3.687	2.393	2.458	2.644	3,000,000	86
			2.472	3.681	2.406	2.455	1.996		
			2.487	4.584					
			2.488	4.582	2.397	2.476	3.191		
			2.482	3.948					
			2.483	3.947					
			2.478	3.672					
			2.487	4.423	2.388	2.48	3.710		
Polk	8	STP-160-1(10)--2C-77	2.474	3.032	2.389	2.475	3.475		
			2.481	3.426					
			2.483	3.907					
			2.478	4.036	2.368	2.475	4.323		
			2.486	3.781					
			2.488	4.100					
Lyon	9	STP-009-1(39)--2C-60	2.446	3.802					
			2.45	3.837					
			2.453	3.954					
			2.453	4.117	2.342	2.452	4.486		
			2.45	4.204					
			2.454	4.482					
			2.456	4.886	2.321	2.448	5.188		
			2.452	4.812					

County	Project No.	Iowa DOT Project No.	Constructed		Iowa DOT			ESAL	N_{design}
			G_{mm}	AV	G_{mb}	G_{mm}	AV		
Linn	10	NHSX-151-3(119)--3H-57	2.603	3.419				10,000,000	96
			2.602	3.420	2.522	2.608	3.298		
			2.633	5.735					
			2.609	4.446					
			2.629	3.576					
			2.63	3.460					
Jefferson	11	NHSX-034-8(143)--3H-51	2.577	3.454					
			2.59	4.595	2.488	2.582	3.641		
			2.529	3.440	2.454	2.53	3.004		
			2.541	3.817					
			2.558	4.730					
Hamilton	12	MP-020-1(705)136--76-40	2.469	4.617	2.36	2.473	4.569		
			2.46	4.593					
			2.47	4.332	2.37	2.47	4.049		
			2.46	3.455					

APPENDIX C: DATA AIR VOID ANALYSES (300,000–10,000,000 ESALS)

Table 22. Data for air void analyses

Project Location	Average of N_{design}	Avg AV 4 yrs Post-const.	Average of AV at const.	Average of AADT	% G_{mm} at 0 years	% G_{mm} at 4 years	Change AV
Boone E-26	68	2.859	4.353	690	95.647	97.053	1.495
Boone E-26	68	5.841	4.312	690	95.688	95.959	-1.528
Boone E-26	68	4.029	5.351	690	94.649	95.971	1.322
Emmet A-34	68	4.068	5.968	320	94.032	96.259	1.901
Emmet A-34	68	4.128	5.824	320	94.176	96.295	1.695
Emmet A-34	68	3.085	6.010	730	93.990	97.456	2.925
Story E-29	68	5.016	6.258	560	93.742	94.643	1.242
Story E-29	68	4.255	6.418	560	93.582	95.755	2.163
Story E-29	68	4.701	6.491	560	93.509	95.140	1.790
Clinton IA	76	5.402	6.634	1230	93.366	94.912	1.233
Clinton IA	76	4.797	6.007	2110	93.993	95.345	1.210
Clinton IA	76	5.535	5.983	1230	94.017	94.852	0.448
Guthrie IA 25	76	3.040	6.598	1100	93.402	97.125	3.557
Guthrie IA 25	76	4.420	6.598	1100	93.402	95.581	2.179
Guthrie IA 25	76	5.500	6.606	1100	93.394	95.415	1.106
Tama Rd E-43	76	5.674	7.407	740	92.593	94.660	1.733
Tama Rd E-43	76	8.309	7.404	740	92.596	91.923	-0.905
Tama Rd E-43	76	6.126	7.391	740	92.609	94.125	1.265
Lyon IA 9	86	5.453	7.463	3290	92.537	94.296	2.010
Lyon IA 9	86	4.046	7.542	3290	92.458	95.476	3.496
Lyon IA 9	86	4.636	7.542	3290	92.458	95.320	2.905

Project Location	Average of N_{design}	Avg AV 4 yrs Post-const.	Average of AV at const.	Average of AADT	% G_{mm} at 0 years	% G_{mm} at 4 years	Change AV
Polk IA 17	86	3.350	6.780	980	93.220	93.645	3.430
Polk IA 17	86	3.127	6.956	980	93.044	94.025	3.829
Polk IA 17	86	4.440	6.767	980	93.233	95.434	2.327
Polk IA 160	86	3.127	4.903	21600	95.097	96.559	1.775
Polk IA 160	86	3.350	4.872	21600	95.128	95.717	1.522
Polk IA 160	86	4.440	5.080	21600	94.920	96.268	0.640
Hamilton US 20	96	6.418	7.236	8200	92.764	93.301	0.818
Hamilton US 20	96	5.385	7.490	8200	92.510	93.451	2.105
Hamilton US 20	96	6.234	7.487	8200	92.513	92.793	1.253
Jefferson US 34	96	5.610	7.084	5200	92.916	94.575	1.473
Jefferson US 34	96	5.381	6.998	5200	93.002	94.932	1.617
Jefferson US 34	96	5.805	7.256	6600	92.744	92.000	1.451
Linn US 151	96	3.083	4.842	7300	95.158	97.018	1.760
Linn US 151	96	4.684	4.945	7300	95.055	96.464	0.261

APPENDIX D: DENSITY INFORMATION (30,000,000 ESALS)

Table 23. Density information for 30,000,000 ESALs

Project No.	Project Name	Sample ID	A = Mass of dry sample	C= submerged wt. of sample in water	G_{mm}	G_{mb}	Air Voids Post-const.	Const. Year	Cores Drilled	% Voids at Const.
13	Pottawattamie I-29 NB	I-29 NB 70.0 mp	2008.3	1199.4	2.483	2.314	6.792	2008	2009	4.5
13	Pottawattamie I-29 NB	I-29 NB 68.0 mp	2004.2	1184	2.444	2.290	6.284	2008	2009	9.8
14	Warren I-35	Warren I-35 NB 59.50	2032.3	1216.4	2.491	2.357	5.372	2008	2009	7.4
14	Warren I-35	I-35 NB 57.75 Warren	2013.5	1201.3	2.479	2.378	4.085	2008	2009	6.2
14	Warren I-35	I-35 NB 58.3 Warren	1512.8	920	2.552	2.354	7.773	2008	2009	7.1
15	Fremont I-29 NB	I-29 NB 5.0 mp	2025.9	1211.7	2.488	2.307	7.293	2007	2009	7.2
15	Fremont I-29 NB	I-29 NB 4.0	1933.8	1141.9	2.442	2.349	3.816	2007	2009	6.4
16	Story I-35	Story I-35 NB 123.90	2004.5	1195.4	2.477	2.359	4.785	6/29/2009	6/30/2009	6.9
16	Story I-35	Story I-35 NB 123.85	2003	1194	2.476	2.323	6.157	6/29/2009	6/30/2009	6.9
16	Story I-35	I-35 NB 122.50 Story	1372.5	833	2.544	2.356	7.410	6/29/2009	6/30/2009	6.9
17	Iowa I-80	I-80 EB between 210.20 and 210.25	2004.3	1245.4	2.641	2.434	7.823	2008	2009	6.4
17	Iowa I-80	I-80 EB 211.30	967	489	2.528	2.422	5.260		2009	5.9
18	Pottawattamie I-680	I-680 WB 2.10	1398.5	834	2.477	2.317	6.455	1997	2009	7.9
18	Pottawattamie I-680	I-680 EB 2.0 mp	2013.2	1192.8	2.454	2.318	5.546	1997	2009	7.9
18	Pottawattamie I-680	I-680 WB 1.75	2026.6	1201.2	2.455	2.327	5.215		2009	7.9
19	Johnson I-80 EB/WB	I-80 WB 234.10	2016.5	1240.4	2.598	2.447	5.809	6/15/2009	6/16/2009	6.8
19	Johnson I-80 EB/WB	I-80 Wb 235.80	2048.7	1265.4	2.615	2.463	5.816	6/15/2009	6/16/2009	6.5
20	Johnson I-380	I-380 North 3.50	1707.6	1054	2.613	2.475	5.259	2008	2009	7.8

Table 24. Project information for 30,000,000 ESALs

Sample ID	Project Number	Estimated Stationing	Construction Year	Cores were Drilled in 2009	Type and Design No.
I-80 EB 212.70 Lower Course	Base course--Don't use			2009	
I-29 NB 70.0 mp (I29(80) pg. 45, 87) HMA 30M L-2 Surface	IM-029-4(80)58--13-78	776+06	2008	2009	4BD8-17R1
I-29 NB 69.10 mp	IM-029-4(80)58--13-78	728+54	2008	2009	4BD8-17R1
I-29 NB 68.0 mp	IM-029-4(80)58--13-78	670+46	2008	2009	4BD8-17R1
Warren I-35 NB 59.50 (Pg42, 94)	IM-035-2(347)54--13-91	877+44	2008	2009	IBD8-056
I-35 NB 57.75 Warren Co.	IM-035-2(347)54--13-91	785+04	2008	2009	IBD8-056
I-35 NB 58.3 Warren Co	IM-035-2(347)54--13-91	814+08	2008	2009	IBD8-056
I-235 EB Before I-80WB overpass	IM-035-3(159)87--13-77	2050+00.00 ish	2006	2009	
I-29 NB 5.0 mp (pg. 209)	IM-29-1(65)0--13-36	273+85.81	2007	2009	4BD7-21/4B7-7-21
I-29 NB 3.0	IM-29-1(65)0--13-36	167+98.81	2007	2009	4BD7-21/4B7-7-21
I-29 NB 4.0	IM-29-1(65)0--13-36	220+78.81	2007	2009	4BD7-21/4B7-7-21
Story Co, I-35 NB 123.90 (pg.139,433)	IMX-035-5(97)121--02-85	1213+77.6	6/29/2009	6/30/2009	IBD9-055
Story I-35 NB 123.85	IMX-035-5(97)121--02-85	1211+13.6	6/29/2009	6/30/2009	IBD9-055
I-35 NB 122.50 Story	IMX-035-5(97)121--02-85	1139+85.6	6/29/2009	6/30/2009	IBD9-055
I-80 EB between 210.20 & 210.25 (pg. 29)	IM-80-6(242)210--13-48	289+36	2008	2009	ABD6-6011 SURF
I-80 EB 211.30	IM-80-6(242)210--13-48	346+12		2009	ABD6-6011 SURF
I-680 WB 2.10	IM-680-1(126)00--13-78	222+08	1997	2009	ABD7-31
I-80 WB 214.25 **Maybe EB??	IMX-080-6(283)226--02-48	581+56.4		2009	ABD9-6014
I-680 EB 2.0 mp (pg.6)	IM-680-1(126)00--13-78	216+80	1997	2009	ABD7-31
I-680 WB 1.75	IM-680-1(126)00--13-78	203+60		2009	ABD7-31
I-235 EB 13.1 mp				2009	
I-80 WB 234.10	IMX-080-6(283)226--02-48	374+88	6/15/2009	6/16/2009	ABD9-6014 (pg. 97,101)
I-80 Wb 235.80	IMX-080-6(283)226--02-48	464+64	6/15/2009	6/16/2009	ABD9-6014 (pg. 97,101)

Sample ID	Project Number	Estimated Stationing	Construction Year	Cores were Drilled in 2009	Type and Design No.
I-380 North 3.50	IM-380-6(240)0--13-52	1348+34	2008	2009	ABD7-6012/6011r1 (pg. 354 & 368)
I-380 North 2.40	IM-380-6(240)0--13-52	1290+26	2008	2009	ABD7-6012/6011r1 (pg. 354 &p. 366)

APPENDIX E: GYRATION CURVES FOR EACH ESAL LEVEL

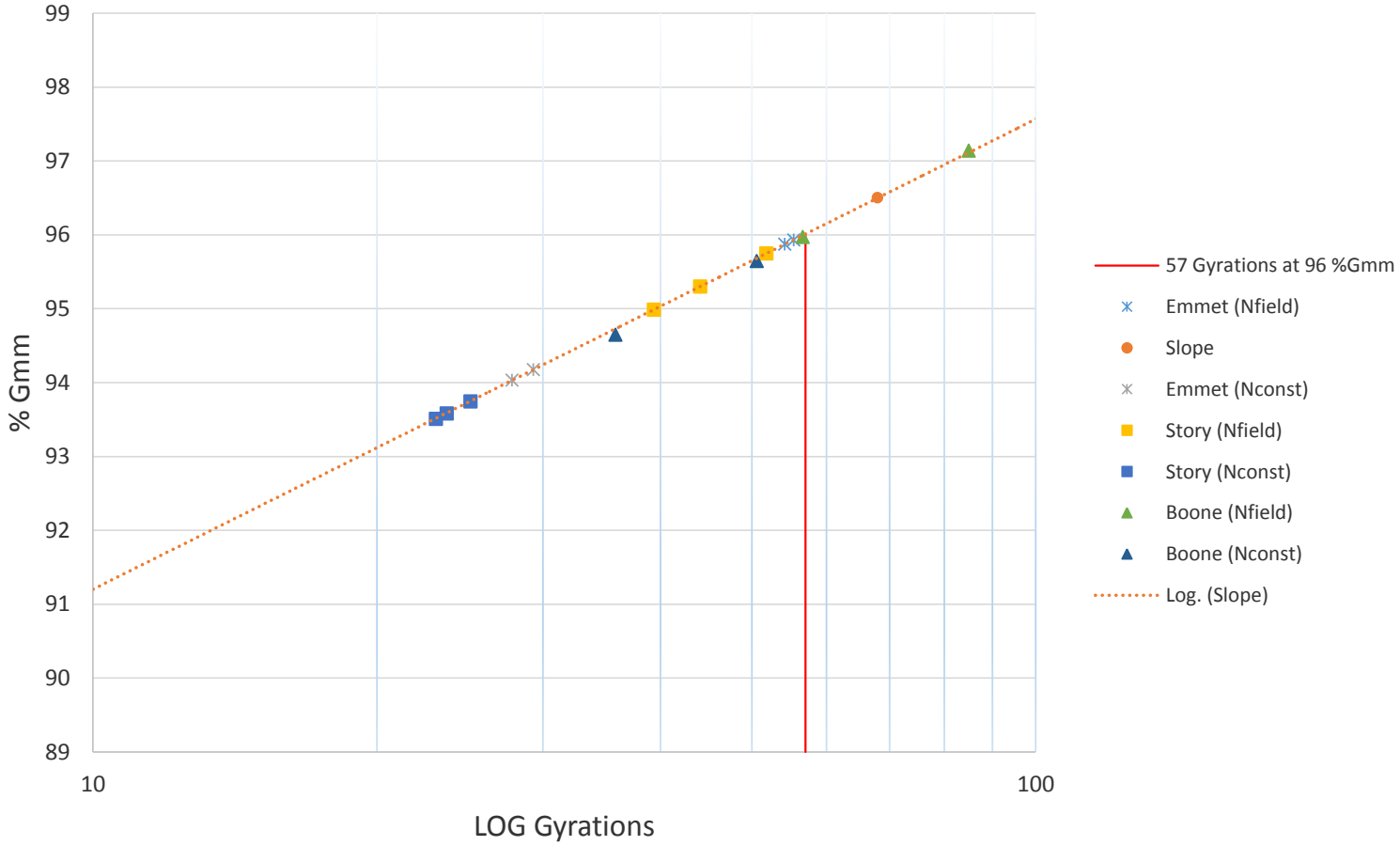

Figure 44. Gyration curve for 300,000 ESALs

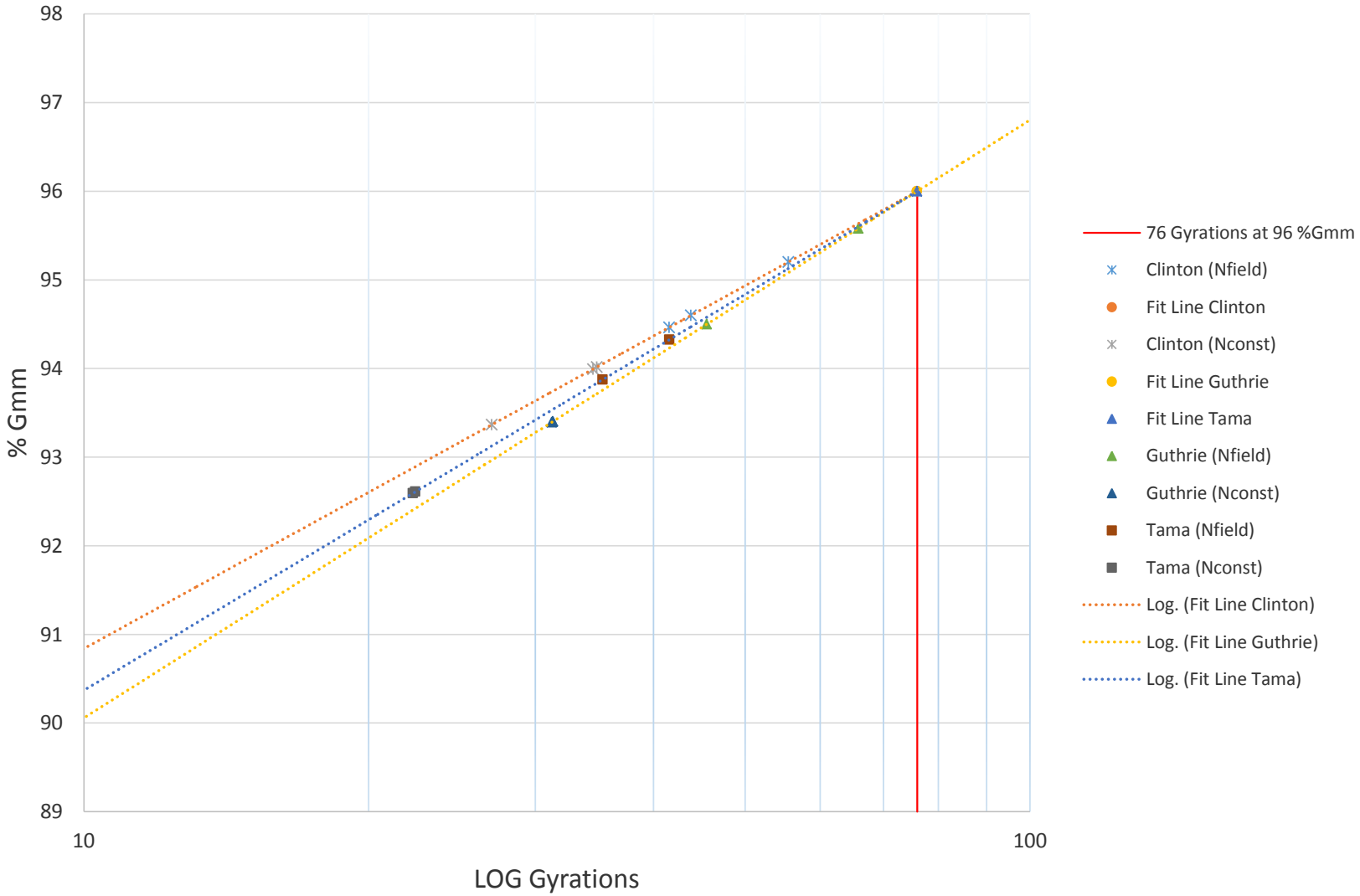

Figure 45. Gyratory curve for 1,000,000 ESALs

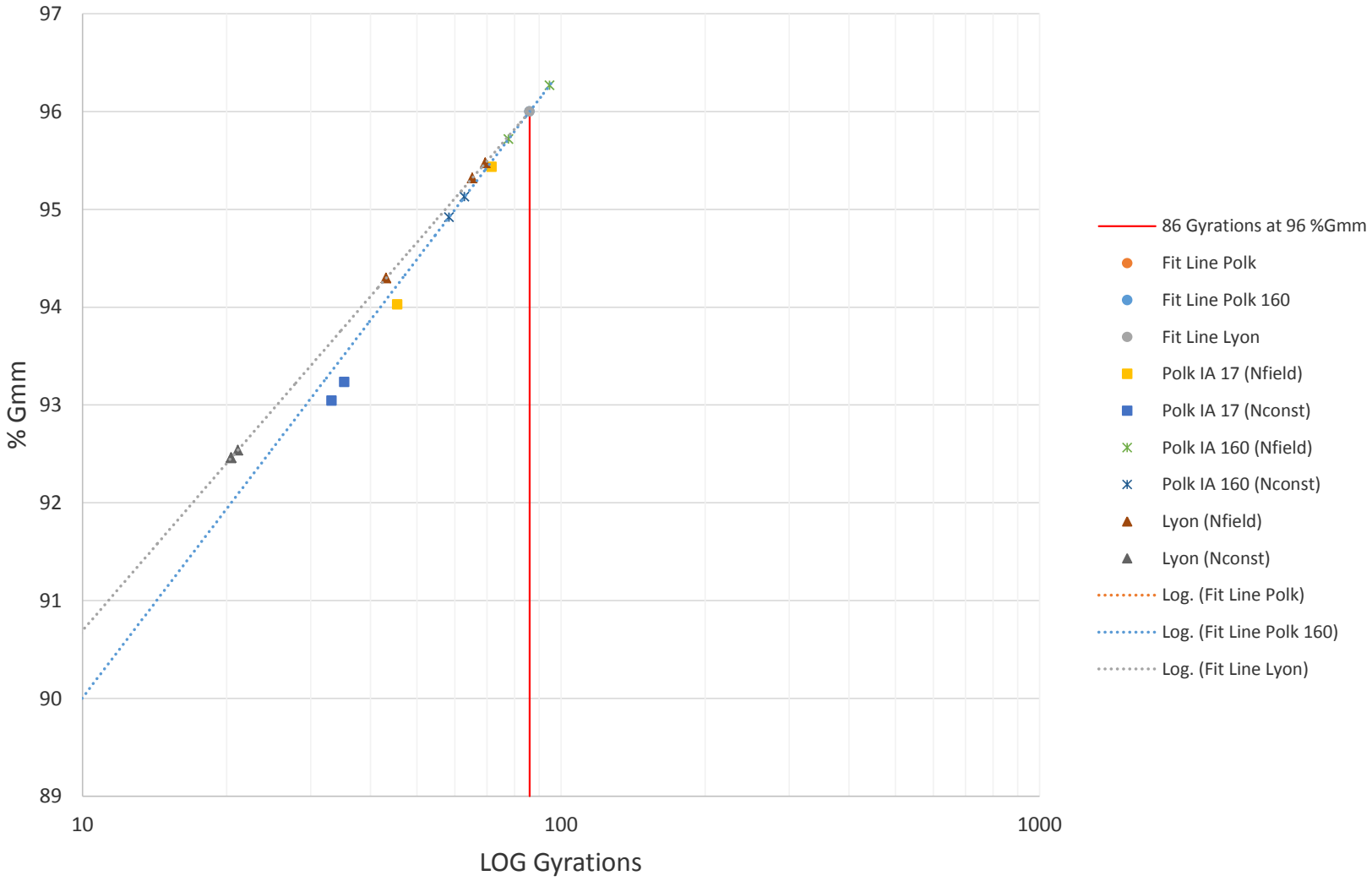

Figure 46. Gyratory curve for 3,000,000 ESALs

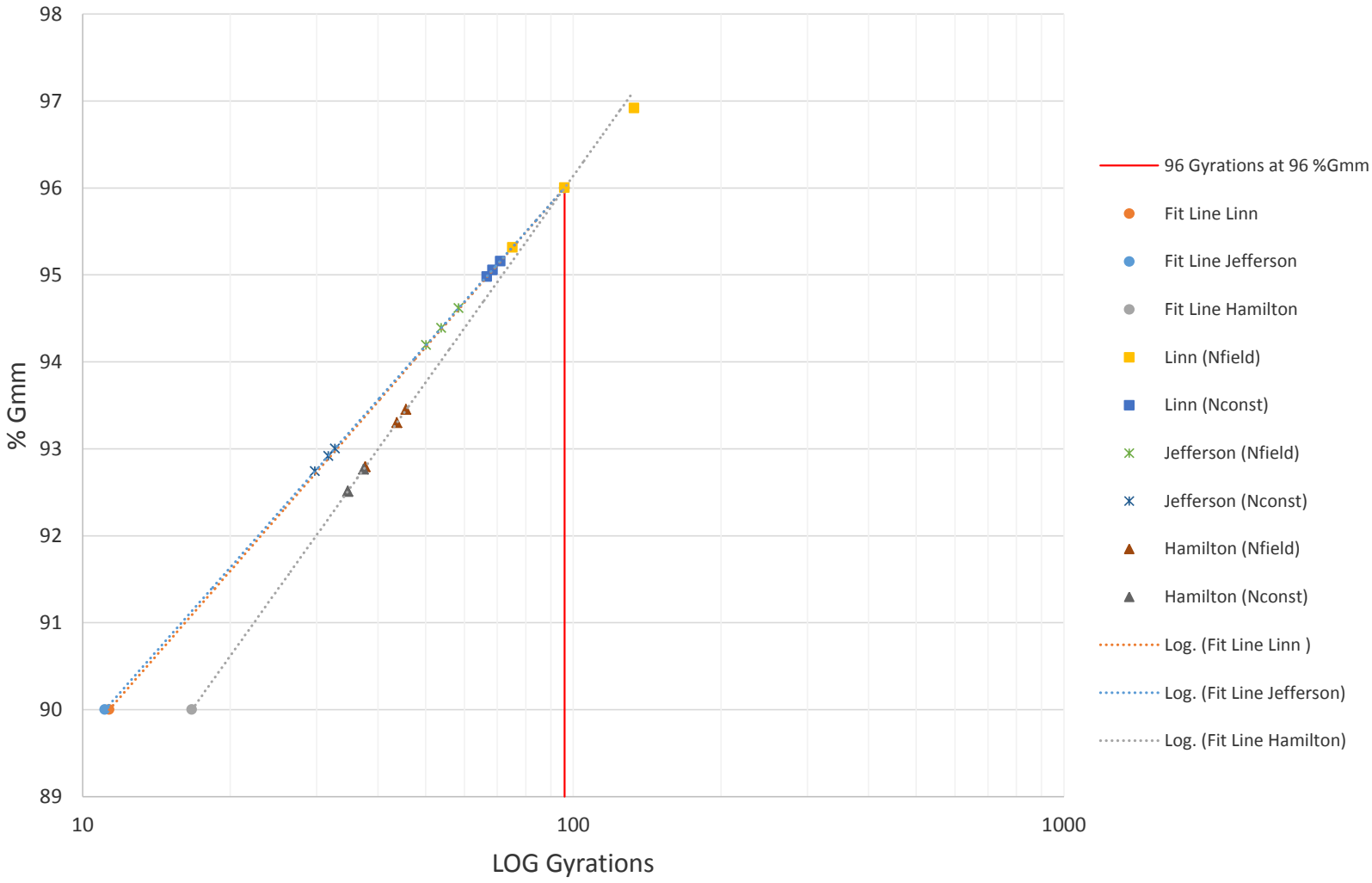

Figure 47. Gyratory curve for 10,000,000 ESALs

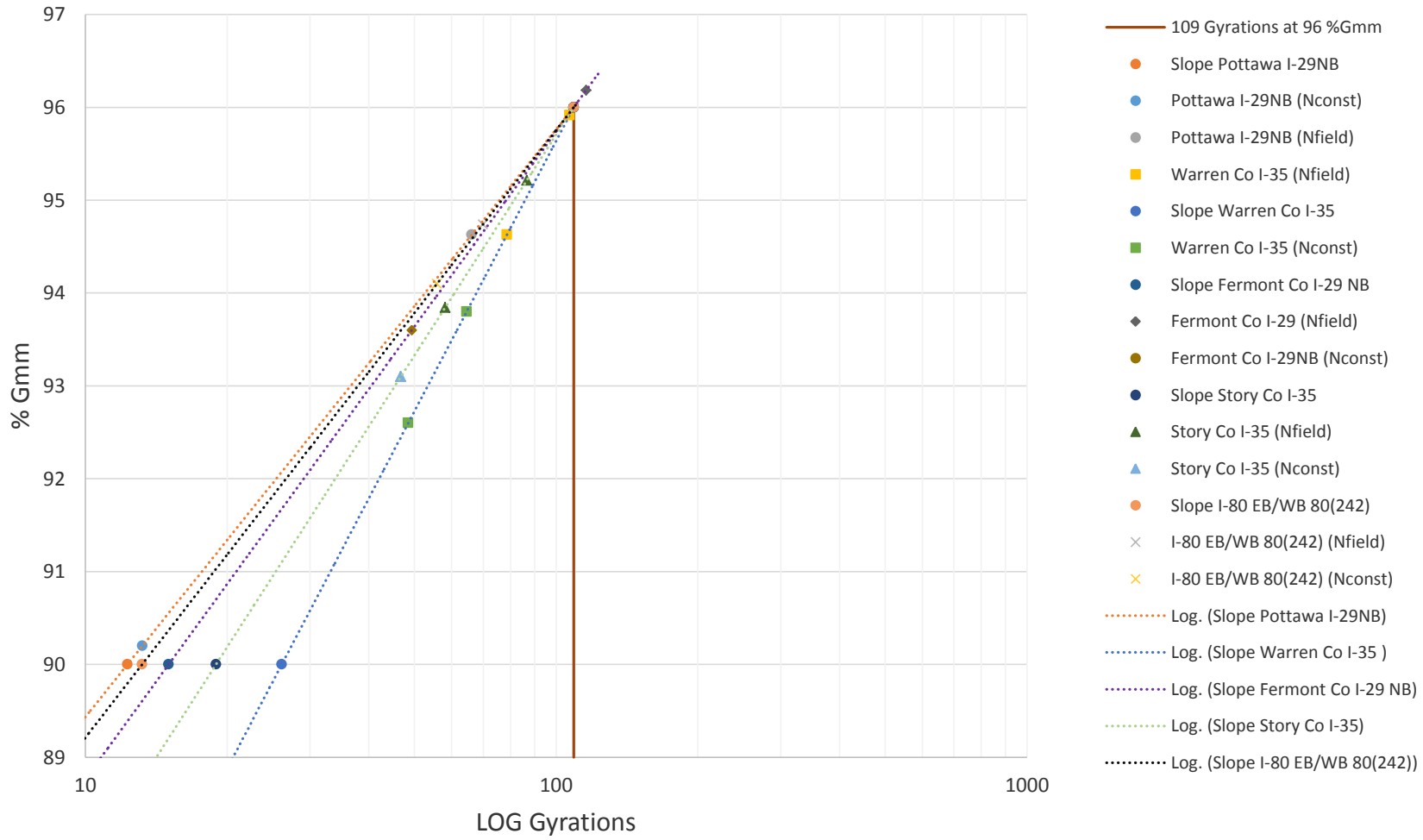

Figure 48. Gyratory curve for 30,000,000 ESALs